Output Factsheet

Output title: Strategy of EMS take-up on city scale

Summary of the output (max. 2500 characters)

Potential for the application of 3Smart tool on the level of infrastructure in cities, towns and villages is analyzed. Special emphasis is put on using similar mathematical optimization based methodologies within infrastructures to make these potential infrastructure-level energy management modules compatible for interaction with the modules in the 3Smart tool. In order to encompass in the analysis settlements of different size, the analysis relies on the case studies performed in a city, a town and a village in the Danube region: city of Zagreb, town of Idrija and village of Strem.

For the case of Zagreb, interaction of electricity grid with buildings and with the following 3Smart-like-managed infrastructure systems is analyzed: water distribution, electric vehicles charging and electrified city rail. Also the effects of 3Smart-managed buildings on the load in heat distribution grid are assessed.

For the case of Idrija, mine water pumping system is analyzed for maintaining the water level in Idrija mines, in interaction with electricity grid.

For the case of Strem, the central biogas and wood pellets combined heating/electricity plant and heat distribution grid operation under demand management is analyzed.

Based on the performed analyses, a strategy for up-scaling the use of building-side EMS tool is assessed. It elaborates how the modules of energy management on the side of infrastructure should look like, the envisioned IT environment and commissioning.

The strategy also points out the significance of inclusion of an infrastructure management system in demand response scheme since it can be a turning point for providing enough flexibility on a geographically localized area where it is needed for the distribution system operator. And then, once enough flexibility is available, other small flexibility providers can join.

The strategy also stresses the possibility of installation of an autonomous trading system between different flexibility providers which further increases economical gains for those capable of flexibility provision and reduces a risk for running into penalties when temporarily the system or infrastructure is not in a position to provide flexibility. Thus, it seems that infrastructure and buildings can form a symbiosis and support each other in the energy transition process.

Contribution to the project and Programme objectives (max. 1500 characters)

The main objective of 3Smart is to provide a technological and legislative setup for cross-

spanning energy management of buildings, energy grids and major city infrastructures in the DR. The output clearly addresses the extension of the tool which is within the project focussed on buildings and grids towards city infrastructures and various benefits that stem out of that.

As the DTP major objective is to harmonize policies across different countries in the Danube region in crucial priority fields, one of them being also energy, the strategy contributes to it by showing what role the city infrastructures can have in energy transition. Especially it is important to note that infrastructure is usually operated by public companies where local and state influence in introducing energy management and demand response measures can be more direct and represent an additional motivator for other private entities to enter the demand response scheme.

Transnational impact (max. 1500 characters)

The strategy was derived based on case studies performed for settlements of different size in different countries of the Danube region. Moreover, its results are indeed not in any way constrained to certain national environment such that it is transnationally valid.

Contribution to EUSDR actions and/or targets (max. 1500 characters)

The output contributes to Priority Area 2 "To encourage more sustainable energy" of the EUSDR within which the following actions are required: „To explore the possibility to have an increased energy production originating from local renewable energy sources to increase the energy autonomy", „To promote energy efficiency and use of renewable energy in buildings and heating systems", „To facilitate networking and cooperation between national authorities in order to promote awareness and increase the use of renewable energies".

The up-scale of energy management platform which significantly enlarges demand response capacities in a geographical area or even represents an outweigh point for accepting demand response is thus very important for local renewable energy integration.

Performed testing, if applicable (max. 1000 characters)

The strategy is based on performed case studies. Especially relevant when considering the actual application of the 3Smart tool is the Zagreb case study which can be also considered as a sequence of preliminary tests – namely within Zagreb case study it was assessed how the up-scaled 3Smart tools would operate on a water distribution, an electrified rail system or on an electric vehicles charging system.

Integration and use of the output by the target group (max. 2000 characters)

Main target groups for usage of the output are local authorities, infrastructure companies and national regulators.

Local authorities can learn how to better use the infrastructure they have within local authority assets to reduce its operation costs and also help the proliferation of demand response services locally which then also induces secondary benefits of renewable energy capacities increase.

Similar position is for infrastructure operators – it shows how the infrastructure operation costs can be lowered via demand response and optimization.

National regulators can put more emphasis on smart energy management of infrastructure since through this strategy the infrastructure should be recognized as a turning point for demand response functionality initiating in different geographical areas.

Geographical coverage and transferability (max. 1500 characters)

The strategy is transnationally relevant and transferrable to different local contexts and different infrastructure setups compared to the ones considered in performed case studies.

Durability (max. 1500 characters)

The strategy validity is not constrained with time and should become more and more relevant as the demand response legal framework becomes clear.

Synergies with other projects/ initiatives and / or alignment with current EU policies/ directives/ regulations, if applicable (max. 1500 characters)

The strategy has a synergy effect with Clean Energy for all Europeans package – it shows how city infrastructure can be smartly managed and participate in demand response.

Output integration in the current political/ economic/ social/ technological/ environmental/ legal/ regulatory framework (max. 2000 characters)

The strategy integrates well into the technology framework for demand response provision, as it is based on open tool for integrated energy management of buildings and grids. The strategy can be also considered in an environmental context, showing that demand response can be substantial with very little negative environmental effect, e.g. in water distribution system management one may see a significant flexibility power provision with very small increase in water losses in the distribution system.

Project Deliverable Report

Smart Building – Smart Grid – Smart City

http://www.interreg-danube.eu/3smart

DELIVERABLE D3.3.1

Strategy for EMS take-up on city scale and technical implications on distribution grid development and major city infrastructures

Project Acronym	3Smart
Grant Agreement No.	DTP1-502-3.2-3Smart
Funding Scheme	Interreg Danube Transnational Programme
Project Start Date	1 January 2017
Project Duration	30 months
Work Package	3
Task	3.3
Date of delivery	**Contractual:** 30 Jun 2019 **Actual:** 30 June 2019
Code name	**Version:** 1.0 Final ☒ Final draft ☐ Draft ☐
Type of deliverable	Report
Security	Public
Deliverable participants	HEP, UNIZGFER, E3, EEE, EnergyG
Authors (Partners)	Mario Vašak, Tomislav Capuder, Hrvoje Novak, Vinko Lešić, Paula Perović, Nikola Hure, Anita Martinčević, Danko Marušić (UNIZGFER), Ivona Štritof, Helena Božić (HEP), Marko Baša (E3), Tadej Rupnik (IDRIJA), Andrea Moser (EEE)
Contact person	Mario Vašak (UNIZGFER)
Abstract (for dissemination)	In this deliverable potential for the application of 3Smart tools on the level of infrastructure in cities, towns and villages is analyzed and assessed via case studies. Based on this assessment a strategy for up-scaling the 3Smart tool on the infrastructure level is assessed.
Keyword List	Analysis, EMS effects, city infrastructure, deliverable, 3Smart, D3.3.1, Water distribution system, Electrified light city rail, vehicle charging infrastructure, Central heating distribution system, Street lighting, mine water pump

Revision history

Revision	Date	Description	Author (Organization)
v0.1	22 February 2018	First draft – Zagreb case study	Ivona Štritof (HEP)
v0.2	7 May 2018	First draft – Idrija case study	Marko Baša (E3)
v0.3	11. July 2018	First draft – Strem case study	Andrea Moser (EEE)
v0.4	15 December 2018	Improvement of the technical content: Summary, Introduction and Zagreb case study	Mario Vašak, Hrvoje Novak, Tomislav Capuder (UNIZGFER)
v0.5	11 January 2019	Improvement of the content on the Austrian case study	Andrea Moser (EEE)
V0.6	3 June 2019	Economic assessment for Idrija case, finishing the Strem case study	Marko Baša (E3), Andrea Moser (EEE)
v0.7	26 June 2019	Finishing the analysis of water distribution system, electrified city rail, electric vehicles charging and heating energy flexibility	Hrvoje Novak, Vinko Lešić, Nikola Hure, Mario Vašak (UNIZGFER)
v0.8	28 June 2019	Transforming the case studies results in inputs for smart city up-scale strategy. Finishing the electrical grid analysis. Finishing the document	Paula Perović, Mario Vašak (UNIZGFER)
v1.0	29 June 2019	Finalization of the document after performed quality check	Mato Baotić, 3Smart quality assessment manager, Mario Vašak (UNIZGFER)

Table of Contents

Executive summary

Making a smart city and community impact of smart buildings and smart grids necessitates to integrate also major infrastructures of settlements of different size into energy management schemes to lift to a higher level the energy efficiency, energy security and renewable energy integration effects. This document analyses the possible approaches for upscaling the 3Smart management scheme to infrastructure systems in cities, towns and villages. Special emphasis is put on using a similar mathematical optimization based methodologies within infrastructures to make these potential infrastructure-level energy management modules compatible for interaction with the modules developed for the buildings and for the grid. In order to encompass in the analysis settlements of different size, the analysis relies on the case studies performed in a city, a town and a village in the Danube region: city of Zagreb, town of Idrija and village of Strem.

For the case of Zagreb, interaction of 3Smart-managed building and electricity grid with the following 3Smart-like-managed infrastructure systems is analyzed: water distribution system, electric vehicles charging system and electrified rail public transport. Also the effects of 3Smart-managed buildings on the consumption patterns within the heat distribution grid are assessed.

For the case of Idrija, the following infrastructure system in interaction with the 3Smart-managed building and grid are encompassed: Idrija mine water pumping system (water pumping for maintaining the water level in Idrija mine).

For the case of Strem, the central biogas and wood pellets combined heating/electricity plant and heat distribution grid in interaction with the 3Smart-managed buildings is analyzed.

Based on the performed analyses, a strategy for expansion of the building-side (consumer-side) EMS is assessed. Also, technical implications are elaborated regarding how the modules of energy management on the side of infrastructure should look like.

1. Introduction

The effects, potentials and technical possibilities of up-scaling the 3Smart concept on the smart city level is addressed in this document. Crucial for ensuring a significant effect in grid management, energy efficiency and energy security is to encompass also infrastructure systems.

One of the key terms in this document is flexibility – it is designated as possibility of a certain consumer to change its consumption profile by a certain amount compared to its previously assessed predictions for it, if an entity in the energy system requests that.

From one side it is expected that it will leverage the demand response potential of buildings and make the introduction of demand response more lucrative for local communities – their attractiveness for providing demand response services rises with the flexibility amount they can provide. Also it is possible that the community members help one another in providing the contracted flexibility and that penalties risk is lowered. From the other side it might also prove that public investment in infrastructure management will be a motivator for the surrounding private buildings to step into different energy management and demand response schemes.

In this analysis 3Smart-like management of infrastructures characteristic for settlements of different size in the Danube region is addressed. In that sense, three case studies are performed – for Zagreb as a representative of larger cities, for Idrija as a representative of middle-sized towns and for Strem as a representative of villages.

For the case of the city of Zagreb the following two large infrastructure systems will be encompassed: water distribution system, including water pumping, pumping into district storages and pressure regulation, and electrified public transport, including light city rail and electric vehicles charging infrastructure. It will be also analyzed how the heating energy consumption pattern of 3Smart-controlled buildings can be changed with demand response service provision – finally based on it the potential beneficial effects of 3Smart-operated buildings on the heat distribution grid will be assessed.

Case study in Idrija addresses the potential of energy management in water pumping from the mines. The aim of water pumping from the mines is to keep the water level in the mines on a particular level, and there is an inherent choice of timing when the pumps for the water are engaged which is a source of flexibility.

Case study in Strem is focussed on the central heating plant that uses a combination of biogas and wood remains and also besides heat produces electricity. Here the case study focusses on benefits that can be induced on the central heating plant level when there is a possibility to shift heat demand of buildings.

After the performed presented case studies, a strategy for expansion of the 3Smart-based energy management to infrastructures on the city level will be assessed. Also technical implications will be elaborated regarding how the modules of energy management on the side of infrastructure should be structured and organized.

The document is organized as follows. First the three case studies are presented, and then the smart-city upscale strategy elaborated.

2. Zagreb case study

Zagreb case study focuses on the following infrastructures:

- Water distribution system,
- Electrified light city rail,
- Electric vehicles charging infrastructure, and
- Central heat distribution system.

All future plans for previously mentioned infrastructures are here written in accordance to Smart City Strategy of Zagreb which has passed through the public consultation process at the end of 2018. Fundamentals of the Strategy are:

- Connection and co-operation of all city systems and systems of key stakeholders (public administration, private sector, academic community, citizens and others) with the aim of stimulating economic activity and long-term sustainability of the city;
- Analysis of the real needs of key stakeholders, especially citizens, through their active co-operation in city activities, with the aim of improving the quality of life and the satisfaction of stakeholders;
- Collecting and analyzing data related to city services and city activities, with addition of feedback on the collected data, with the aim of proactive and reactive action.

The case study for Zagreb will be performed for the buildings, electricity grid and other selected infrastructure in the neighbourhood of the two pilot buildings, with some assumptions. It will encompass the flexibility that can be obtained from a building and then the mentioned infrastructure elements are analyzed, and their flexibility potential assessed.

2.1 Exemplary building flexibility

The potential for flexibility provision of individual buildings is assessed by computations performed for different typical days of the year via 3Smart model predictive control modules that decide through interaction with long-term grid-side modules what are the maximum amounts of flexibilities the buildings can offer in different time periods in which the grid-side modules have assessed the flexibility need. The exemplary building used is UNIZGFER pilot building.

The grid part in focus is provided in Figure 2.1 – it consists of two radially operated 10 kV feeders of different substations which supply the buildings in the 3Smart pilot for Croatia:

- HEP building is supplied from TS 30/10 kV Vrbik. HEP`s feeder supplies a total of 3 MV/LV substations and 7 customers with connection power over 100 kW, including HEP pilot building
- UNIZGFER building is supplied from TS 110/10 kV Savica. UNIZGFER`s feeder supplies a total of 6 MV/LV substations and 11 customers with connection power over 100 kW, including UNIZGFER pilot building.

Distribution of large consumers throughout the pilot grid is also presented in Figure 2.1.1.

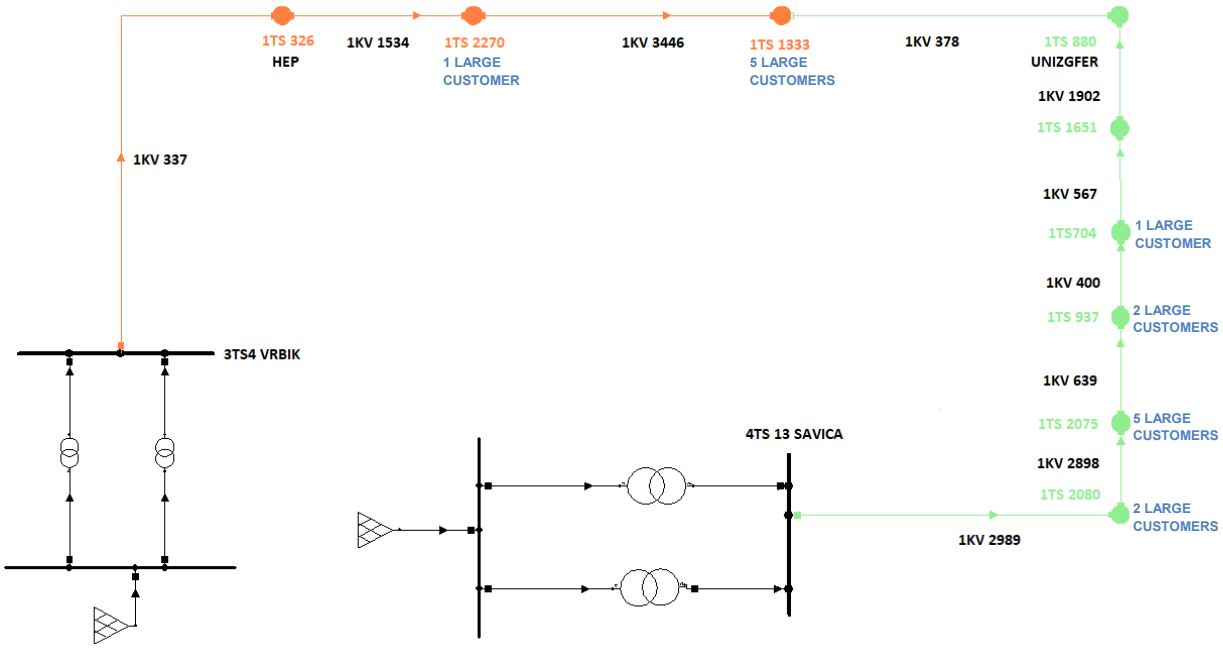

Figure 2.1.1. Croatian pilot grid single line diagram.

Load profiles (15-minute intervals) of customers with connection power equal or greater than 100 kW connected to the pilots` feeders for year 2016 are analysed, as well as customer data (category, connection power, yearly consumption for 2016) for all consumers connected to the pilots` feeders.

As both pilot buildings are located in the city centre with strong and well-developed grid, there are no issues in the network (high voltage drops or high loads) so no major investments are needed. To test the benefits of flexibility, for simulation purposes the threshold network loads are decreased.

UNIZGFER pilot building is analyzed for a typical sunny workday in July. From the grid side the following flexibility intervals are assessed:

- 11:30-11:45
- 13:00-13:30
- 14:30-15:00

The prices determined for flexibility are:

- 0.027 EUR/kW/(15 min) for flexibility reservation
- 0.109 EUR/kWh for flexibility activation
- 0.219 EUR/kWh penalty for non-delivered flexibility within the 90% threshold with respect to the activated flexibility

By activating all three levels of building operation within 3Smart (zone, central HVAC, microgrid), the reservation for flexibility is provided as in Figure 2.1.2.

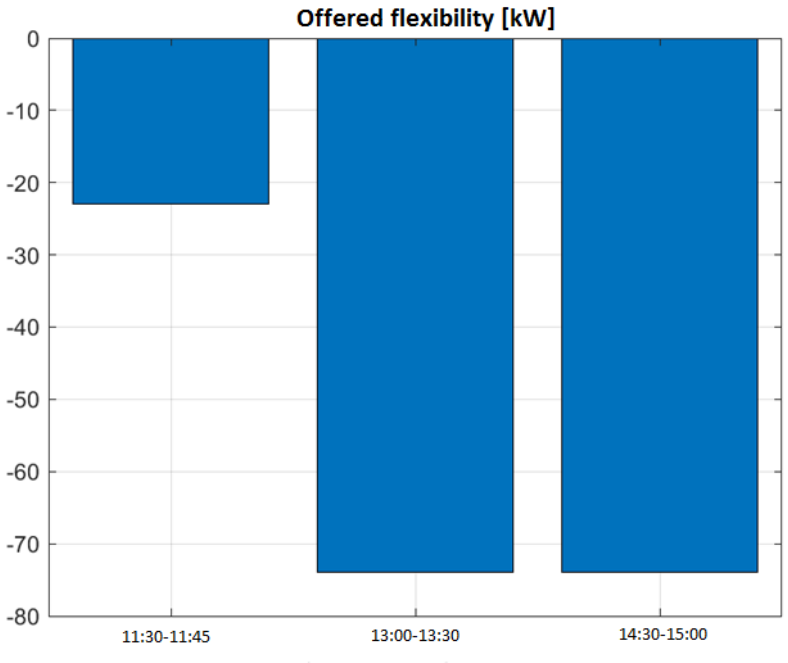

Figure 2.1.2. Offered flexibility powers for the three flexibility intervals.

In Figure 2.1.3 are shown: the planned profile of the building electricity consumption for the situation without 3Smart tool, electricity consumption profile with the 3Smart tool for the case of non-activation of flexibility, and electricity consumption profile with the 3Smart tool for the case when all offered flexibility is engaged by the grid in the maximum amount.

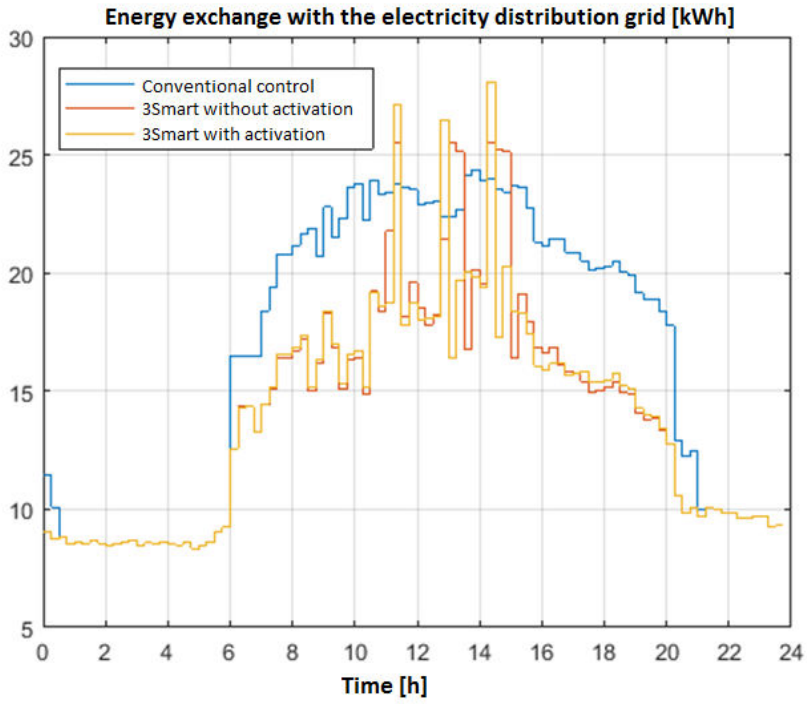

Figure 2.1.3 Planned energy exchange of the building with the electricity distribution grid.

From the responses in the figure one may note that the flexibility can be provided by the building if it is called within the flexibility intervals. Finally, in Figure 2.1.4 one may see the economic performance of the building under 3Smart control which shows that the 3Smart tool brings a significant cost reduction in building operation.

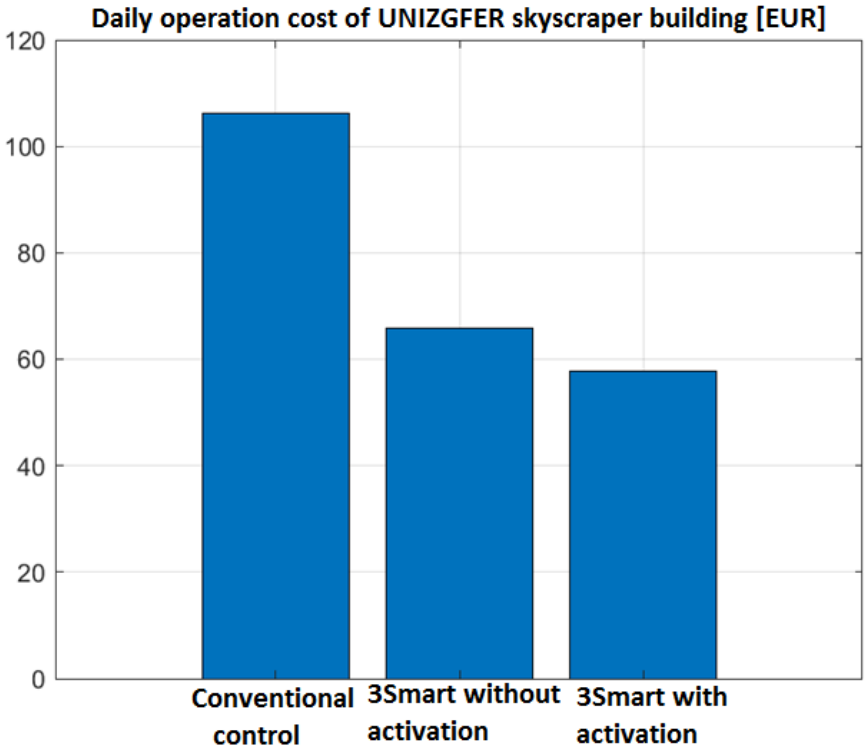

Figure 2.1.4. Daily operation cost of the 3Smart building in July.

2.2 Water distribution system

The considered pilot area is based on the Zagreb's water distribution network pressure zone I which is accounted for roughly 89% of the overall water consumption in the Zagreb city area. Zone I is supplied from water intakes Mala Mlaka, Zaprađe, Sašnjak, Žitnjak, Petruševec and Strmec from which the water is pumped to water reservoirs Jurjevska-Tuškanac, Sokolovac, Bukovac, Laščina, Oporovec, Lisičina and Jačkovina via 4 watermains, as depicted in Figure 2.2.1. The water is then repumped from pressure zone I water reservoirs to pressure zones II and III, which are elevated 80 and 160 meters in relation to pressure zone I, respectively.

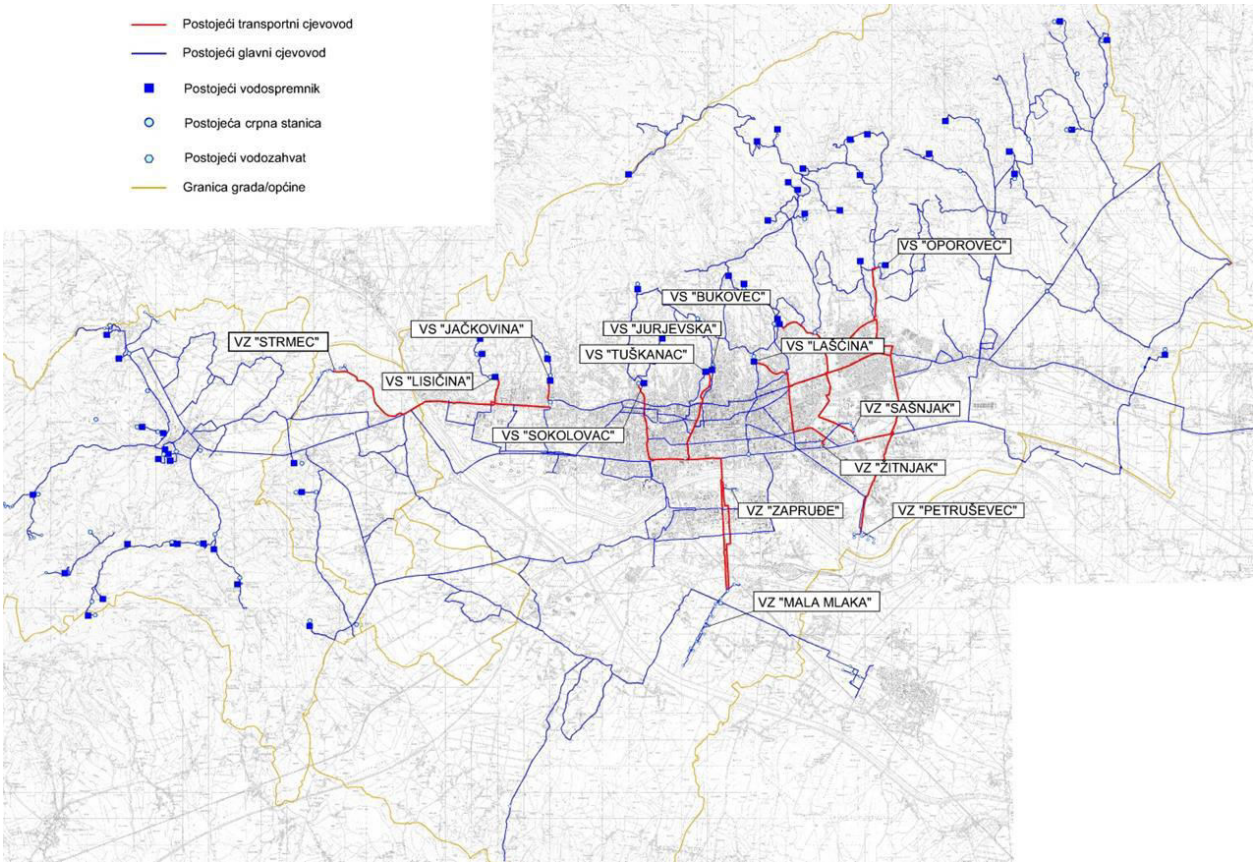

Figure 2.2.1 Water distribution network in Zagreb - watermains, water intakes VZ and water reservoirs VS.

A simplified configuration of a water distribution network is considered for the pilot area with pressure regulation via a water storage filled with a pump, where only one watermain from water intake Mala Mlaka to water reservoir Tuškanac is considered for regulation of the required water pressure in the downscaled distribution network of pressure zone I. Configuration of the considered water distribution network is depicted in Figure 2.2.2**Error! Reference source not found.**, with the corresponding water pump, water reservoir, model of the water distribution network, all with respect to the altitude of different system components. Water intake Mala Mlaka has a nominal water flow of 1500 l/s on its disposal although around 820 l/s are used on average (data measured in the 2011-2014 period). In the downscaled configuration, water pump with 60 l/s nominal water flow is considered. Water reservoir Tuškanac is considered with a possible water column height of 30 m

that ensures the minimal water pressure of 2 bars in all end-points of the distribution network with hydrants. Overall 9 different consumption points are considered in the network model.

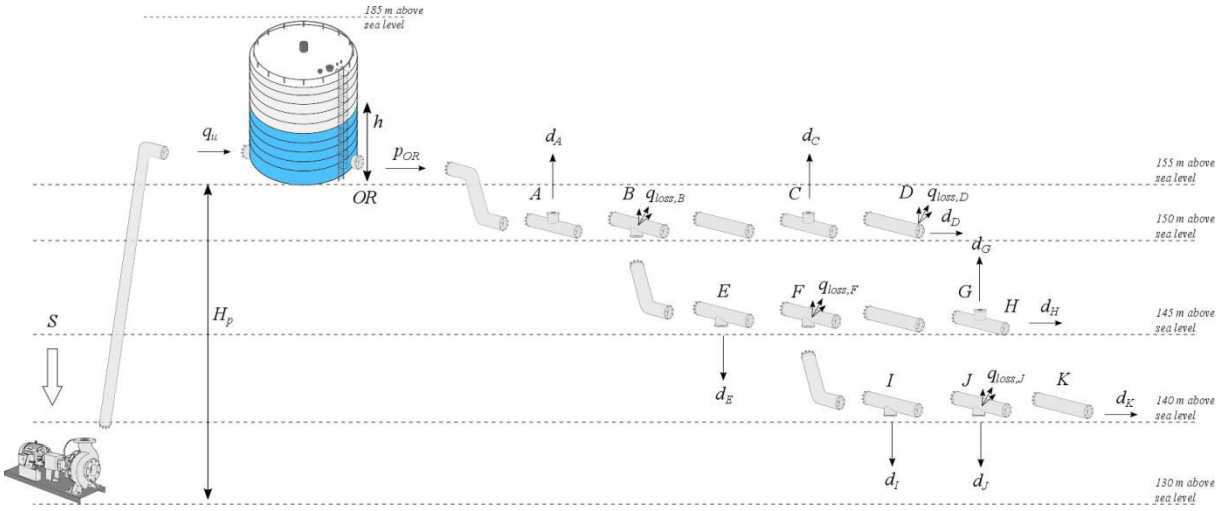

Figure 2.2.2. Water distribution system model based on pressure zone I of the water distribution network in the city of Zagreb.

Some of the piping segments are subject to losses, proportional to the local pressure. It is presumed that the demand in all parts of the network is perfectly predictable (idealized scenario). The goal of the water distribution system is to provide correct pressure according to technical norms in all its supply points, while minimizing the overall costs, where the costs consist of electricity costs and the costs for lost water (the water will be also assigned a monetary value).

Predictive control of water distribution will be performed with also perfectly known models of all the piping segments. Through predictive control, reference water flow values for the pump that fills the water reservoir will be computed. Flows and pressures will be selected as typical ones for water consumption in the test-site area. The consumptions in different considered cummulative supply points will be presumed to be known in advance, in reality they need to be predicted, which is viable.

The connection to electricity distribution grid will be put in focus. Such a management system will offer significant ancillary services due to its flexibility in filling the water reservoir and ensuring proper pressure in the system. The system will function similarly as any other flexible node which is governed by a module analogous to the building microgrid-level module.

2.2.1 System configuration

Configuration of the WDS for the case study is shown in **Error! Reference source not found.**2.2.2. It is a system with a single storage, a pump and the piping branched from the tank outlet. The parameters of the case study system are provided in 0and particularly the parameters related to piping are provided in 0Pipes diameters are determined based on presumed maximum water demands such that the linear velocity of water in the pipes does not exceed 3 m/s and that the pressure drop along pipes allows to attain minimum allowed pressure in all end-points with maximum pressure nowhere exceeding the amount $5P_0$.

TABLE 2.2.1 PARAMETERS USED IN THE WDS CASE STUDY

Parameter	Description	Value
ν	Kinematic coefficient of water viscosity (at 15°C)	$1.15 \cdot 10^{-6}$ m^2/s
ρ	Density of water	1000 kg/m^3
g	Gravity acceleration	9.81 m/s^2
A_{leak}	Area of leak surfaces on pipes	10^{-5} m^2
P_0	Atmospheric pressure	101325 Pa
A	Area of the tank cross section surface	10 m^2
$Q_{u,max}$	Maximum flow of the pump	$2.78 \cdot 10^{-2}$ m^3/s (100 m^3/h)
P_{min}	Minimum allowed pressure at end-points	$2P_0$=202650 Pa
H_{max}	Tank height from bottom to top	30 m
η	Pump efficiency	0.85
H_p	Elevation of the tank bottom above the pump	25 m
D_{max}	Maximum demand at different piping supply points	$2.78 \cdot 10^{-3}$ m^3/s (10 m^3/h)

The WDS serves the demands in the following 9 points: A, C, D, E, G, H, I, J, K. These demands are referred to as d_A, d_C, d_D, d_E, d_G, d_H, d_I, d_J, d_K, respectively. Flows through different pipes are denoted with endpoints of particular pipes in subscript, i.e. they are denoted as follows: q_{OR_A}, q_{A_B}, q_{B_C}, q_{C_D}, q_{B_E}, q_{E_F}, q_{F_G}, q_{G_H}, q_{F_I}, q_{I_J}, q_{J_K}. The leaks are assumed to occur in points B, D, F and J and are denoted with $q_{loss,B}$, $q_{loss,D}$, $q_{loss,F}$ and $q_{loss,J}$, respectively.

TABLE 2.2.2 WATER DISTRIBUTION SYSTEM PIPING PARAMETERS

Parameter	Description	Value
d_{OR_A}	Pipe diameter from output of the reservoir (OR) to point A	0.125 m
d_{A_B}	Pipe diameter from A to B	0.125 m
d_{B_C}	Pipe diameter from B to C	0.1 m
d_{C_D}	Pipe diameter from C to D	0.1 m
d_{B_E}	Pipe diameter from B to E	0.125 m
d_{E_F}	Pipe diameter from E to F	0.125 m
d_{F_G}	Pipe diameter from F to G	0.1 m
d_{G_H}	Pipe diameter from G to H	0.065 m
d_{F_I}	Pipe diameter from F to I	0.1 m
d_{I_J}	Pipe diameter from I to J	0.1 m
d_{J_K}	Pipe diameter from J to K	0.065 m
l_{OR_A}	Pipe length from OR to A	100 m
l_{A_B}	Pipe length from A to B	100 m
l_{B_C}	Pipe length from B to C	300 m
l_{C_D}	Pipe length from C to D	200 m
l_{B_E}	Pipe length from B to E	300 m
l_{E_F}	Pipe length from E to F	300 m

Parameter	Description	Value
l_{F_G}	Pipe length from F to G	300 m
l_{G_H}	Pipe length from G to H	200 m
l_{F_I}	Pipe length from F to I	300 m
l_{I_J}	Pipe length from I to J	200 m
l_{J_K}	Pipe length from J to K	200 m
Δh_{OR_A}	Height difference between OR and A	5 m
Δh_{A_B}	Height difference between A and B	0 m
Δh_{B_C}	Height difference between B and C	0 m
Δh_{C_D}	Height difference between C and D	0 m
Δh_{B_E}	Height difference between B and E	5 m
Δh_{E_F}	Height difference between E and F	0 m
Δh_{F_G}	Height difference between F and G	0 m
Δh_{G_H}	Height difference between G and H	0 m
Δh_{F_I}	Height difference between F and I	5 m
Δh_{I_J}	Height difference between I and J	0 m
Δh_{J_K}	Height difference between J and K	0 m
ε	Pipe roughness	0 m

2.2.2 Water distribution system model

The WDS dynamic model resides on the water mass balance equation in the tank:

$$\frac{\mathrm{d}h}{\mathrm{d}t} = \frac{1}{A}\left(q_{\mathrm{u}} - q_{\mathrm{OR\_A}}\right), \qquad (1)$$

where t [s] denotes time, h [m] is the height of water in the tank and q_{u} [m^3/s] is the input flow from the pump into the tank. Relation between pressures on end-points X and Y of a certain pipe with fluid flowing from point X to point Y is

$$p_{\mathrm{Y}} = p_{\mathrm{X}} + \rho g \Delta h_{\mathrm{X\_Y}} - \alpha \frac{l_{\mathrm{X\_Y}}}{d_{\mathrm{X\_Y}}^{4.75}} \cdot q_{\mathrm{X\_Y}}^{1.75}, \qquad (2)$$

where Δh_{X_Y} is the difference in elevation between points X and Y and α [Pa·$s^{1.75}$/$m^{0.5}$] is calculated as

$$\alpha = 0.241434 \rho \sqrt[4]{\nu}. \qquad (3)$$

We assume that the tank is open such that the water top in the tank is at the pressure P_0. Thus the pressure at point OR (output of the tank) is

$$p_{OR} = P_0 + \rho g h. \qquad (4)$$

The leakage flow at certain point X is modelled as

$$q_{\mathrm{loss,X}} = A_{\mathrm{leak}} \sqrt{\frac{2}{\rho}\left(p_{\mathrm{X}} - P_0\right)}. \qquad (5)$$

The flow through a certain pipe is equal to sum of all demands and leaks downstream the pipe, e.g.

$$q_{\mathrm{OR\_A}} = d_{\mathrm{A}} + d_{\mathrm{C}} + d_{\mathrm{D}} + d_{\mathrm{E}} + d_{\mathrm{G}} + d_{\mathrm{H}} + d_{\mathrm{I}} + d_{\mathrm{J}} + \\ + d_{\mathrm{K}} + q_{\mathrm{loss,B}} + q_{\mathrm{loss,D}} + q_{\mathrm{loss,F}} + q_{\mathrm{loss,J}}, \qquad (6)$$
$$q_{\mathrm{E\_F}} = d_{\mathrm{G}} + d_{\mathrm{H}} + d_{\mathrm{I}} + d_{\mathrm{J}} + d_{\mathrm{K}} + q_{\mathrm{loss,F}} + q_{\mathrm{loss,J}}.$$

Assuming that the pressure in water entering the pump is P_0, the electrical power of the pump S [W] is calculated as

$$S = \frac{1}{\eta}\rho g\left(H_p + h\right)q_{\mathrm{u}}. \qquad (7)$$

The pump is driven via variable frequency drive such that the flow can be continuously set from 0 to $Q_{\mathrm{u,max}}$. Model of the pump is simplified and it is assumed that the pump system can provide the maximum flow for any water height in the tank up to H_{max}.

2.2.3 Optimal Control Problem Formulation and Solution

Nonlinear optimal control problem

The operation cost of the WDS in a certain period of time corresponds to the sum of costs for the spent electrical energy on the pump and for the volume of lost water through leaks during that period. The goal in operation of the WDS is to satisfy all demands with sufficient pressure in all end-points, while keeping the operation cost at minimum. The methodology of optimal control is employed to compute the optimal profile of the input flow q_{u} for a certain prediction horizon as well as to decide on the optimal starting water height in the tank.

The computation of optimal controls is performed on a control computer which considers states of the system in a finite number of time instants influenced with a finite number of control inputs and requires a finite time for re-computation of the optimal control sequence in a receding horizon fashion when switching from planning to operation. The system is thus discretized with sampling time T, and the input flow q_{u} is maintained constant within each time step $[kT,(k+1)T)$,

$$q_{\mathrm{u}}\left(t\right) = q_{\mathrm{u},k} \quad \forall \mathrm{t} \in I_k = \left[kT,\left(k+1\right)T\right), \ \ k \in \mathrm{Z}, \qquad (8)$$

where Z is the set of integers. The cost function for the control problem is defined as follows:

$$J = \sum_{k=0}^{N-1} p_{e,k}E_k + p_w W_k, \qquad (9)$$

where $p_{\mathrm{e},k}$ [EUR/kWh] is the price of electricity in time interval I_k, p_{w} [EUR/m^3] is the price of water, NT is the prediction horizon, E_k [kWh] is the electrical energy spent on the pump in time interval I_k, i.e.

$$E_k = \frac{1}{1000 \cdot 3600}\int_{kT}^{(k+1)T} S\left(t\right)\mathrm{d}t, \qquad (10)$$

while W_k [m^3] is the volume of lost water in I_k, i.e.

$$W_k = \int_{kT}^{(k+1)T}\left(q_{\mathrm{loss,B}}\left(t\right) + q_{\mathrm{loss,D}}\left(t\right) + q_{\mathrm{loss,F}}\left(t\right) + q_{\mathrm{loss,J}}\left(t\right)\right)\mathrm{d}t \ . \qquad (11)$$

The lowest pressures in the WDS occur at end-points as long as there is no up-hill water path after the tank output. Since there are none such paths in the WDS considered, it is enough to pose pressure constraints at the end-points D, H and K. Although pressure constraints will be only posed at the discrete-time instants kT, the aperiodic behaviour of the system under constant input flow q_{u}, within the time interval will assure that the constraints are maintained throughout the prediction horizon. The posed pressure constraints are:

$$\begin{aligned} p_{\mathrm{D},k} &\geq P_{\min}, \quad k=0,\ldots,\mathrm{N}, \\ p_{\mathrm{H},k} &\geq P_{\min}, \quad k=0,\ldots,\mathrm{N}, \\ p_{\mathrm{K},k} &\geq P_{\min}, \quad k=0,\ldots,\mathrm{N}, \end{aligned} \tag{12}$$

where $p_{\mathrm{X},k}=p_{\mathrm{X}}(kT)$. Similarly the constraints are posed also for the water heights in the tank along the prediction horizon:

$$0 \leq h_k \leq H_{\max}, \quad k=0,\ldots,\mathrm{N}, \tag{13}$$

where $h_k=h(kT)$. Constraints are also posed for the input flow from the pump:

$$0 \leq q_{\mathrm{u},k} \leq Q_{\mathrm{u,max}}, \quad k=0,1,\ldots,N\text{-}1. \tag{14}$$

Finally, the periodicity constraint is imposed such that the water height at the end of the prediction horizon is equal to the height at the beginning:

$$h_0 = h_N. \tag{15}$$

The nonlinear optimization problem can be now posed as follows:

$$\begin{aligned} &\min_{h_0, q_{\mathrm{u},0}, q_{\mathrm{u},1}, \ldots, q_{\mathrm{u},N-1}} J \\ &\text{subject to (12)-(15).} \end{aligned} \tag{16}$$

Note that the optimization problem (16) addresses not just the pumping sequence, but also the optimal starting height of the water in the tank since it is focussed on WDS daily operation planning. The sampling time T is selected to be T=15 min in order to correspond to the presumed period of change of the electricity prices, and the prediction horizon is selected to be 1 day long, i.e. N=96. In this way one can for predicted demand sequences in the WDS supply points determine the optimal behaviour of the WDS. Here focus is not on techniques for water demand prediction and it is assumed that these prediction sequences can be obtained based on historical data for different day types and predicted weather conditions.

Due to the nonlinearity of the WDS model, the problem (16) cannot be easily solved. The WDS model thus needs to be linearized and then the problem (16) replaced with an approximate problem based on linearization performed. With such problem it will be possible to decide on the direction of change of the optimization variables and finally to reach the optimum through iterations.

Linearization of the water distribution system model

For a fixed water height H_0, input flow Q_{u0} and demands D_{A0}, D_{C0}, D_{D0}, D_{E0}, D_{G0}, D_{H0}, D_{I0}, D_{J0}, D_{K0} the linearization of the model is performed in order to approximate the behaviour of pressures, flows and leaks in the WDS for small changes in water height or input flow.

First all pressures, flows and leaks need to be determined for given height and demands. This is done by numerically solving the system of equations (2) with insertions from (3) to (6) which gives 11 equations for pressures in different points of the WDS with 11 unknowns being these pressures, i.e. P_{A0}, P_{B0}, P_{C0}, P_{D0}, P_{E0}, P_{F0}, P_{G0}, P_{H0}, P_{I0}, P_{J0}, P_{K0}. After they are determined, the losses and flows are determined by applying relations (5) and (6), consecutively. Recall that (6) contains only two exemplary relations, while actually there are 11 different relations for flows. The determined losses are: $Q_{\mathrm{loss,B,0}}$, $Q_{\mathrm{loss,D,0}}$, $Q_{\mathrm{loss,F,0}}$, $Q_{\mathrm{loss,J,0}}$. The determined flows are: $Q_{\mathrm{OR\_A,0}}$, $Q_{\mathrm{A\_B,0}}$, $Q_{\mathrm{B\_C,0}}$, $Q_{\mathrm{C\_D,0}}$, $Q_{\mathrm{B\_E,0}}$, $Q_{\mathrm{E\_F,0}}$, $Q_{\mathrm{F\_G,0}}$, $Q_{\mathrm{G\_H,0}}$, $Q_{\mathrm{F\_I,0}}$, $Q_{\mathrm{I\_J,0}}$, $Q_{\mathrm{J\_K,0}}$. The procedure for determining the pressures, losses and flows in the operating point (OP) we will denote shortly with:

$$\left[P_{X,0}, Q_{\mathrm{loss,X,0}}, Q_{\mathrm{X\_Y,0}}\right] = OP\left(H_0, D_{\mathrm{X,0}}\right). \tag{17}$$

The linearization of the considered WDS is performed further as follows. For the water height h, each pressure p_{X}, loss $q_{\mathrm{loss,X}}$ and flow $q_{\mathrm{X\_Y}}$ one can write the following:

$$\begin{aligned} h &= H_0 + \Delta h \\ p_{\mathrm{X}} &= P_{\mathrm{X},0} + \Delta p_{\mathrm{X}}, \\ q_{\mathrm{X\_Y}} &= Q_{\mathrm{X\_Y},0} + \Delta q_{\mathrm{X\_Y}}, \\ q_{\mathrm{loss,X}} &= Q_{\mathrm{loss,X},0} + \Delta q_{\mathrm{loss,X}}, \end{aligned} \qquad (18)$$

where Δh, Δp_{X}, $\Delta q_{\mathrm{X\_Y}}$ and $\Delta q_{\mathrm{loss,X}}$ are small changes around the operating point. By inserting (18) into (2), (4), (5) and (6) and by approximating all the nonlinear mappings with a first-order Taylor polynomial, the following linear relations are obtained for the small changes:

$$\begin{aligned} \Delta p_{\mathrm{X}} &= K_{\mathrm{X}} \Delta h, \\ \Delta q_{\mathrm{loss,X}} &= K_{\mathrm{loss,X}} \Delta h, \\ \Delta q_{\mathrm{OR\_A}} &= K_h \Delta h, \end{aligned} \qquad (19)$$

where K_{X}, $K_{\mathrm{loss,X}}$ and K_{h} are the computed linearization coefficients.

For a fixed sequence of flows $q_{\mathrm{u},k}=Q_{\mathrm{u},k,0}$ and predicted demands $d_{\mathrm{X},k}$ along the prediction horizon, i.e. k=0,...,N-1, and for initial water height in the tank $H_{0,0}$, first a sequence of heights $H_{\mathrm{k},0}$ is obtained by performing simulation of the nonlinear model via some numerical integration procedure. For each of the operating points defined with $H_{k,0}$ and $D_{\mathrm{X},k}$ the pressures, flows and losses are computed by following (17). After that linearization is performed with introduced changes of input flow and height

$$\begin{aligned} q_{u,k} &= Q_{u,k,0} + \Delta q_{u,k}, \\ h_k &= H_{k,0} + \Delta h_k, \end{aligned} \qquad (20)$$

such that finally linearization coefficients $K_{\mathrm{X},k}$, $K_{\mathrm{loss,X},k}$ and $K_{\mathrm{h},k}$ can be computed. With computed coefficients $K_{\mathrm{h},k}$ also a sequence of linear dynamical WDS models along the prediction horizon adhering to the following difference equation can be found:

$$\frac{\mathrm{d}\Delta h(t)}{\mathrm{d}t} = \frac{1}{A}\left(\Delta q_{\mathrm{u},k} - K_{\mathrm{h},k}\Delta h(t)\right),\ t \in I_k\,. \qquad (21)$$

For each time interval I_k, k=0,...,N-1, the following relation for water height h is obtained:

$$\begin{aligned} h(t) = H_{k,0} &+ \Delta h_k e^{-\frac{K_{\mathrm{h},k}}{A}(t-kT)} + \\ &+ \left(\frac{1}{K_{\mathrm{h},k}}\Delta q_{\mathrm{u},k} + \beta_k\right)\left(1 - e^{-\frac{K_{\mathrm{h},k}}{A}(t-kT)}\right),\ t \in I_k, \end{aligned} \qquad (22)$$

where $\beta_k = \dfrac{H_{k+1} - H_k}{1 - e^{-\frac{K_{h,k}}{A}T}}$. The following discrete relation holds for the small changes of height at sampling instants:

$$\begin{aligned} \Delta h_{k+1} &= \Phi_k \Delta h_k + \Gamma_k \Delta q_{\mathrm{u},k}, \\ \Phi_k &= e^{-\frac{K_{\mathrm{h},k}}{A}T},\ \Gamma_k = \frac{1}{K_{\mathrm{h},k}}\left(1 - e^{-\frac{K_{\mathrm{h},k}}{A}T}\right). \end{aligned} \qquad (23)$$

By introducing

$$\begin{aligned} \Delta\mathbf{h} &= \begin{bmatrix} \Delta h_0 & \Delta h_1 & \cdots & \Delta h_N \end{bmatrix}^{\mathrm{T}}, \\ \Delta\mathbf{q}_u &= \begin{bmatrix} \Delta q_{\mathrm{u},0} & \Delta q_{\mathrm{u},1} & \cdots & \Delta q_{\mathrm{u},N-1} \end{bmatrix}^{\mathrm{T}}, \end{aligned} \qquad (24)$$

the following can be written based on (23):

$$\Delta\mathbf{h} = \mathbf{A}\cdot\Delta h_0 + \mathbf{B}\cdot\Delta\mathbf{q}_u\,, \qquad (25)$$

$$\mathbf{A}=\begin{bmatrix}1\\ \Phi_0\\ \Phi_0\Phi_1\\ \vdots\\ \prod_{i=0}^{N-1}\Phi_i\end{bmatrix},\quad \mathbf{B}=\begin{bmatrix}0 & 0 & 0 & \cdots & 0\\ \Gamma_0 & 0 & 0 & \cdots & 0\\ \Phi_1\Gamma_0 & \Gamma_1 & 0 & \cdots & 0\\ \vdots & \vdots & \vdots & \cdots & \vdots\\ \left(\prod_{i=1}^{N-1}\Phi_i\right)\Gamma_0 & \left(\prod_{i=2}^{N-1}\Phi_i\right)\Gamma_1 & \left(\prod_{i=3}^{N-1}\Phi_i\right)\Gamma_2 & \cdots & \Gamma_{N-1}\end{bmatrix}.$$

By employing (22) and (25) in (7), (10) and (11) one can now also obtain the expressions for E_k and W_k needed for the criterion of the cost function of the optimal control problem, now expressed through Δh_0 and $\Delta\mathbf{q}_u$. These are as follows:

$$\begin{aligned}E_k &= \frac{1}{2}\begin{bmatrix}\Delta h_0 & \Delta\mathbf{q}_u^{\mathrm{T}}\end{bmatrix}\mathbf{A}_{\mathrm{E},k}\begin{bmatrix}\Delta h_0 & \Delta\mathbf{q}_u^{\mathrm{T}}\end{bmatrix}^{\mathrm{T}}+\mathbf{B}_{\mathrm{E},k}\begin{bmatrix}\Delta h_0 & \Delta\mathbf{q}_u^{\mathrm{T}}\end{bmatrix}^{\mathrm{T}}+c_{\mathrm{E},k},\\ W_k &= \mathbf{B}_{\mathrm{loss},k}\begin{bmatrix}\Delta h_0 & \Delta\mathbf{q}_u^{\mathrm{T}}\end{bmatrix}^{\mathrm{T}}+c_{\mathrm{loss},k},\end{aligned}\quad (26)$$

where $\mathbf{A}_{\mathrm{E},k}\in R^{(N+1)\times(N+1)}$, $\mathbf{B}_{\mathrm{E},k}\in R^{1\times(N+1)}$, $c_{\mathrm{E},k}\in R$, $\mathbf{B}_{\mathrm{loss},k}\in R^{1\times(N+1)}$, $c_{\mathrm{loss},k}\in R$, $k=0,1,...,N-1$, are properly constructed. The overall cost J for the linearized WDS can now be expressed as

$$J=\frac{1}{2}\begin{bmatrix}\Delta h_0 & \Delta\mathbf{q}_u^{\mathrm{T}}\end{bmatrix}\mathbf{H}\begin{bmatrix}\Delta h_0 & \Delta\mathbf{q}_u^{\mathrm{T}}\end{bmatrix}^{\mathrm{T}}+\mathbf{F}\begin{bmatrix}\Delta h_0 & \Delta\mathbf{q}_u^{\mathrm{T}}\end{bmatrix}^{\mathrm{T}}+c,\quad (27)$$

where $\mathbf{H}=\sum_{k=0}^{N-1}p_{\mathrm{e},k}\mathbf{A}_{\mathrm{E},k}$, $\mathbf{F}=\sum_{k=0}^{N-1}p_{\mathrm{e},k}\mathbf{B}_{\mathrm{E},k}+p_{\mathrm{w}}\mathbf{B}_{\mathrm{loss},k}$, $c=\sum_{k=0}^{N-1}p_{\mathrm{e},k}c_{\mathrm{E},k}+p_{\mathrm{w}}c_{\mathrm{loss},k}$.

Constraints for the problem (12)-(15) can now also be expressed by employing (25), e.g.

$$\begin{aligned}p_{H,k} &= P_{H,0,k}+\Delta p_{H,k}=P_{H,0,k}+K_{H,k}\Delta h_k=\\ &= P_{H,0,k}+K_{H,k}\left(\mathbf{A}_{(k+1,:)}\cdot\Delta h_0+\mathbf{B}_{(k+1,:)}\cdot\Delta\mathbf{q}_u\right)\geq P_{\min},\end{aligned}\quad (28)$$

where $\mathbf{M}_{(i,:)}$ denotes the ith row of matrix $\mathbf{M}$. Besides constraints (12)-(15), also additional constraints need to be introduced to keep the assumptions of the linearization fulfilled, i.e. to keep Δh_0 and $\Delta q_{\mathrm{u},k}$ sufficiently small.

Finally, all constraints stacked together can for the linearized WDS be expressed as

$$\begin{aligned}\mathbf{A}_{\mathrm{ineq}}\begin{bmatrix}\Delta h_0 & \Delta\mathbf{q}_u^{\mathrm{T}}\end{bmatrix}^{\mathrm{T}}&\leq\mathbf{b}_{\mathrm{ineq}},\\ \mathbf{A}_{\mathrm{eq}}\begin{bmatrix}\Delta h_0 & \Delta\mathbf{q}_u^{\mathrm{T}}\end{bmatrix}^{\mathrm{T}}&=\mathbf{b}_{\mathrm{eq}}.\end{aligned}\quad (29)$$

Relations (27) and (29) define a mathematical programme. Usually **H** due to the change of the dynamics along the prediction horizon is not positive semidefinite which then requires further to approximate J for small changes Δh_0 and $\Delta\mathbf{q}_u$ with

$$J=\mathbf{F}\begin{bmatrix}\Delta h_0 & \Delta\mathbf{q}_u^{\mathrm{T}}\end{bmatrix}^{\mathrm{T}}+c,\quad (30)$$

finally coming to a Linear Programme (LP) formulation of the WDS perturbation problem with (29) and (30).

Once the LP (29)-(30) is solved, the optimal solution denoted with $\begin{bmatrix}\Delta h_0^* & \Delta\mathbf{q}_u^{*\mathrm{T}}\end{bmatrix}^{\mathrm{T}}$ is added to the input flow sequence and the initial height to get their values for the new iteration of optimization:

$$\begin{bmatrix}H_{0,0}\\ \mathbf{Q}_{u,0}\end{bmatrix}_{iter+1}=\begin{bmatrix}H_{0,0}\\ \mathbf{Q}_{u,0}\end{bmatrix}_{iter}+\begin{bmatrix}\Delta h_0^* & \Delta\mathbf{q}_u^{*\mathrm{T}}\end{bmatrix}^{\mathrm{T}}.\quad (31)$$

The iterative procedure of optimization involving Sequential Linear Programming (SLP) is stopped if the criterion J is decreased for less than the tolerance value or the norm of the optimal solution $\left[\Delta h_0^* \quad \Delta \mathbf{q}_u^{*\mathrm{T}}\right]^{\mathrm{T}}$ is close to zero.

2.2.4 Case Study Results and Analysis

The derived optimal control methodology is applied to the WDS case study. The predicted demand profiles for the considered 9 supply points are provided in 0Figure 2.2.3.

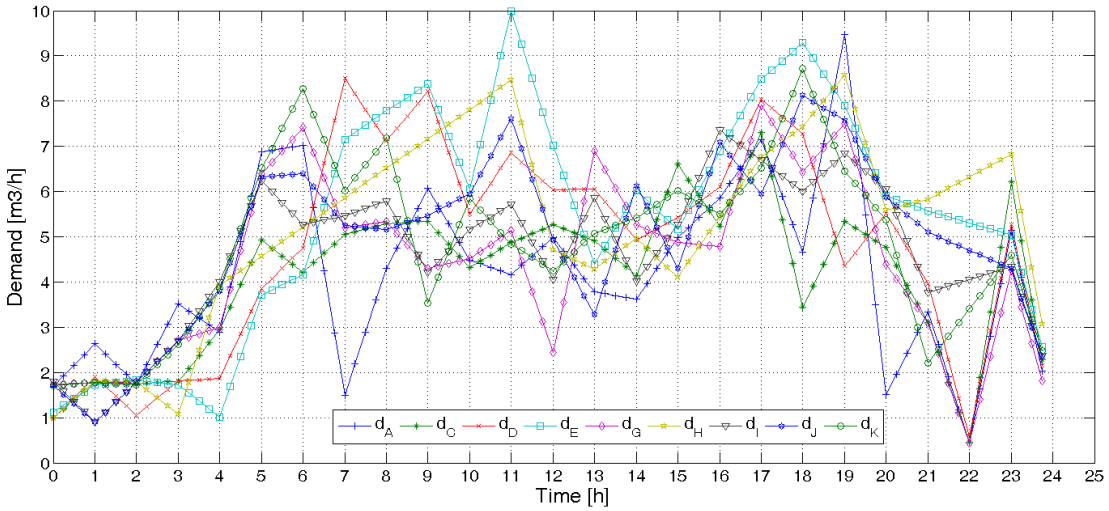

Figure 2.2.3. Predicted demands for the 9 supply points of the considered WDS.

The electricity price profile is shown in Figure 2.2.4. Water price is set at 2 EUR/m^3 throughout the day.

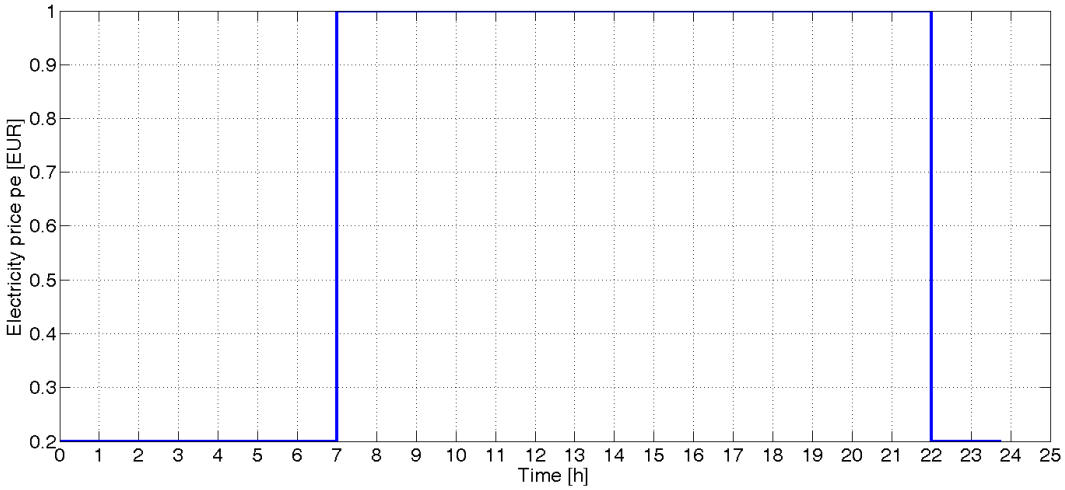

Figure 2.2.4. Electricity price profile.

The optimization of the WDS behaviour is regarding $(\mathbf{Q}_{u,0})_{iter=1}$ started from a random input flow profile uniformly sampled between 0 and $Q_{u,max}$, and it is shown in 0 with the thin line. The initial height $(H_{0,0})_{iter=1}$ was set at 10 m.

The finally obtained optimal input flow profile after the application of the SLP procedure described in Section 2.2.3 is shown in 02.2.5 with the thick line.

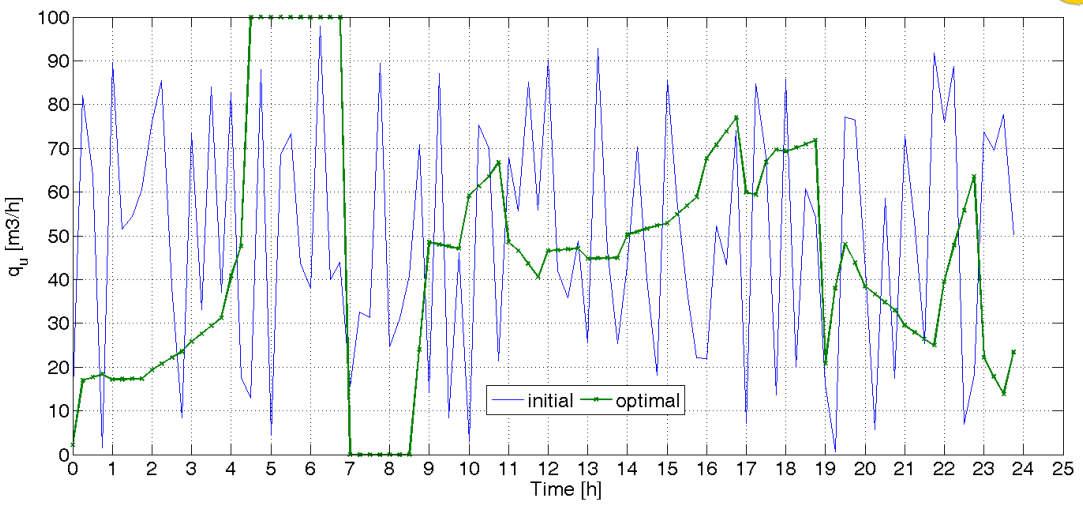

Figure 2.2.5. The initial and computed optimal input flow q_u.

The behaviour of the water height profile *h* through iterations is shown in Figure 2.2.6. The height profile related to the initial random flow $(\mathbf{Q}_{u,0})_{iter=1}$ is denoted in the figure and also the final optimal water height profile. One may notice that the initial height has lowered from 10 m to somewhat less than 6 m at the optimum. The optimization procedure also takes care that the initial height corresponds to the final height which makes it possible to use this behaviour repeatedly, i.e. the optimization does not use the initial water height for a single-day economics. One may see the shaped behaviour of the WDS which exploits the variability of electricity prices to fill the tank during the period of low electricity price. The tank is however not filled to the full (H_{max}=30 m) since in that case the cost for lost water would prevail over the gains in electricity cost.

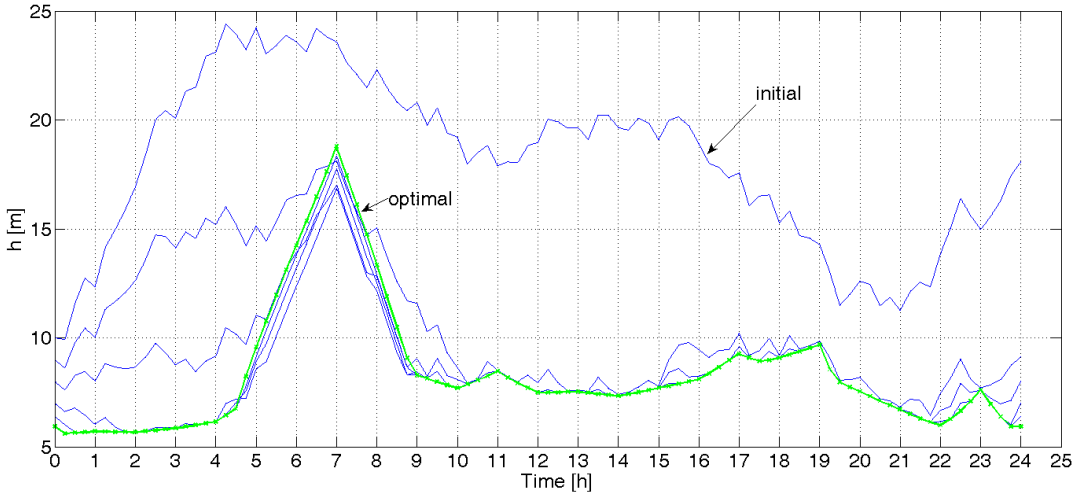

Figure 2.2.6. The initial profile of height h, h profiles through iterations and the optimal h profile.

The behaviour of pressures in end-points of the considered WDS for the optimal solution is shown in Figure 2.2.7. One may notice that the pressure constraints for ensuring quality supply are fulfilled all the time.

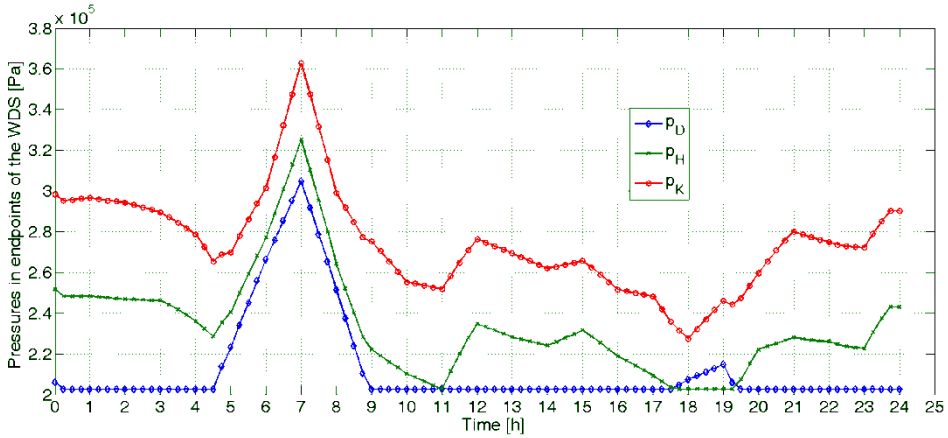

Figure 2.2.7. Optimal profiles of pressure in WDS end-points.

The electricity consumption profile for the optimal behaviour of the WDS is shown in Figure 2.2.8.

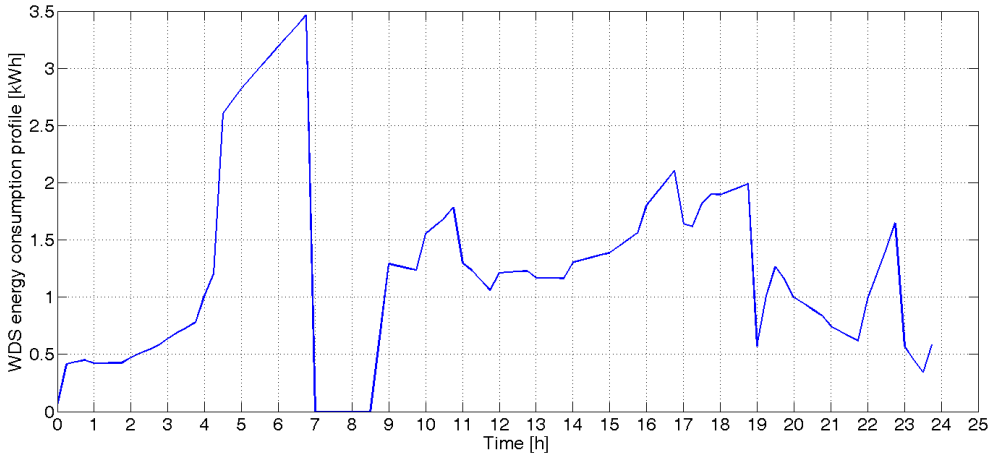

Figure 2.2.8. Optimal electrical energy consumption. The points in the graph at time kT correspond to Ek from (10), i.e. represent 15-minute energy consumption from kT to (k+1)T.

Finally Figure 2.2.9 shows the change of the total cost of WDS operation within the 24-hours period through iterations, starting from the initial random flow and 10 m initial height to the optimized behaviour. The maximum allowed changes in h_0 and $q_{u,k}$ between iterations were set at 1 m and $0.2Q_{u,max}$, respectively. The optimization procedure ended within 10 iterations due to a negligible change of the optimizer or cost at the final iteration according to the stopping criterion – the threshold was set to 10^{-8} for either the norm of the optimizer change or the cost change.

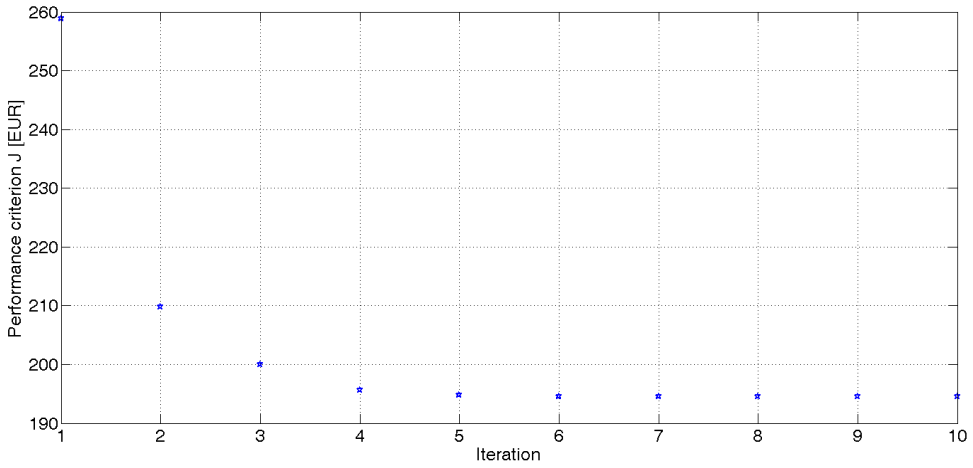

Figure 2.2.9. Total cost of daily operation of the WDS through iterations of the optimization procedure.

2.2.5 Flexibility provision study

Possibility of flexibility provision by the water distribution system is analyzed in a simplistic way for the purpose of this case study. The flexibility provision is considered for the same conditions as for the building, i.e. as follows.

From the grid side the following flexibility intervals are assessed:

- 11:30-11:45
- 13:00-13:30
- 14:30-15:00

The prices determined for flexibility are:

- 0.027 EUR/kW/(15 min) for flexibility reservation
- 0.109 EUR/kWh for flexibility activation
- 0.219 EUR/kWh penalty for non-delivered flexibility within the 90% threshold with respect to the activated flexibility

The day-ahead electricity price is constant and set to 0.016 EUR/kWh. The water loss cost of 2 EUR/m^3 is dominant in the overall operation of the WDS, which needs to be respected also when flexibility is provided.

Simplified analysis is performed in a way that the optimization is performed with disregarding flexibility provision in order to compute the optimal overall cost of the water distribution system operation. Then the optimization was performed with enforced all input flows in the flexibility intervals equal to the maximum value – in this way the declared consumption profile of the WDS for the case of flexibility provision is assessed. Finally, the optimization was performed with enforced all input flows in the flexibility intervals to be zero. When flexibility is activated, in the electricity cost also the cost for deviation from the declared energy consumption is accounted (deviation is priced with 20% higher prices than day-ahead prices).

Possible flexibilities of the water distribution system obtained in this way in the three grid flexibility intervals are as follows:

- for 11:30-11:45 : -10.75 kW
- for 13:00-13:30 : -11.06 kW
- for 14:30-15:00 : -11.04 kW

The results of the three optimizations are summarized in the following table.

TABLE 2.2.3. ECONOMICAL ANALYSIS OF DAILY OPERATION OF THE CONSIDERED WDS WITH FLEXIBILITY PROVISION

	1: Operation without flexibility provision	2: Operation with reserved flexibility, but not called	3: Operation with reserved flexibility called in the entire amount
A: Optimized daily water loss cost [EUR]	110.41	110.97	110.88
B: Optimized electricity consumption cost (including deviation from the declared amount) [EUR]	1.83	1.84	2.36
C: Daily gain for flexibility reservation [EUR]	-	1.48	1.48
D: Daily gain for flexibility activation when called in the entire amount [EUR]	-	-	1.50
E: Overall daily electricity cost (B-C-D) [EUR]	1.83	0.36	-0.62
F: Overall daily cost of the WDS operation (A+B-C-D) [EUR]	112.24	111.33	110.26
Daily gain when flexibility is not called (F1-F2) [EUR]		0.91	
Daily gain when flexibility is called in full amount (F1-F3) [EUR]		1.98	

From the table it follows that it pays off to the water distribution system to participate in the flexibility provision scheme: if flexibility is not called per day it has a reduced overall cost of operation by 0.91 EUR; if flexibility is called (activated) by the grid in full amount the WDS has a reduction of daily operation costs by 1.98 EUR. Considering that the overall daily electricity cost is on the level 1.8-2.3 EUR, the decrease induced by flexibility provision is very significant and it even reverses the money flow between the WDS and the electricity provider when flexibility provision service is activated. The water loss cost, which is in the example above the dominant cost, is taken into account and the flexibility provision does not change the water loss significantly.

The optimized daily electricity consumption profiles in the performed analysis are shown in Figure 2.2.10. The optimal operation without flexibility provision is denoted with 'Optimal' in the graph, the operation of the system when flexibility is not called is represented with 'Declared' in the graph, and the operation of the system when flexibility is called in maximum amount is represented with 'Alternative'.

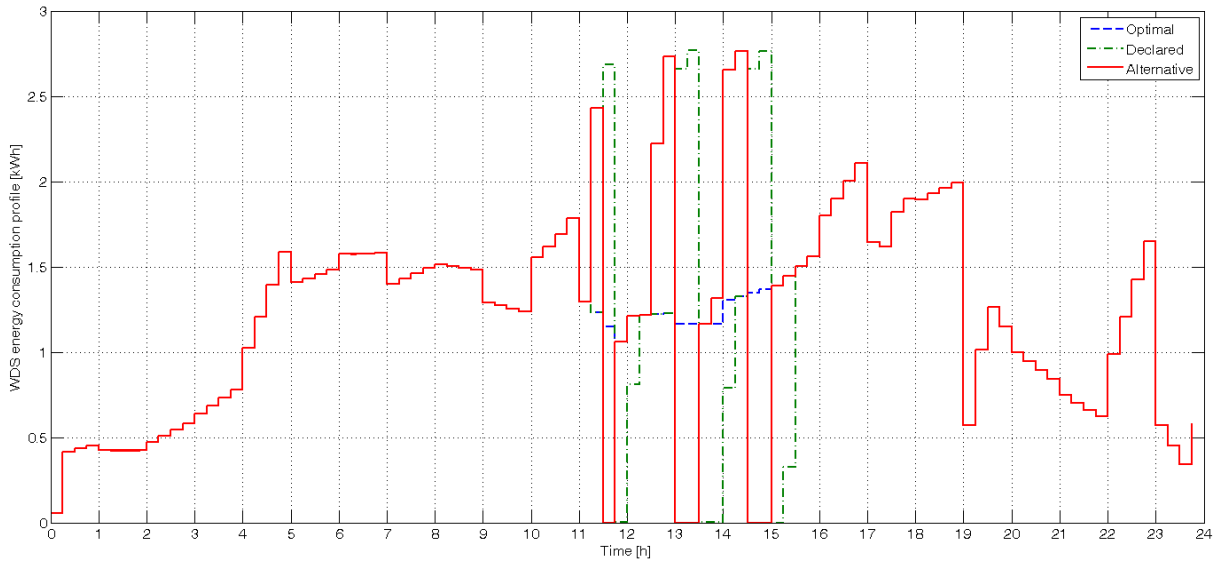

Figure 2.2.10. WDS energy consumption profiles for the cases of: optimal operation without flexibility provision ('Optimal'); operation when flexibility is just reserved, but not called ('Declared'); and for the cases when flexibility is reserved and called in maximum amount ('Alternative').

One may also see from Figure 2.2.10 that practically the behaviours differ just after 11:15, so the flexibility can be called even just 45 minutes before the activation time.

2.3 Electrified light city rail

Electrified light city rail validation environment and simulation models are put together such that a realistic system behaviour is simulated for application of the developed control algorithms. The case study is based on actual trains, time schedules and rail route configurations. The trains time-schedule and rail route configuration are taken from the railway section of Corridor X of Croatian Railways Infrastructure which is supplied from ETS Andrijevci in Slavonia region (eastern Croatia). The train configuration considered belongs to the low-floor electromotive train (EMT) for urban and commuter operation manufactured by Končar – Electric Vehicles Inc. The chosen simulation environment serves as a base case representative for many different railway systems. Railway segment comprised of straight rail tracks with no slopes or curves and electromotive trains with the ability of regenerative braking, all together supplied from the power grid through a single connection point in the ETS is one of the most commonly found railway system setups and is easily extended towards different, more complex setups. It is possible to extend the presented algorithm on more complex railway configurations including slopes, curves and tunnels.

2.3.1 Train composition model

The considered electromotive train (EMT) is intended for urban and commuter operation and is designed as a low-floor four-part train with the total length of 75 m. It is built for rails electrified with catenary power supply of 25 kV voltage and 50 Hz frequency with maximum speed of 160 km/h.

Train braking system is designed as a combination of regenerative and pneumatic frictional brakes which together provide the necessary braking force. Pneumatic frictional braking is utilized in lower speeds when regenerative braking is not able to provide enough braking force to stop the train. Parameters of the Končar EMT are presented in Table 2.3.1 together with resistance and available traction/braking force curves in Figure 2.3.1. For optimal train traction control law computation a discrete-time piecewise affine (DTPWA) train model is computed. The resistance force F_r is linearized and conservative constraints for available traction and braking force F_{tr} are introduced to the DTPWA model (Figure 2.3.1).

Table 2.3.1 Končar low-floor electromotive train parameters.

Parameter	Value
Catenary supply voltage	25 [kV], 50 [Hz]
Composition weight	139 [t]
Max. weight	172 [t]
Overall length	75 [m]
Gauge	1435 [mm]
Powered bogie axle/wheel radius	180/750 [mm]
Trailer bogie axle/wheel radius	180/860 [mm]
Continuous power (on wheel)	2000 [kW]
Starting traction force	200 [kN]
Max. acceleration at gross weight	1 [m/s^2]
Max. deceleration	1.3 [m/s^2]
Max. velocity	44.44 [m/s]
Specific resistance force	856+36v+5.4432v^2
Motor-reductor efficiency	0.939
Converter efficiency	0.92

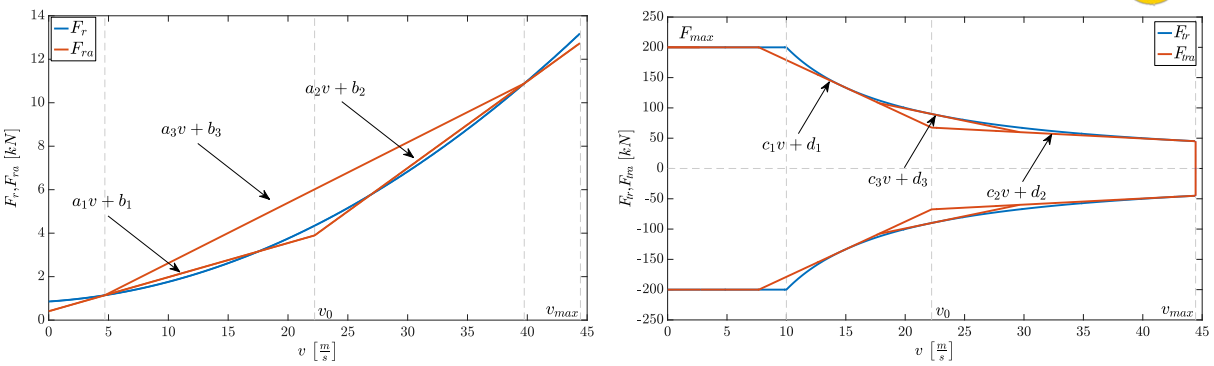

Figure 2.3.1 Končar low-floor electromotive train linearized train resistance F_{ra} and available traction force boundaries F_{tra}.

Optimal train traction force for the corresponding DTPWA model of Končar's EMT is calculated also for a straight rail segment, for different train travel times and distances from the stopping station.

2.3.2 Rail configuration

The considered ETS selected within the so-called Corridor X of the Croatian railway operator, which is entirely electrified, can withstand the maximum train velocity of 160 km/h and has double track gauges for simultaneous two-way traffic. A part of Corridor X supplied from ETS Andrijevci is selected with small to none track gradient and no curves or tunnels. Andrijevci ETS is situated between ETS Jankovci and ETS Nova Kapela. The area supplied by ETS Andrijevci covers track length between two facilities with neutral conduit sections (NS), namely NS Ivankovo and NS Sibinj. Following from distance between NS Ivankovo and NS Sibinj, it is assumed that ETS Andrijevci supplies a traction segment of ~56 km including 10 passenger stations. The considered rail path is depicted in Figure 2.3.2.

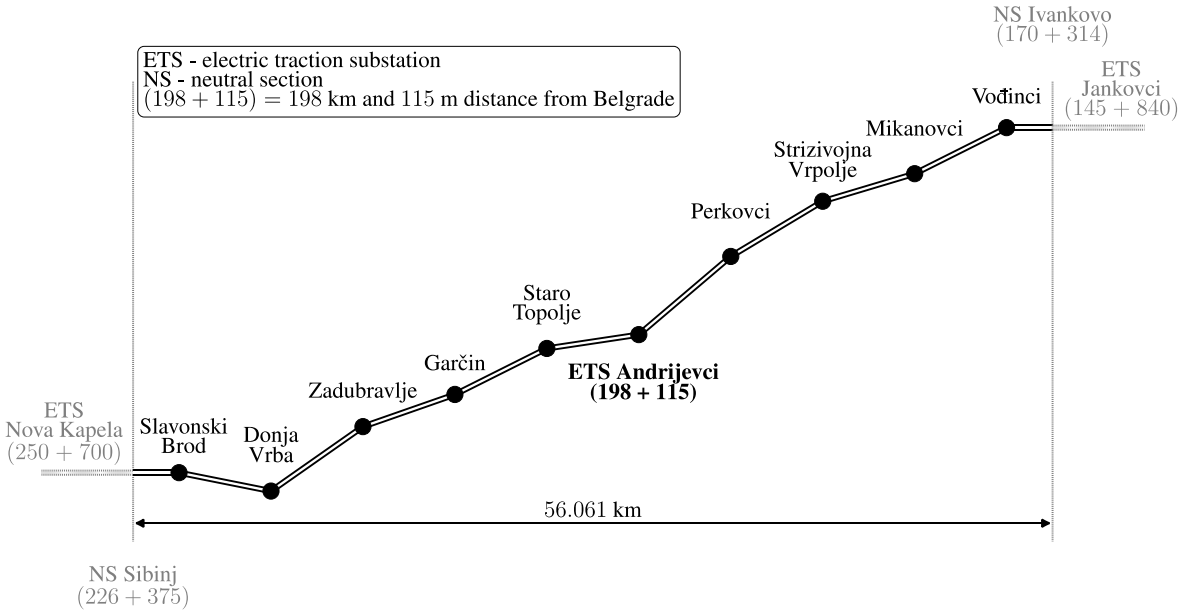

Figure 2.3.2 Croatian Railways Corridor X section area supplied from ETS Andrijevci with the corresponding passenger stations.

The corresponding passenger stations locations with travel distances and times are presented in Table 2.3.2. Traveling times between passenger stations have been obtained from the official railway timetable of Croatian Railways for the period from 14/12/2014 to 12/12/2015. Since different trains

have different travel times, average travel times are used and presented in Table 2.3.2. It is assumed that each train spends one minute in each passenger station in order to allow passengers to board and leave the train. When summed, the whole trip from Slobodnica station to Ivankovo station lasts 62 minutes and 30 seconds. It is important to notice that during the whole trip the train is supplied from ETS Andrijevci only between two neutral sections NS Sibinj and NS Ivankovo, therefore the route considered in the simulation lasts around one hour.

Table 2.3.2 Passenger stations supplied from ETS Andrijevci.

Station (location in km+m from Belgrade)	Distance to next station [km]	Travel time to next station [km]
Slobodnica (227+468)	6.777	7
NS Sibinj (226+375)	-	-
Slavonski Brod (220+691)	8.755	6.5
Donja Vrba (211+936)	2.582	3
Zadubravlje (209+354)	2.611	3
Garčin (206+743)	4.920	4
Staro Topolje (201+823)	3.635	4
ETS Andrijevci (198+118)	4.869	4.5
Perkovci (193+249)	5.452	5
Strizivojna-Vrpolje (187+797)	10.846	7
Stari Mikanovci (176+951)	5.873	4.5
Vođinci (171+078)	4.329	4
NS Ivankovo (170+314)	-	-
Ivankovo (166+749)	10.885	7

2.3.3 ETS parameters

ETS validation environment is considered from a standpoint of energy flows between the trains consumption and regeneration, ETS with the corresponding energy storage system and the power grid with volatile energy prices. Renewable energy sources like photovoltaic panels or small scale wind turbines built in/on passengers stations are not considered because of a rather small power production contribution in comparison to the overall trains consumption in megawatt scale but can be easily introduced as disturbance in HHL optimization problem. Therefore, the only considered power generation in the ETS is the regenerative braking energy produced by trains.

2.3.4 Utility grid connection

Connection to the utility grid is made via two 110/25 kV transformers of 7.5 MVA power each. The ETS power rating of 15 MVA is the most commonly found case of ETS transformers in Croatian railways. The transformers have the ability to return energy back to the utility grid which offers a

possibility for interaction with the power grid and better utilization of excessive regenerative and/or stored energy. However, there are also constraints on the power grid side, limiting the amount of energy that can be returned back to the grid in order to ensure grid stability. The limit for energy returned into the grid is set to 1 MW.

In the case of excessive regenerative braking power that cannot be delivered to the utility grid, the proposed control system distributes the amount of excessive energy among the trains supplied from the ETS that are in braking, proportionally to their braking energy. The regenerative braking on each train is then reduced to fit the available amount during one time instant while the remaining braking force is substituted with the use of frictional brakes and modelled with energy dissipated on the resistors. If the power consumption of the trains auxiliary systems is considered on the LHL, it is expected that the amount of excessive regenerative energy is reduced since the power consumption of all trains would increase, i.e. the use of frictional brakes would decrease.

The current energy pricing scheme in Croatia is based on a two-tariff pricing for buying energy with higher prices set during the day and lower during the night, and with no reimbursement when selling energy, i.e. returning it to the grid. However, it is expected that price profiles varying on hourly or even smaller time-scales will be implemented in the near future. The considered prices for energy exchange are based on European Power Exchange prices (EPEX), which are available one day ahead. For simplicity, prices for energy exchange with the grid do not change when buying or selling energy, while the case with no reimbursement for selling energy is simulated with the 0 MW limit on the energy returned to the grid.

2.3.5 Energy storage system

The considered energy storage system is modeled as a joint operation of battery energy storage system and a supercapacitor. Selection of the supercapacitor is justified for collecting the regenerative braking energy with a large number of charging/discharging cycles, due to its large power density, while battery storage is selected with the aim of collecting larger amounts of energy during longer periods of time, due to the batteries high energy density. The considered energy storage system parameters are listed in Table 2.3.3.

Table 2.3.3 Energy storage system parameters.

Parameter	Battery storage	Supercapacitor
Rated power [MW]	0.3	1.2
Capacity [kWh]]	140	30
Charge/discharge efficiency	0.8	0.8
Maximum SoC	0.9	0.9
Minimum SoC	0.1	0.1
Initial SoC	0.1	0.1

2.3.6 Problem formulation

Railway system is considered through coordination of on-route trains energy consumption and electric traction substation (ETS) energy flows management with the goal of increasing energy efficiency, decreasing operational costs and enabling integration of railways into smart electricity grids. The algorithm for hierarchical coordination is developed in several steps and described here together with an extensive case study scenario designed for verification of the developed control system within a realistic scenario taken from Croatian railways. The method for energy consumption minimization of a single train travelling between two stations employs explicit constrained finite-time optimal control of piecewise affine systems for calculation of the optimal traction force control law. On the higher, energy flows optimization level, model predictive control (MPC) problem is formulated with the linear cost function for the price-optimal energy flows. A single ETS is observed from the point of balancing energy flows between the accelerating and decelerating trains, the energy storage system and a connection to the utility grid with variable energy prices and various demands from the utility grid operator. Energy flows optimization results in optimal charging/discharging profiles for storage components that guarantee the optimal economic cost on the prediction horizon while taking into account the current state-of-charge of the energy storages, predicted trains consumption profile, volatile electricity price profile representing the economic criterion of the utility grid, and technical constraints on system components. The initial algorithm for coordination between the two levels is based on iterative improvement of the lower level solution through revisiting of both levels. Energy flows level model predictive control problem is locally solved parametrically with the lower level (optimal) energy consumption solution as a parameter. Lower level solution is then reoptimized with respect to higher level value function while taking into account the inherited lower level constraints. The developed algorithm is extended and validated on various simulation scenarios for different railway system operation set-ups showing the possibility for cost reductions of up to 25% for specific scenarios. The modularity and hierarchical structure of the presented algorithm keeps the considered subsystems operation apart since they are often required to remain infrastructurally and technologically independent, but also usually legally separated to infrastructure companies for operating power supply and different transportation companies for operating the trains. Due to the modular structure of the algorithm, the levels are able to operate independently when e.g. the train operation on the lower level cannot be changed. It is also possible to extend the proposed algorithm with new levels e.g. for simultaneous coordination of multiple traction substations such that a longer rail segment is considered.

Optimization problems for both on-route trains energy consumption (lower) and ETS energy flows management (higher) levels are described in the sequel. Superscripts 'l' and 'h' denote lower hierarchical level (LHL) and higher hierarchical level (HHL) variables, respectively. Lower and uppercase letters are used to denote vectors and matrices, respectively, while bold notation is used to denote variables stacked over the prediction horizon.

2.3.6.1 Lower hierarchical level

Train motion along the rail tracks is described with a simple continuous-time model:

$$\mathrm{m}\frac{d\mathrm{v}}{\mathrm{d}t} = \mathrm{F_{tr}} - \mathrm{F_r}(\mathrm{v}, \mathrm{s}), \tag{1a}$$

$$\frac{\mathrm{d}s}{\mathrm{d}t} = \mathrm{v}, \tag{1b}$$

where m is the train mass, v the train velocity, $\mathrm{F_{tr}}$ the train traction force (in breaking $\mathrm{F_{tr}} < 0$), $\mathrm{F_r}$ the overall resistance force and s the traversed path. The resistance force $\mathrm{F_r}$ includes roll resistance (friction), aerodynamic resistance and track resistance (caused by track grade, curves and tunnels) and is nonlinear due to quadratic speed dependency and variable rail configuration:

$$F_{\mathrm{r}}(v,s) = \alpha_0(s) + \alpha_1 v + \alpha_2 v^2, \tag{2}$$

where α_0, α_1 and α_2 are resistance coefficients derived from the train shape, power train and other parameters.

Due to the non-linearity from (1a) and model discretization effects, the train dynamics is described with a discrete-time piecewise affine (PWA) model:

$$\begin{aligned} \mathrm{x_{k+1}} &= \mathrm{A_{di}x_k} + \mathrm{B_{di}u_k} + \gamma_{\mathrm{di}}, \\ \text{if} \quad \mathrm{H_i x_k} &+ \mathrm{L_i u_k} \le \mathrm{K_i}, \quad \mathrm{i} = 1,2,3,4, \end{aligned} \tag{3}$$

where $x = \left[\frac{v}{s}\right]$, $\mathrm{u} = \mathrm{F_{tr}}$, matrices A_{di}, B_{di} and γ_{di} are obtained by Zero-Order Hold discretization of the continuous-time PWA model $\dot{x} = \mathrm{A}_i\mathrm{x} + \mathrm{B}_i\mathrm{u} + \gamma_i$ with sampling time T, $\mathrm{A}_i = \begin{bmatrix} -\frac{a_i}{m} & 0 \\ 1 & 0 \end{bmatrix}$, $\mathrm{B}_i = \begin{bmatrix} \frac{1}{m} \\ 1 \end{bmatrix}$, $\gamma_i = \begin{bmatrix} -\frac{b_i}{m} \\ 1 \end{bmatrix}$, coefficients a_i and b_i are obtained from linearization of the nonlinear resistance force from (2), and matrices $\mathrm{H_i}$, $\mathrm{L_i}$ and $\mathrm{K_i}$ are formed according to constraints for each PWA dynamics.

Mechanical energy required for the train within one sampling interval $\mathrm{I} = [\mathrm{kT}, (\mathrm{k}+1)\mathrm{T})$ under constant $\mathrm{F_{tr}(kT)}$ applied along the entire interval I is:

$$\begin{aligned} E_I\big(F_{\mathrm{tr}}(kT), v(kT)\big) &= \int_{kT}^{(k+1)T} F_{\mathrm{tr}}(kT)v(kT)dkT \\ &= p_i\big(F_{\mathrm{tr}}(kT)\big)^2 + q_i F_{\mathrm{tr}}(kT) + r_i F_{\mathrm{tr}}(kT)v(kT), \end{aligned} \tag{4}$$

where $\mathrm{T_i} = \frac{\mathrm{m}}{\mathrm{a_i}}$, $\mathrm{p_i} = \frac{1}{\mathrm{a_i}}\left[\mathrm{T} - \mathrm{T_i}\left(1 - \mathrm{e}^{-\frac{\mathrm{T}}{\mathrm{T_i}}}\right)\right]$, $\mathrm{q_i} = -\mathrm{b_i p_i}$, $\mathrm{r_i} = \mathrm{T_i}\left(1 - \mathrm{e}^{-\frac{\mathrm{T}}{\mathrm{T_i}}}\right)$, the index i represents the currently activated dynamics. It is important to mention that $\mathrm{p_i} > 0$ if $\mathrm{a_i} > 0$, which leads to convex energy optimization problems with respect to the traction force.

Optimization of trains on-route energy consumption is formed as a minimization of trains energy cost during the travel time T^* dictated by the timetable:

$$J^{l*} := \min_{\mathbf{u}^l,\mathbf{i}} \sum_{k=0}^{k^*} E_I\left(u_k^l, x_k^l\right),$$
$$s.t. \begin{cases} x_{k+1}^l = A_{di_k} x_k^l + B_{di_k} u_k^l + \gamma_{di_k}, \\ H_{i_k} x_k + L_{i_k} u_k \leq K_{i_k}, \\ G^l \begin{bmatrix} x_k^l \\ u_k^l \end{bmatrix} \leq w^l, \\ x_{k^*}^l = \begin{bmatrix} 0 \\ s_{k^*} \end{bmatrix}, \end{cases} \tag{5}$$

where $u^l = F_{tr}$ is the train traction force, $x_l = \begin{bmatrix} v \\ s \end{bmatrix}$ are the train states, i.e. train speed and traversed path, $k^* = T^*/T, i = 1,2,3,4,$ mark the corresponding affine train dynamics, E_I is described in (4), train dynamics are described with A_{di}, B_{di} and γ_{di}, with corresponding dynamics constraints in H_i, L_i and K_i, maximal allowable and possible train traction force $F_{tr,max}$ and speed v_{max} are described with G^l and w^l, and s_{k^*} is the train position at the end of the route.

Control problem formulated in (5) is a mixed-integer quadratic program and is solved backwards in time with dynamic programming through k^* steps. The sampling time $T = 15$ seconds is chosen as a good trade-off between model precision and number of prediction instants on the prediction horizon of the LHL for the considered scenario.

The optimization problem on the LHL is composed of energy consumption minimization problems of all $j = 1, \dots, N_{tr}$ trains currently supplied from the considered ETS. It is initially solved for all N_{tr} trains individually, while taking into account the train and rail path limitations together with preset timetables. The LHL problem results in energy-optimal traction/braking force sequences u_j^l and train speed and traversed path x_j^l, together with fixed PWA dynamics switching sequences i_j^* for all trains:

$$u_j^l = \left[u_{j,0}^{l*}, \dots, u_{j,k^*}^{l*}\right], \tag{6}$$

$$\boldsymbol{x_j^l} = \left[x_{j,0}^{l*}, \dots, x_{j,k^*}^{l*}\right]. \tag{7}$$

Optimal train traction sequence u_j^l and speed profile is plugged in (4), resulting in energy cost for a single train E_j^l:

$$E_j^l = \left[E_{j,0}^{l*}, \dots, E_{j,k^*}^{l*}\right]. \tag{8}$$

Energy costs of all N_{tr} trains are summed to obtain the total ETS energy consumption, which is passed to the HHL level as a parameter θ^h:

$$\theta^h = \sum_{j=1}^{N_{tr}} E_j^l. \tag{9}$$

In order to include the LHL problem from (5) in the hierarchical coordination algorithm, trains mechanical energy E_I from (4) needs to be linearized with respect to the train traction force F_{tr}. Adaptation of the LHL problem to enable tuning of the traction profiles via hierarchical coordination is described in the following sections.

2.3.6.2 Higher hierarchical level

Electric traction substation energy flows are consisted of accelerating trains energy consumption, decelerating trains energy production, wayside energy storage system energy flows and energy exchanged with the electrical grid. The power balance of the system is:

$$P^{\mathrm{TR}} = P^{\mathrm{G}} + P^{\mathrm{SC}} + P^{\mathrm{BAT}} + P^{\mathrm{R}}, \tag{10}$$

where P^{TR} denotes the cumulative power consumption ($P^{\mathrm{TR}} > 0$) or production ($P^{\mathrm{TR}} < 0$) by trains supplied from the ETS, P^{G} denotes the power exchanged with the electrical power grid, P^{SC} and P^{BAT} denote supercapacitor and battery power flows, respectively, and P^{R} is the power dissipated on the ETS resistors.

The considered energy storage systems are modelled with:

$$\begin{aligned} x_{k+1}^{\mathrm{BAT}} &= x_k^{\mathrm{BAT}} - \frac{T}{C^{\mathrm{BAT}}}\left(\frac{1}{\eta_{\mathrm{dch}}^{\mathrm{BAT}}} P_{\mathrm{dch},k}^{\mathrm{BAT}} + \eta_{\mathrm{ch}}^{\mathrm{BAT}} P_{\mathrm{ch},k}^{\mathrm{BAT}}\right), \\ x_{k+1}^{\mathrm{SC}} &= x_k^{\mathrm{SC}} - \frac{T}{C^{\mathrm{SC}}}\left(\frac{1}{\eta_{\mathrm{dch}}^{\mathrm{SC}}} P_{\mathrm{dch},k}^{\mathrm{SC}} + \eta_{\mathrm{ch}}^{\mathrm{SC}} P_{\mathrm{ch},k}^{\mathrm{SC}}\right), \end{aligned} \tag{11}$$

where states x_k^{BAT} and x_k^{SC} are normalized battery and the supercapacitor state-of-charge (SoC), respectively, C is storage capacity, η_{ch} and P_{ch} are charging efficiency and charging power component of the storage system ($P_{\mathrm{ch}} \leq 0$), while η_{dch} and P_{dch} are discharging efficiency and discharging power component of the storage system ($P_{\mathrm{dch}} \geq 0$). Separation of charging and discharging is introduced to avoid additional integer formulation.

Traction substation microgrid energy flows optimization is formulated as a model predictive control (MPC) HHL problem with the cost function set as the economic criterion of overall system operation on the prediction horizon N:

$$J^{\mathrm{h}*} := \min_{P_{\mathrm{ch,dch},k}^{\mathrm{BAT}}, P_{\mathrm{ch,dch},k}^{\mathrm{SC}}, P_k^{\mathrm{R}}} T \sum_{k=0}^{N-1} c_k \, P_k^{\mathrm{G}}, \tag{12}$$

where c denotes the utility electricity price in €/MWh.

The MPC problem takes into account the ETS physical constraints, energy storage SoC and charging/discharging power limitations and limitations on energy exchanged with the grid. Microgrid physical constraints are introduced to the control problem as state and input constraints. With respect to energy storage system dynamics from (11), constraints include supercapacitor and battery SoC limitations in order to preserve the health of the storage systems:

$$\begin{aligned} x_{\mathrm{min}}^{\mathrm{SC}} \leq x_k^{\mathrm{SC}} \leq x_{\mathrm{max}}^{\mathrm{SC}}, \\ x_{\mathrm{min}}^{\mathrm{BAT}} \leq x_k^{\mathrm{BAT}} \leq x_{\mathrm{max}}^{\mathrm{BAT}}, \end{aligned} \tag{13}$$

and maximum charging and discharging power of the supercapacitor and batteries:

$$\begin{aligned} \mathrm{P}_{\mathrm{dch,min}}^{\mathrm{BAT}} \leq \mathrm{P}_{\mathrm{dch,k}}^{\mathrm{BAT}} \leq \mathrm{P}_{\mathrm{dch,max}}^{\mathrm{BAT}}, \\ P_{\mathrm{ch,min}}^{\mathrm{BAT}} \leq P_{\mathrm{ch},k}^{\mathrm{BAT}} \leq P_{\mathrm{ch,max}}^{\mathrm{BAT}}, \\ P_{\mathrm{dch,min}}^{\mathrm{SC}} \leq P_{\mathrm{dch},k}^{\mathrm{SC}} \leq P_{\mathrm{dch,max}}^{\mathrm{SC}}, \end{aligned} \tag{14}$$

$$P^{\mathrm{SC}}_{\mathrm{ch,min}} \leq P^{\mathrm{SC}}_{\mathrm{ch},k} \leq P^{\mathrm{SC}}_{\mathrm{ch,max}}.$$

Constraints on utility grid power rating are defined as follows:

$$P^{\mathrm{G}}_{\mathrm{min}} \leq P^{\mathrm{G}}_{k} \leq P^{\mathrm{G}}_{\mathrm{max}}, \tag{15}$$

and constraints on the power dissipated in the resistors as:

$$0 \leq P^{\mathrm{R}}_{k} \leq P^{\mathrm{R}}_{\mathrm{max}}. \tag{16}$$

For simplification, excess regenerative energy is dissipated on the virtual resistors bank, while it is actually substituted with the use of frictional brakes instead of regenerative braking proportionally distributed over all trains in braking. Due to the MPC philosophy, the system takes into account future electricity prices c, available one day in advance, as well as the predicted energy consumption/production of all trains currently supplied from the ETS and is therefore able to plan the future consumption in advance such that the system acts as a flexible and proactive consumer connected to the grid.

The HHL optimization problem minimizes the cost of energy exchanged between the ETS that supplies the considered rail section and the transmission power grid. The HHL problem introduced in (12) is reformulated as a multi-parametric MPC optimization problem with the parameters set θ^h obtained from the LHL solution (9):

$$\begin{aligned} \mathrm{J}^{h*} &:= \min_{\mathbf{u}^h} \mathbf{h}^h \begin{bmatrix} \mathrm{x}^{\mathrm{h}} \\ \mathrm{u}^{\mathrm{h}} \end{bmatrix} + \mathbf{f}^h \theta^h, \\ s.t. &\begin{cases} \mathbf{x}^{\mathrm{h}} = \mathbf{A}^h \mathrm{x}^{\mathrm{h}}_0 + \mathbf{B}^h \mathrm{u}^{\mathrm{h}}, \\ \mathbf{G}^{\mathrm{h}} \begin{bmatrix} \mathbf{x}^{\mathrm{h}} \\ \mathbf{u}^{\mathrm{h}} \end{bmatrix} \leq \mathbf{w}^{\mathrm{h}} + \mathbf{E}^h \boldsymbol{\theta}^h, \end{cases} \end{aligned} \tag{17}$$

where h^h and f^h are computed from (12) and represent the cost of the energy exchanged with the transmission grid, x^h is the storages SoC with $\mathbf{A}^h$ and $\mathbf{B}^h$ representing the dynamics of the storage systems from (11), $\mathbf{u}^{\mathrm{h}} = \left[\boldsymbol{P}^{BAT}_{ch}, \boldsymbol{P}^{BAT}_{dch}, \boldsymbol{P}^{SC}_{ch}, \boldsymbol{P}^{SC}_{dch}, \boldsymbol{P}^{\boldsymbol{R}}\right]$ incorporates charging/discharging energies of the energy storage system and dissipating on the resistor bank, while $\mathbf{G}^{\mathrm{h}}$, $\mathbf{w}^{\mathrm{h}}$ and $\mathbf{E}^h$ are used to describe the HHL physical constraints and limitations presented in (13)-(16).

2.3.6.3 Hierarchical coordination for energy management

Hierarchical coordination between the LHL and HHL is performed through revisiting of both control levels with the goal of improving the initial energy-optimal LHL solution for individual trains with respect to the HHL cost for energy exchange, thus transforming it into a global, price-optimal, solution for all trains. The iterative coordination scheme is depicted in Figure 2.3.3, executed until the LHL solution converges with respect to the global criteria under the given constraints, i.e. when the train traction force energy-optimal profile is shifted to the price-optimal profile.

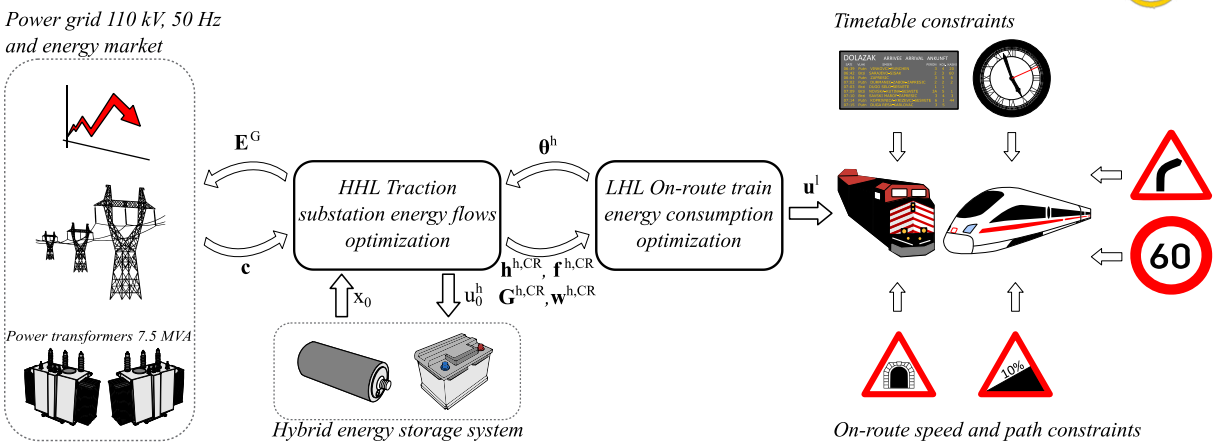

Figure 2.3.3 Scheme and information flow of hierarchical coordination between LHL and HHL optimizations.

Local multi-parametric HHL problem from (17) is solved for the initial LHL solution θ^{h} as a parameter. In the case of an infeasible HHL optimization problem (17) with initially obtained θ^{h}, the nearest feasible θ^{h} is calculated and introduced into the HHL. By applying the geometric multi-parametric algorithm only a single critical region (CR) is computed around the LHL solution and no additional partitioning of the parameter space is performed. A critical region is a subset of parameters θ^{h} that yield the same set of active constraints, i.e. constraints that are satisfied with equality in the optimal solution. For the computed LHL solution, CR boundaries around it are defined as:

$$G^{h,CR}\theta^{\mathrm{h}} \leq w^{\mathrm{h,CR}}, \tag{18}$$

while the optimal control law and value function characterization are linear over the CR, i.e. for any cumulative trains consumption profiles within the CR, are formulated as:

$$\mathbf{u}^{\mathrm{h}*}(\theta^{\mathrm{h}}) = \mathbf{D}^{h,CR}\theta^{\mathrm{h}} + \mathbf{Q}^{h,CR}, \tag{19}$$
$$\mathrm{J}^{\mathrm{h,CR}*}(\theta^{\mathrm{h}}) = \mathbf{h}^{h,CR}\theta^{\mathrm{h}} + \mathbf{f}^{h,CR}. \tag{20}$$

The calculated CR boundaries and value function are then passed to the LHL in order to reoptimize the previously obtained train traction sequences. Since HHL is set on minimization of the cost for energy exchanged with the power grid, CR boundaries $G^{h,CR}$, $w^{\mathrm{h,CR}}$ and value function $\mathbf{h}^{h,CR}$, $\mathbf{f}^{h,CR}$ are functions of trains energy and need to be transformed in order to adapt them to LHL traction force based optimization (5). Otherwise, the optimization problem on the LHL becomes nonlinear since the trains consumed energy (4) is a quadratic function of the traction force which would be introduced in CR constraints (18), thus making the LHL problem non-convex and hard to solve in real-time applications. The linearization is performed around the current solution of the traction force sequence from LHL (6). Although the CR value function from (20) could be kept quadratic with respect to the traction forces u^l, it is linearized since linear programs are easier to solve and have better solving properties in terms of speed and convergence. After linearization, LHL is optimized with respect to the CR value function and CR boundaries for all N_{tr} simultaneously, while taking into account LHL constraints of all N_{tr} trains currently supplied from the ETS. The reformulated LHL optimization problem is solved for all N_{tr} trains while keeping the new solution in close vicinity of the initial LHL solution in order to ensure the linearization accuracy:

$$\mathrm{J}^{h,CR*} := \min_{\Delta \mathbf{u}^{\boldsymbol{l}}} \mathbf{h}_{\boldsymbol{lin}}^{h,CR}(\mathrm{u}^{\boldsymbol{l}} + \Delta \mathrm{u}^{\boldsymbol{l}}) + \mathbf{f}_{\boldsymbol{lin}}^{h,CR},$$
$$s.t. \begin{cases} -\boldsymbol{\varepsilon} \leq \Delta \mathbf{u}^{\boldsymbol{l}} \leq \boldsymbol{\varepsilon}, \\ \mathbf{G}_{\boldsymbol{lin}}^{\boldsymbol{h,CR}}(\mathrm{u}^{\boldsymbol{l}} + \Delta \mathrm{u}^{\boldsymbol{l}}) \leq \mathbf{w}_{\boldsymbol{lin}}^{h,CR}, \\ \mathbf{G}_{\boldsymbol{j}}^{\boldsymbol{l}} \begin{bmatrix} \boldsymbol{x}_{\boldsymbol{j}}^{\boldsymbol{l}} \\ (\boldsymbol{u}_{\boldsymbol{j}}^{\boldsymbol{l}} + \Delta \boldsymbol{u}_{\boldsymbol{j}}^{\boldsymbol{l}}) \end{bmatrix} \leq \mathbf{w}_{\boldsymbol{j}}^{l}, \\ \vdots \\ \mathbf{G}_{\boldsymbol{N_{tr}}}^{\boldsymbol{l}} \begin{bmatrix} \boldsymbol{x}_{\boldsymbol{N_{tr}}}^{\boldsymbol{l}} \\ (\boldsymbol{u}_{\boldsymbol{N_{tr}}}^{\boldsymbol{l}} + \Delta \boldsymbol{u}_{\boldsymbol{N_{tr}}}^{\boldsymbol{l}}) \end{bmatrix} \leq \mathbf{w}_{\boldsymbol{N_{tr}}}^{l}, \end{cases} \tag{21}$$

where $\mathrm{u}^{\boldsymbol{l}} = [\boldsymbol{u}_{\boldsymbol{j}}^{\boldsymbol{l}}, \cdots, \boldsymbol{u}_{\boldsymbol{N_{tr}}}^{\boldsymbol{l}}]$, $\Delta \mathrm{u}^{\boldsymbol{l}}$ is the change with respect to the initial LHL solution $\mathrm{u}^{\boldsymbol{l}}$, $\boldsymbol{\varepsilon}$ is the change limitation added to insure the linearization accuracy, $\mathbf{h}_{\boldsymbol{lin}}^{h,CR}$ and $\mathbf{f}_{\boldsymbol{lin}}^{h,CR}$ are the linearized coefficients of the CR value function from (20), $\mathbf{G}_{\boldsymbol{lin}}^{\boldsymbol{h,CR}}$ and $\mathbf{w}_{\boldsymbol{lin}}^{h,CR}$ are the linearized CR boundaries and $\mathbf{G}_{\boldsymbol{j}}^{\boldsymbol{l}}$ and $\mathbf{w}_{\boldsymbol{j}}^{l}$ are LHL constraints of train j from (5) with included PWA train dynamics sequence constraints and end-state constraints ensuring punctual arrival at the station. In the reformulated LHL optimization problem (20), the initial LHL cost function J^{l} from (5), for an individual train, is substituted with the CR value function from (20) representing the minimum cost for energy consumption of all the trains simultaneously, with respect to the change of the initial LHL solution $\Delta \mathbf{u}^{\boldsymbol{l}}$.

As presented in Figure 2.3.3, the subproblems interact through exchange of several variables. The LHL subproblem from (21) generates optimal traction profiles for all the trains supplied from a single ETS and sends the overall trains energy consumption profile θ^{h} to the HHL subproblem where it is used as an optimization parameter. The HHL then calculates a single critical region with the corresponding value function parameters $\mathbf{h}^{h,CR}$, $\mathbf{f}^{h,CR}$ and critical region boundaries $G^{h,CR}$, $W^{\mathrm{h,CR}}$ and passes them to the LHL where the trains traction profiles are reoptimized and tuned according to the critical region value function from (21). New traction profiles are created in the LHL and returned to the HHL. There are several different possibilities of how the hierarchical coordination is continued with respect to the constraints activated at the optimal solution of (21):

- linearization accuracy constraints are activated; linearization is then performed around the new force sequence and LHL is solved again,
- CR boundaries are reached; the solution is transferred to the adjacent CR on the HHL which requires to solve (17) and characterize the new CR, and (21) is then solved again,
- dynamics switching sequence constraints of the trains LHL PWA model, found within constraints described with $\mathbf{G}_{\boldsymbol{j}}^{\boldsymbol{l}}$ and $\mathbf{w}_{\boldsymbol{j}}^{l}$ for train j, are activated for some of the trains, new dynamics switching sequences are found through solving a mixed-integer linear program described and (21) is then solved again with these new switching sequences introduced in corresponding constrains formed by $\mathbf{G}_{\boldsymbol{j}}^{\boldsymbol{l}}$ and $\mathbf{w}_{\boldsymbol{j}}^{l}$.

When all options are exhausted and LHL solution converges, i.e. $\|\Delta u^{l}\| \leq \epsilon$, where ϵ is the allowed tolerance, the procedure is concluded. The flowchart of the overall algorithm, including also the details of hierarchical coordination, is depicted in Figure 2.3.4.

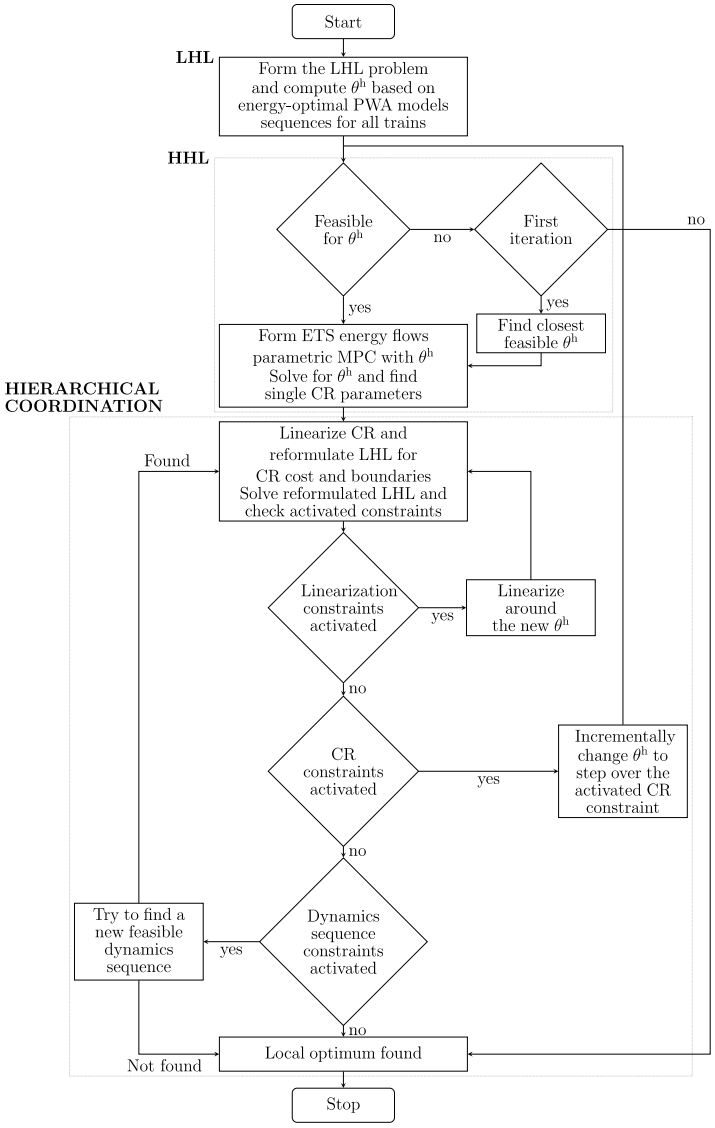

Figure 2.3.4 Hierarchical coordination algorithm flow chart.

Through the described coordination, the trains maintain the schedule in timetables, and respect their physical constraints and route limitations. At the same time they are coordinated with the ETS optimal energy flows through prices $\mathbf{h}_{\boldsymbol{lin}}^{h,CR}$ and $\mathbf{f}_{\boldsymbol{lin}}^{h,CR}$. This way, the energy is distributed among all the trains that are currently supplied from a single ETS and the overall price-optimal system operation is achieved. The railway system is thus transformed from a passive energy consumer into a proactive flexible participant connected to the power grid, which is then able to provide ancillary services (e.g. secondary services such as frequency regulation) to the power grid as well as actively respond to power grid demands (e.g. temporary consumption reduction/increase, power peak shaving etc.).

2.3.7 Results

2.3.7.1 LHL control -- individual train energy consumption

For the train model described with parameters in Table 2.3.1 energy-efficient traction profiles are calculated for a single travel between two stations as well as for the travel throughout the whole ETS Andrijevci supply area with the results presented as follows.

2.3.7.1.1 Single travel

The route between passenger stations Slobodnica and Sl. Brod is simulated with the resulting energy-optimal traction force profile presented together with speed and traversed path profiles in Figure 2.3.5. Stations are distanced 6.8 km with designated travel time of 7 minutes according to Croatian Railways timetable (Figure 2.3.2 and Table 2.3.2).

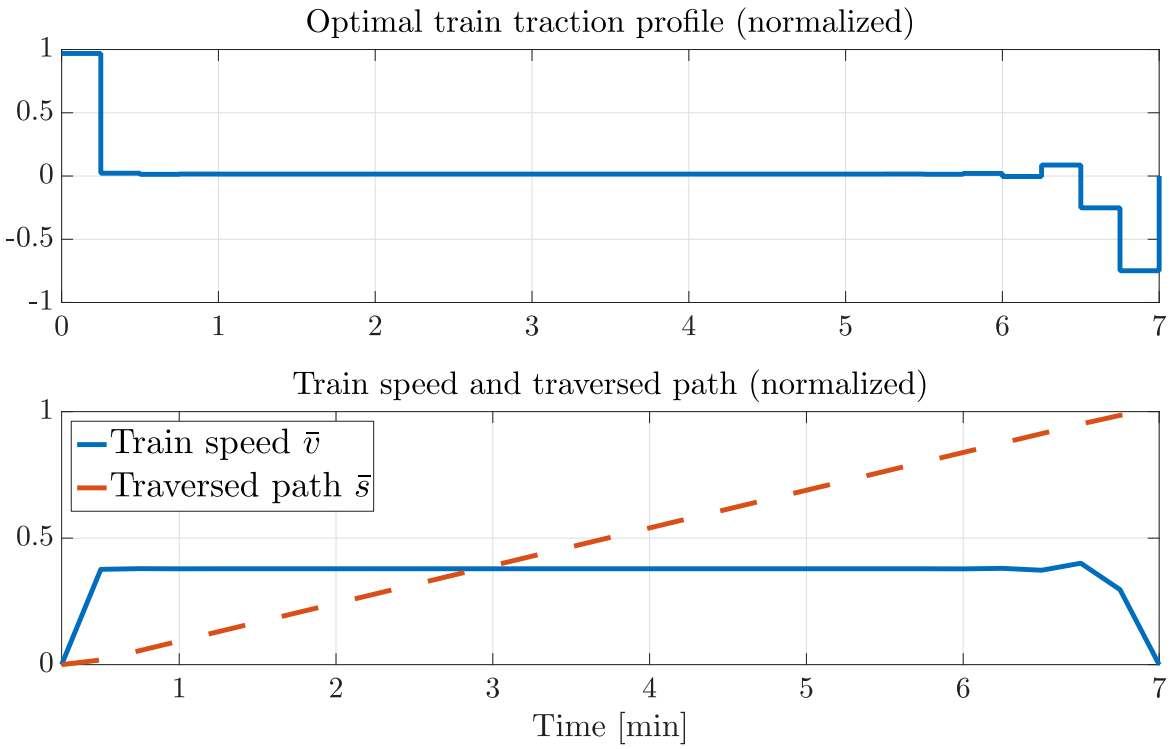

Figure 2.3.5 Energy-optimal train traction force, speed and traversed path profiles while traveling from Slobodnica to Sl. Brod.

2.3.7.1.2 ETS Andrijevci supply area

Traveling through ETS Andrijevci supply area lasts around 60 minutes (including 1 minute stops in all passenger stations) according to the Croatian railways timetable (as presented in Table 2.3.2) for the rail path length of 60.7 km and travel time duration of 62 minutes and 30 seconds (including one-minute stops in passenger stations). The calculated energy-optimal train traction force profile is presented in Figure 2.3.6 together with the corresponding travel speed and traversed path profiles. Figure 2.3.5 and Figure 2.3.6 also show that it is economically more viable to maintain lower speed for most of the path and speed up at the end of the route to satisfy the time-schedule constraints, which is manifested as peaks in traction and speed in the opposite direction at the beginning and end of the cruising phase.

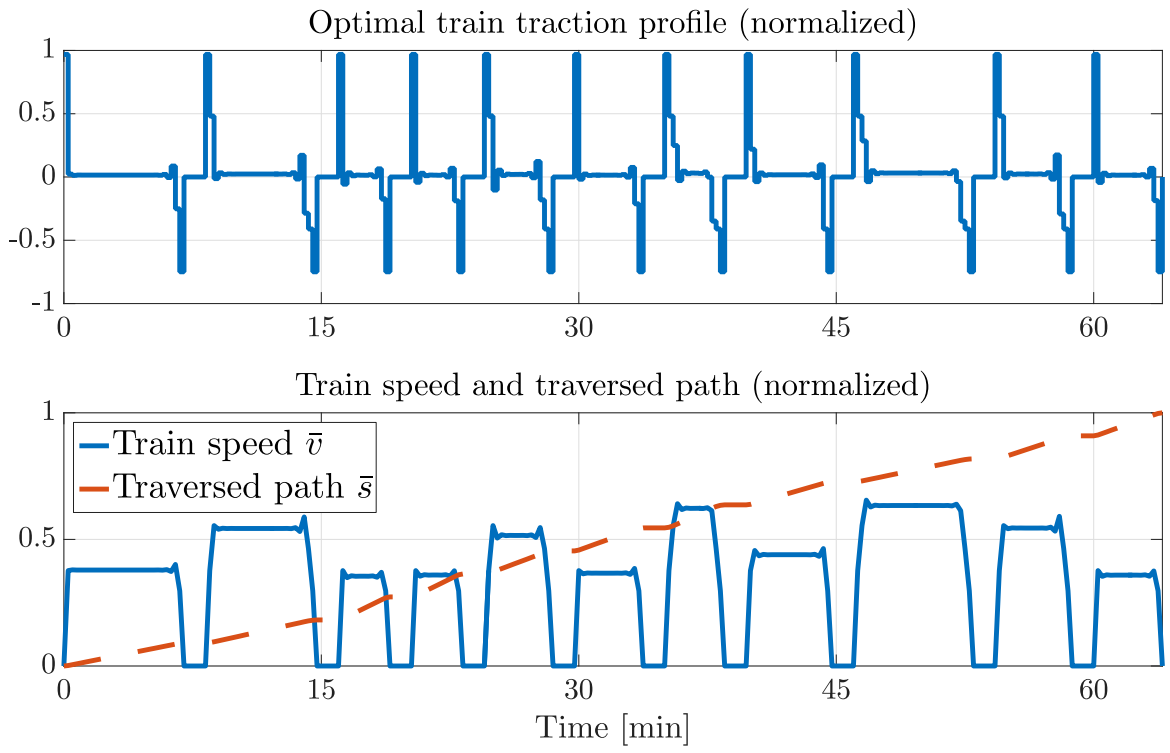

Figure 2.3.6 Energy-optimal train traction force, speed and traversed path profiles while traveling from Slobodnica to Ivankovo.

Since there is no measured data available on the Končar EMV train energy consumption on the Slobodnica-Ivankovo route, the savings from implementation of the sole LHL control system cannot be exactly calculated but are expected to be around 30% compared to average driver performance.

2.3.7.1.3 HHL control -- ETS power flows

After the initial results are obtained from the LHL, energy-optimal train travel consumption profile is created for a train traveling through the ETS Andrijevci supply area, as presented in Figure 2.3.6. To simulate the Croatian railways timetable for the considered ETS Andrijevci area during one day, created travel profiles are stacked in time with all the passenger trains considered identical to the presented Končar EMT.

With the installation of energy storages (as presented in Subsection 2.3.6.2) the higher MPC system is implemented and HHL control system operation is simulated during a daily system operation according to the Croatian railways timetable together with volatile EPEX prices and a prediction horizon of N = 24 h. Simulation scenario results are depicted in Figure 2.3.7 and comprise of: (i) energy exchange price profile, (ii) ETS power flows (summed trains energy consumption/production), (iii) energy exchanged with the utility grid and (iv) energy storage state of charge for both energy storage components (battery system and supercapacitor).

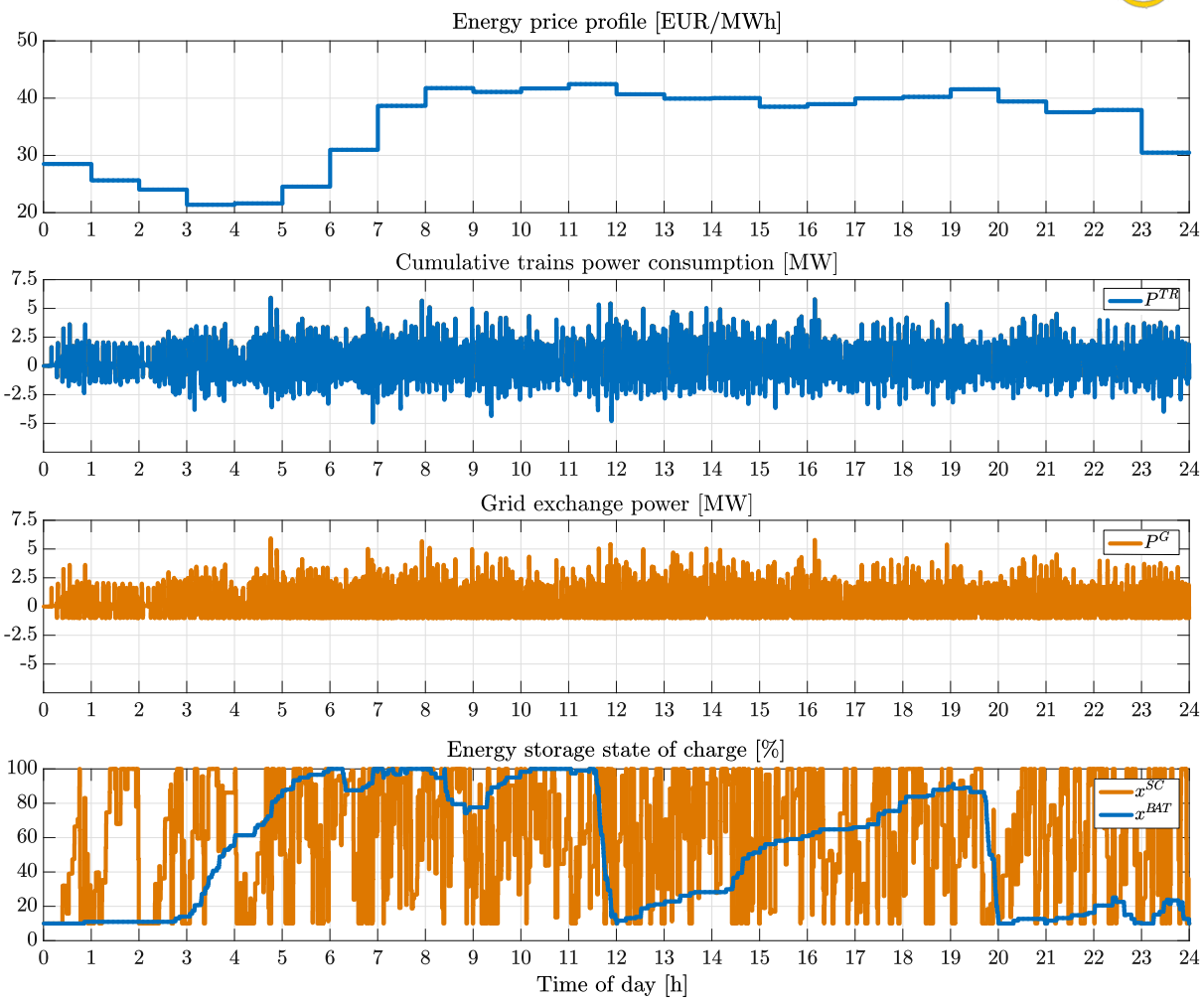

Figure 2.3.7 Daily power flows for system operation with only higher level MPC installed and grid receptiveness of -1 MW.

System operation has been simulated for different grid receptiveness levels of 5, 3, 1 and 0 MW of power that can be returned to the grid. The system is also simulated for a fixed-price tariff (same energy exchange price throughout the day), two-prices tariff (cheaper energy exchange price during the night) and with the variable-price tariff. From the obtained cost savings results, presented in Figure 2.3.8, it can be observed that the possible savings reach 35% on the HHL alone and rise when the grid is more conservative, meaning that little or no energy can be returned to the grid. For the case when grid receptiveness is set to 5 MW (or above), all of the regenerative braking energy can be returned to the grid due to the fact that a maximum of 7 trains is simultaneously supplied from the considered ETS and the regenerative braking power never exceeds 5 MW during one time instant. In such a scenario the algorithm has very little space to reduce the operation costs since there is no excess energy in the system. All that remains is the price variability, which is then exploited through charging and discharging of the energy storage system with little cost reductions (as shown in Figure 2.3.8). Highest savings are obtained for the case when no energy can be returned to the grid (0 MW) meaning that all of the regenerative braking energy that is not immediately used by other trains or stored in the energy storage system is dissipated and lost. In such a scenario there is a significant possibility of storing the regenerative energy for later use which results in cost reductions up to 35%. The behavior obtained with 0 MW grid receptiveness fully corresponds also to the behavior that

would be obtained if the return to the grid is allowed, but not paid by the grid, which is the actual current situation in Croatia.

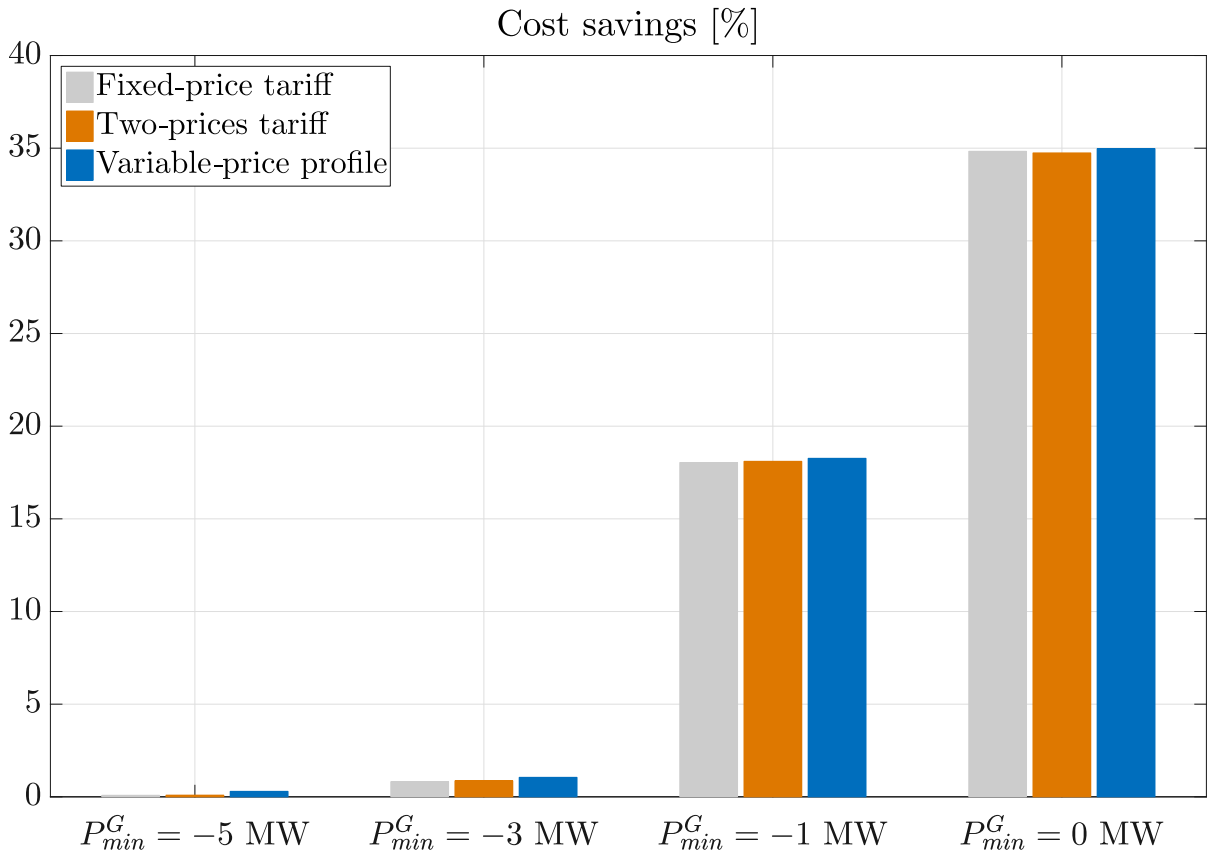

Figure 2.3.8 Cost savings for one-day system operation for different grid receptiveness P^G_{min}, with only HHL MPC installed.

2.3.7.1.4 Coordination between levels

After the introduction of both the LHL and HHL control systems, it is possible to hierarchically coordinate them with the main goal of further increasing the energy efficiency and decreasing the system operation costs.

The hierarchical coordination algorithm is simulated for the period between 13:00 and 14:00 hours with all together 13 trains supplied from ETS Andrijevci at some point during the one-hour period, according to the timetable. Due to the hourly energy exchange price, there are no price changes during the considered period, and the grid receptiveness level is set to 0 MW i.e. no energy can be returned to the grid. Scenario with no energy returned to the grid directly corresponds to the case found in Croatia where the energy returned to the grid is not reimbursed. The simulated system operation is depicted with (i) energy storage power flows (battery and supercapacitor charging/discharging) together with energy dissipated on the resistors, (ii) ETS power flows (summed energy consumption/production of all trains currently supplied from ETS Andrijevci) and (iii) energy storage SoC, all presented in Figure 2.3.9 and Figure 2.3.10 for the system operation before and after hierarchical coordination is employed.

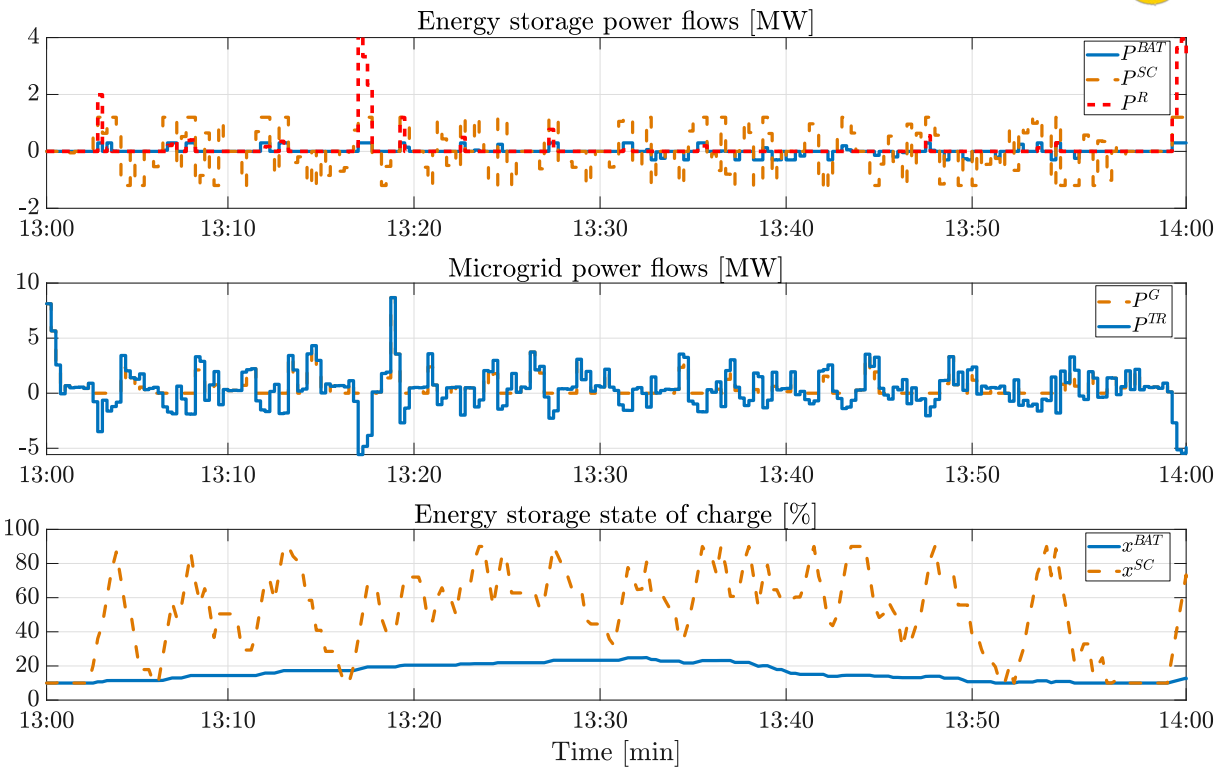

Figure 2.3.9 One-hour system behavior without coordination where only LHL solution θ^h is plugged into the HHL problem (17).

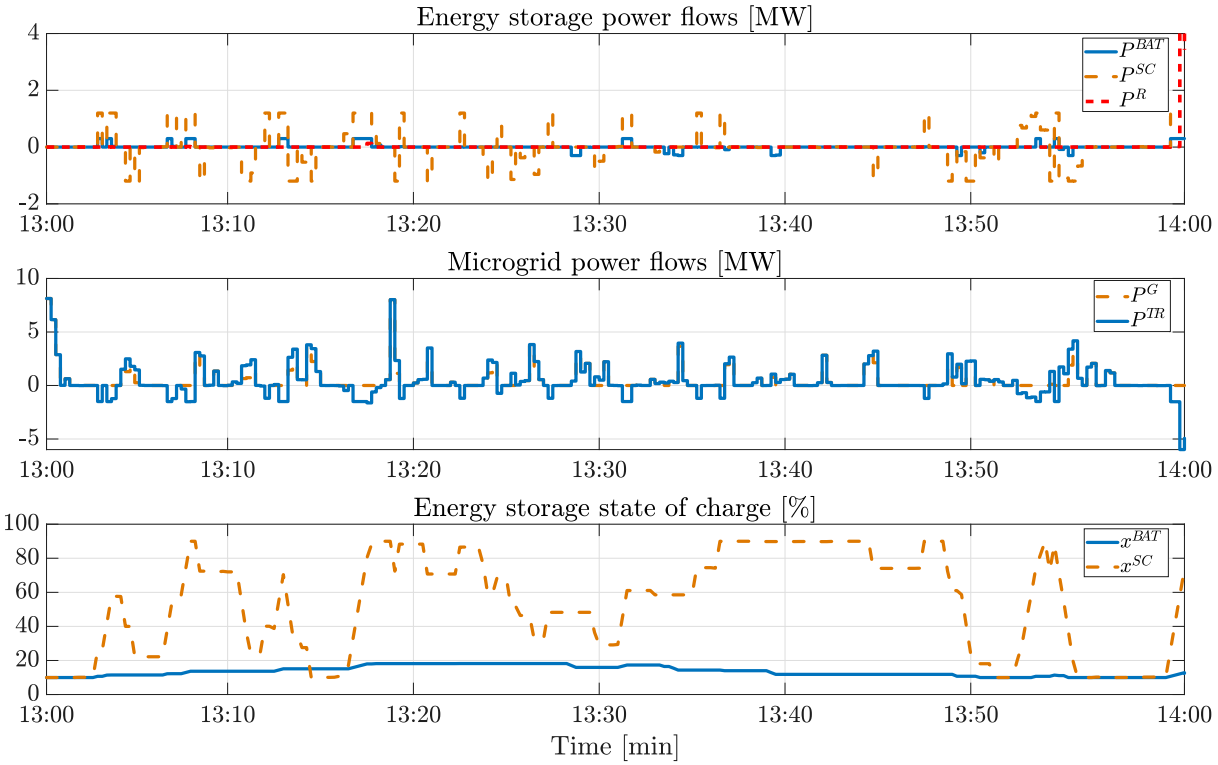

Figure 2.3.10 One-hour system behavior with hierarchical coordination between LHL and HHL employed.

From the results presented in Figure 2.3.9 and Figure 2.3.10, the following is observed: (i) the coordination between the control levels reduces the amount of energy that is being unused (dissipated in the resistors, presented with red line in first plots of both figures) through simultaneous coordination of different trains and their acceleration and deceleration while respecting the previously set timetable constraints, (ii) the peaks of produced regenerative energy are reduced as the regenerative energy production from a single train is being distributed towards other trains that are able to accelerate during that period (presented with blue lines in middle plots of both figures) and (iii) it is also observed that the use of the energy storage systems is reduced since their operation causes energy losses due to energy efficiency of the storage technologies (presented in red and orange lines in first and last plots of both figures). Reduced energy storage usage brings additional benefits in terms of storage system health preservation and extended equipment lifetime.

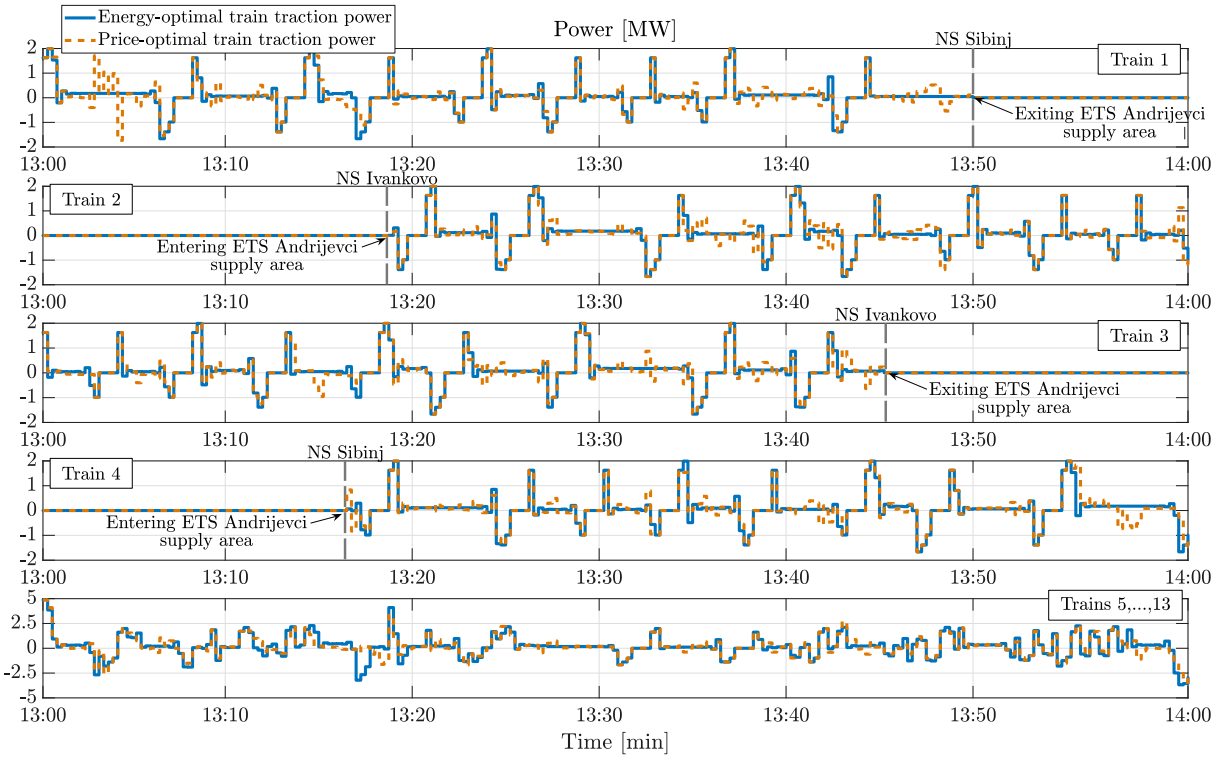

Figure 2.3.11 Power consumption profiles of all trains supplied from ETS Andrijevci, before and after hierarchical coordination, for a one-hour system operation.

Power consumption of individual trains during this one-hour simulation period is presented in Figure 2.3.11, individually for four trains that are supplied during the most of the one-hour period, and cumulatively for the remaining 9 trains. Previously mentioned assumptions are confirmed, the neighbouring trains exchange energy and cooperate in order to reduce system operation costs. Such energy exchange between trains can be seen when more trains are in braking and therefore generate a large amount of energy that is then consumed by other trains currently supplied from the same ETS, which are now deviating from their initial traction profiles in order to consume that energy. Although these trains then operate with a suboptimal traction profile and actually consume more energy, the system benefits from this interaction between trains since most of the regenerative braking energy would be dissipated if the trains would not be coordinated. This behaviour can be seen in Figure 2.3.11 where e.g. Train 1 speeds up at 13:03 to consume the energy generated by the

remaining trains and reduce the cumulative regenerative energy peak (subplot 5), or where trains 3 and 4 brake early at 13:15 and 13:17, respectively, to shift their consumptions profile and reduce the overall regenerative energy production from 13:17-13:18 (subplot 5). Although the trains initial traction profiles are changed when the trains take into account the declared price profile, state of energy storages and various power grid requests, the schedule remains unchanged and operational constraints are respected.

In order to fully investigate the contributions and savings possibilities of hierarchical coordination between energy flows and consumption levels, different variations are introduced to the initial simulation set-up, with corresponding cost and energy consumption reductions compared and results presented in Figure 2.3.12. Cost and energy reduction quantities in all cases are obtained through comparison with the costs and energy consumption of system operation without the HHL control and with trains driven in energy-optimal ways. Results obtained via solely MPC applied to higher level control with energy-optimal traction profiles applied for individual trains, but without coordination are then compared with the baseline case and compared to the results achieved with coordination in order to investigate what the coordination brings in terms of cost and energy efficiency. Presented results show that the energy consumptions reductions reach up to 40% while the costs are reduced up to 45%, as presented in Figure 2.3.12.

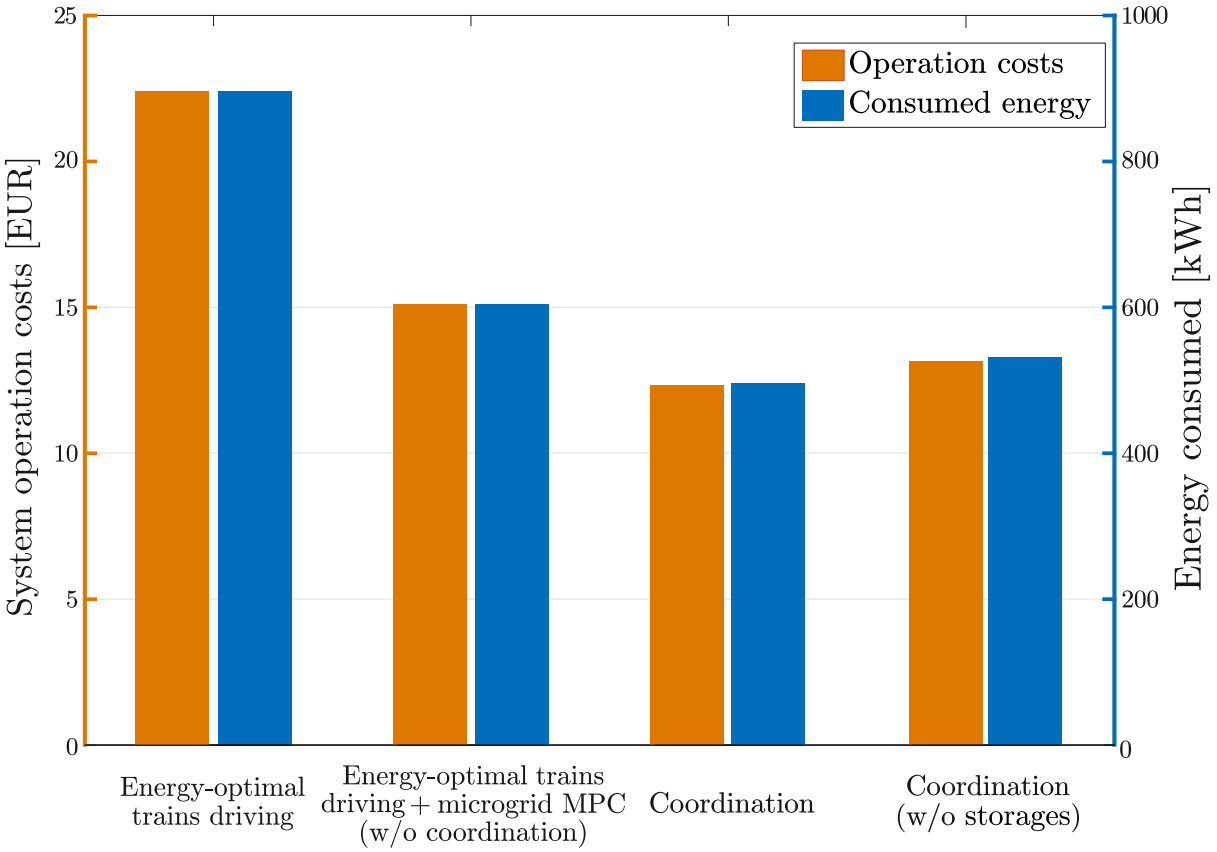

Figure 2.3.12 Energy consumption and system operation costs for different control setups for the one-hour system operation.

An additional simulation case has been added to the setup, in order to investigate system operation without energy storage systems implemented and with coordination between the levels. From the results presented in Figure 2.3.12 it is observed that software-based coordination on the lower level can eliminate the need for storages, since the cost reductions are only slightly decreased when no energy storage systems are installed in the system. Although such control system setup does not provide the best possible results, it also does not require large financial investments for installation of energy storage systems. It is therefore more close to implementation on actual railway systems and shows an important advantage of the analyzed hierarchical coordination.

2.3.8 Flexibility provision study

Possibility of flexibility provision by the electrified rail system is analyzed in a simplistic way for the purpose of this case study. The flexibility provision is considered for the same conditions as for the building, however for only one 15-minute interval since the numerical demands of the optimization procedure keep the simulation scenario on a one-hour timescale from 13:00-14:00.

From the grid side only one flexibility interval is assessed:

- 13:15-13:30

The prices determined for flexibility are:

- 0.027 EUR/kW/(15 min) for flexibility reservation
- 0.109 EUR/kWh for flexibility activation
- 0.219 EUR/kWh penalty for non-delivered flexibility within the 90% threshold with respect to the activated flexibility

The day-ahead electricity price is constant and set to 0.016 EUR/kWh.

Simplified analysis is performed in a way that the optimization is performed with disregarding flexibility provision in order to compute the optimal overall cost of the electrified rail transport system operation. Then the optimization was performed with enforced consumption during the flexibility interval to the maximum value (through setting a very small electricity price during the interval, <0.001 €/kWh) – in this way the declared consumption profile of the system for the case of flexibility provision is assessed. Finally, the optimization was performed with enforced minimal consumption during the flexibility interval through setting a very large electricity price during the interval (>100 €/kWh). When flexibility is activated, in the electricity cost also the cost for deviation from the declared energy consumption is accounted (deviation is priced with 20% higher prices than day-ahead prices).

Possible flexibility of the electrified rail system obtained in this way for the selected grid flexibility interval is as follows:

- for 13:15-13:30: -1.057 MW

The results of the three optimizations are summarized in the following table.

Table 2.3.4 Economical analysis of hourly operation with flexibility provision

	1: Operation without flexibility provision	2: Operation with reserved flexibility, but not called	3: Operation with reserved flexibility called in the entire amount
A: Electricity consumption cost (including deviation from the declared amount for 3.) [EUR]	7.99	8.97	23.01
B: Hourly gain for flexibility reservation [EUR]	-	28.56	28.56
C: Hourly gain for flexibility activation when called in the entire amount [EUR]	-	-	28.82
D: Overall hourly electricity cost (A-B-C) [EUR]	7.99	-19.59	-34.37
Hourly gain when flexibility is not called (D1-D2) [EUR]		27.58	
Hourly gain when flexibility is called in full amount (D1-D3) [EUR]		42.36	

From the table it follows that it pays off to the electrified rail transport system to participate in the flexibility provision scheme: if flexibility is not called it has a reduced overall cost of operation by 27.58 EUR; if flexibility is called (activated) by the grid in full amount the rail system has a reduction of daily operation costs by 42.36 EUR. Considering that the overall hourly electricity cost is on the level of 10 EUR, the decrease induced by flexibility provision is very significant and it reverses the money flow between the rail system and the electricity provider even without flexibility provision service activation. It is also important to keep in mind that the electrified rail transport system is connected to the transmission grid where the energy amounts are usually measured in a MW scale rather than the kW scale which is expected on the distribution grid level. Since the flexibility reservation and activation prices are determined for the distribution grid level, the flexibility amount of 1 MW is significantly rewarded by the grid operator.

The optimized daily electricity consumption profiles in the performed analysis are shown in Figure 2.3.13. The optimal operation without flexibility provision is denoted with ‘Optimal’ in the graph, the operation of the system when flexibility is not called is represented with ‘Declared’ in the graph, and the operation of the system when flexibility is called in maximum amount is represented with ‘Activated’.

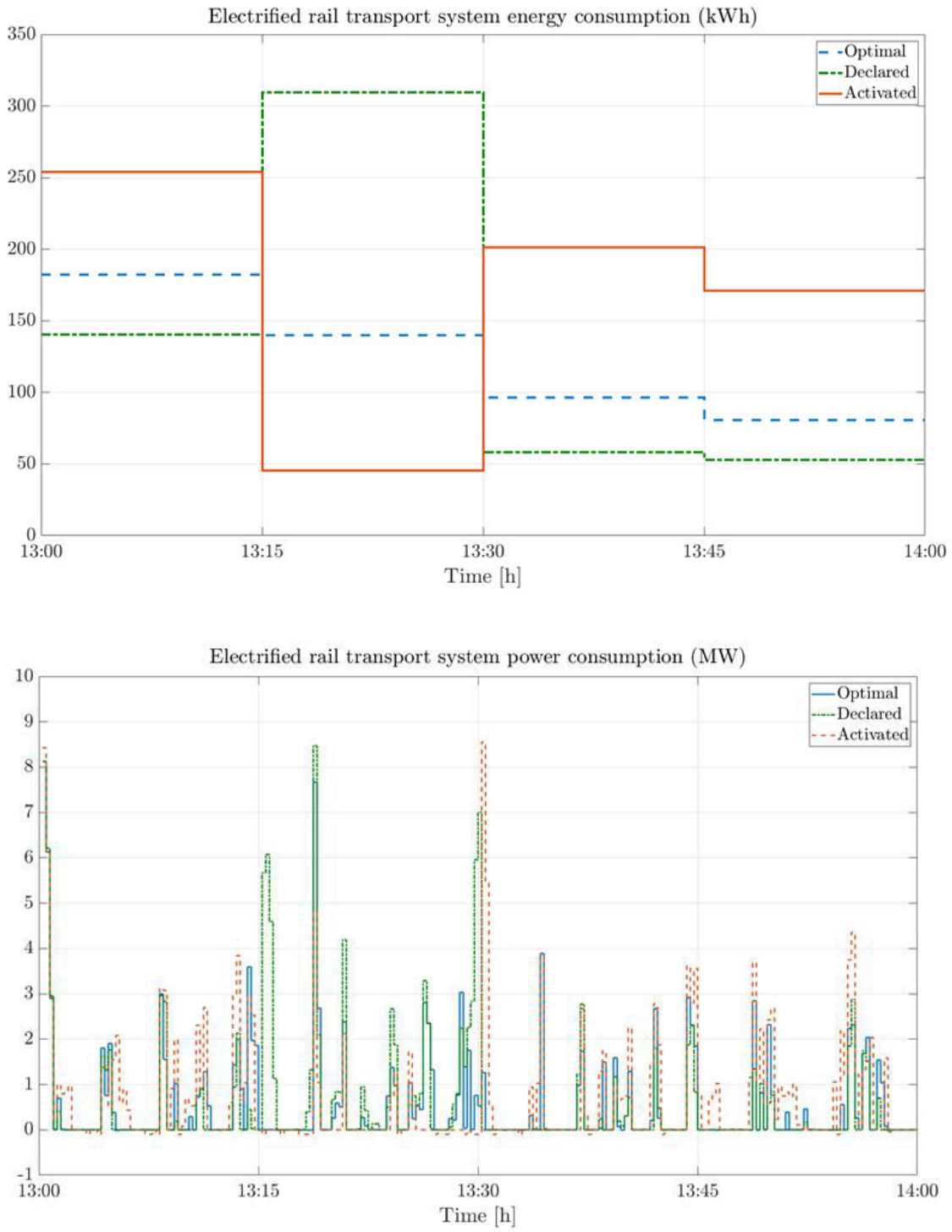

Figure 2.3.13. Electrified rail transport system grid energy and power exchange for: (i) optimal operation without flexibilty provision ('Optimal'), (ii) optimal operation with only flexibility reservation ('Declared') and (iii) optimal operation with flexibility activation in full amount ('Activated').

2.4 Electric vehicles charging infrastructure

Transition from classic traffic systems to electrified ones has a direct effect on reducing pollutant emissions (NO, NOx, SOx), reducing CO2 emissions and reducing noise levels. The current, and certainly the future, available propulsion technologies have a significant potential to radically change and improve public transport as well as personal cars transport, which still represent a very large share in the overall transport scheme of the city of Zagreb, in a holistic approach to a sustainable transport system. As part of the solution, it is also necessary to plan and map the need for electric vehicles charging stations and the integration with the power system, which will map the existing and future needs for the electric vehicle charging infrastructure, as well as take into account the slow and fast charging stations, as potential advanced solutions in terms of battery replacement for electric vehicles. Based on the anticipated needs and the existing capacity of the power system it is necessary to propose and conceptualize the long-term development of the Zagreb power system in cooperation with the Distribution System Operator in order to comply with future EV infrastructure needs. Integration of EV charging stations linked to public buildings in energy-efficient buildings (prosumers) is planned to achieve as low as possible the cost of charging the vehicles for end-users, including public buildings charging stations in an information system that will be able to announce the arrival of vehicles and the anticipated conditions of the work of other energy systems in the building as soon as the prices are lowered, the possible integration with Zagrebparking services, the competition of buildings while selling electricity to vehicles, the introduction of peer-to-peer trading of buildings and vehicle owners, based on blockchain technology.

HEP Group has in its possession 22 electric vehicles distributed throughout the Republic of Croatia, of which 5 Volkswagen e-Golfs, 7 Volkswagen e-Ups, 5 Peugeot Partners and 5 Peugeot Ions.

A total of 50 electric vehicles charging stations were set up throughout the development project EAST-E in several Croatian cities. Most of these are AC 2x22kW charging stations, while 6 of them are AC / DC charging stations (50kW DC, 43kW AC). At all of these charging stations two vehicles can be charged at the same time, at a speed that is independent of the strength of the charging station. It only depends on the inverter in the vehicle itself. For the project, the most important charging station is in Stjepan Radić square on the parking lot of the City government which, in addition to the AC / DC charging station itself, also has solar panels overhangs of about 3kW. The meter of this metering point is bi-directional, so it can power the charging station and also return the produced electricity to the grid.

In addition to publicly available charging stations built through HEP's development project, there is a charging stations system in HEP's business garage built for own needs. It is a master unit that can simultaneously charge two vehicles DC 50kW (CHAdeMO) and AC 43kW, and another 6 wall-box units of AC 3.7kW which are controlled (start and end of charge) via master interface.

Charging stations mentioned above (in HEP's garage and in the parking lot of the City government) are still not connected to any software remote control system, and still do not have great energy management capabilities.

Regarding Li-Ion batteries in HEP's vehicles which were purchased 3-4 years ago, Volkswagen e-Golfs have batteries of 24 kWh, while Volkswagen e-Ups have batteries of 18.7 kWh.

For the case study we opt for the scenario with a fleet consisting of 25 vehicles. Each vehicle has assumed availability and starting SoC for the moment it is connected to the charger. Vehicle connection and disconnection times are selected in the times of the day people usually come from and go to work. In simulation results, vehicle initial SoC when connecting to the system is a random number from interval [0.2, 0.8], while SoC is limited to [0.2, 0.9]. Other limitations are power ratings as 3.5 kW for individual device link and 50 kW for overall energy consumption of the fleet. The efficiency of the charging and discharging are assumed to be 0.9 and 0.75. Capacity of the battery is set to C = 10 kWh. At the moment when leaving the charging station, the vehicle SoC is required to be equal to 0.9, i.e. fully charged battery. Charging and discharging battery amortization costs are used as 0.004 EUR/kWh and -0.007 EUR/kWh.

The starting results presented show simulation for a two-day period with a time step Ts = 15 min and prediction horizon 6 hours. In Figure 2.4.1, results of centralized LP optimization for one vehicle are presented. All local constraints are satisfied. Availability of EV is a binary variable indicating when a vehicle is connected to the charger. In the figures, it is scaled for better visual representation.

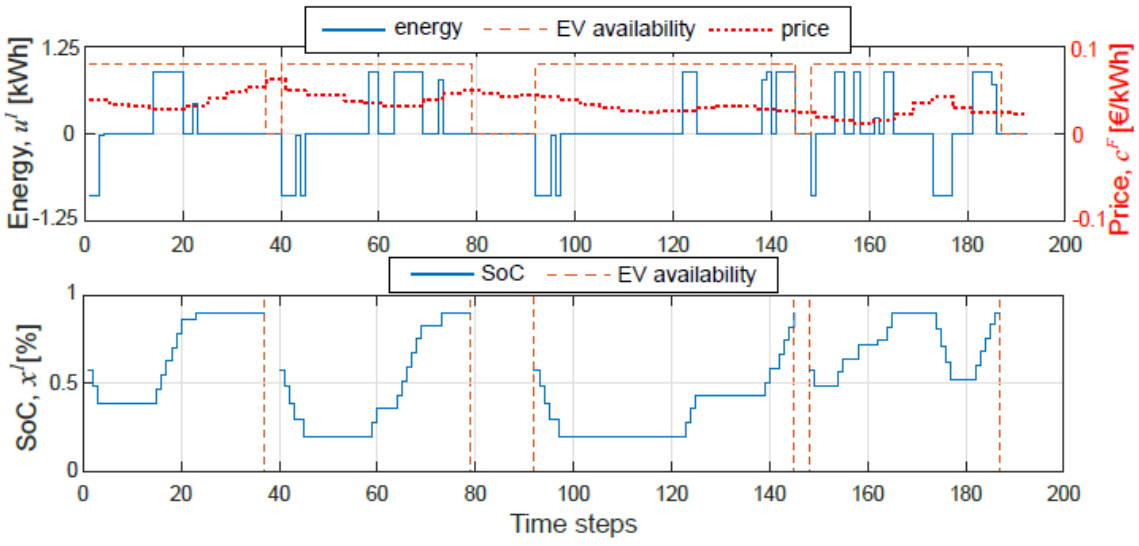

Figure 2.4.1 Centralized linear program solution for all vehicles, presented a result for one of the 25 vehicles used in the scenario.

Here the results are extended such that there is a presumed microgrid level optimization which again computes local perturbation costs for the cumulative energy exchange profile

created by the charging stations, and the lower level here will be a simple linear program that computes the optimal charging profiles for all the vehicles. Through coordination the charging profiles are assessed and respective flexibility the charging infrastructure can offer.

2.4.1. System configuration

Electrical vehicles charging system is an extension of building microgrid with dynamic but predictable availability of vehicles and vehicle batteries to be added to the building microgrid for building hierarchical energy management. The vehicle batteries not only vary in availability but are also different in size, capacitance, efficiency, type, i.e. the parameters, as illustrated in Fig. 2.4.2.

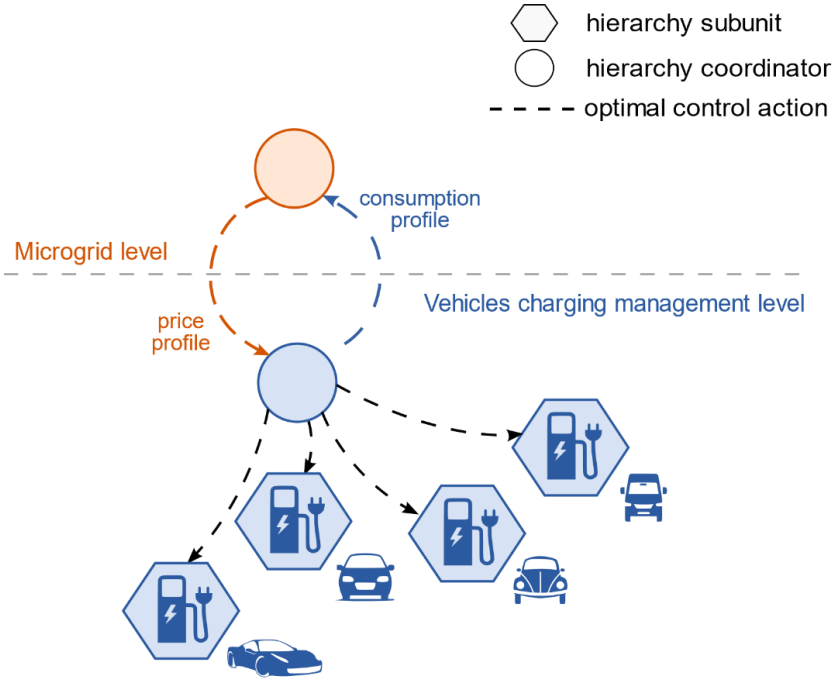

Figure 2.4.2. Proposed methodology of optimal control with dynamic reconfiguration of problem structure for building microgrid and battery charging problems.

In particular, we consider the microgrid as a higher hierarchy level that provides prices and joint constraints for the electrical vehicles charging control problem. The microgrid optimisation problem is simply formed as minimisation of cost for energy exchange with the grid, E_{g}:

$$J^{\mu*}(\mathbf{u}^F) := \min_{\mathbf{u}^\mu} \sum_{k=0}^{n-1} c_{g,k} E_{\mathrm{g},k}, \qquad (32)$$
$$\text{s.t.} \quad \mathbf{G}^\mu \mathbf{u}^\mu \leq \mathbf{w}^\mu + \mathbf{F}^\mu \mathbf{u}^F,$$
$$E_{\mathrm{g},k} = u_k^F + \mathbf{1}_d^\top d_k^\mu + \mathbf{1}_u^\top u_k^\mu,$$

where $\mathbf{G}^\mu$, $\mathbf{w}^\mu$ and $\mathbf{F}^\mu$ are microgrid constraints, $\mathbf{d}^\mu$ is a vector of energy productions of different generation units in the microgrid, $\mathbf{u}^\mu$ is the microgrid control variable and $\mathbf{1}_d$ and $\mathbf{1}_u$ are appropriately sized vectors of ones.

The problem (32) can be more complex to include different layers of pricing such as reduction of maximum power, announced day-ahead profile following or intra-day deviations as energy market incentive as described. The microgrid and fleet charging/discharging problems are connected through the vehicles coupling constraints:

$$\mathbf{G}^F\mathbf{u}^F \leq \mathbf{w}^F, \tag{33}$$

which are constraints of the critical region of multi-parametric solution of (32).

Table 2.44.1 Energy storage system parameters.

Parameter	Description	Value
N	Number of vehicles available at the same time	25
T_s	Sampling time	15 minutes
C	Battery capacity	ranging from 5 to 20 kWh
η_{ch}	Charging efficiency	ranging from 80 to 90%
η_{dch}	Charging efficiency	ranging from 80 to 90%
SoC_{min}	Minimum allowed SoC	ranging from 0.1 to 0.2
SoC_{max}	Maximum allowed SoC	ranging from 0.9 to 1.0
P_{min}	Minimum allowed charging power	ranging from 3 to 5 kW
P_{max}	Maximum allowed charging power	ranging from 3 to 5 kW
E_g	Connection to grid	50% of total capacity for 25 vehicles
SoC_{fin}	SOC at the time of disconnecting from building	0.9

2.4.2. Battery charging model and optimisation problem

From the perspective of high-level energy management systems, vehicle charging is described through the dynamics of its battery. Batteries are modelled via state-of-charge (SoC) dynamic equation:

$$x_{k+1}^i = x_k^i + \frac{1}{C^i}\left(\frac{1}{\eta_{dch}^i}E_{dch,k}^i + \eta_{ch}^i E_{ch,k}^i\right), \tag{34}$$

where $k \in \mathbb{Z}$ is the sampling time index, C, E and η denote storage capacity, energy and efficiency, respectively. Electric vehicles are indexed with i. Energy and efficiency are separated to discharging and charging components, $E^i_{dch} \leq 0$ and $E^i_{ch} \geq 0$, which avoids high calculation complexity of a mixed-integer problem formulation under some mild assumptions. Equation (1) is reformulated into state-space representation suitable for model predictive control (MPC) standard form:

$$x^i_{k+1} = A^i x^i_k + B^i u^i_k, \tag{35}$$

where x^i_k is a vehicle batteries SoC vector, $u^i_k = [E^i_{ch,k},\ E^i_{dch,k}]^\mathsf{T}$ is a vector of energies, exchanged between the microgrid and the charger, from time instant k to $k+1$, while A^i and B^i are corresponding model matrices. The sampling time for the model discretisation should be large enough to disregard the transients on energy links, but smaller or equal to the sampling times of price and behaviour predictions.

Chargers are bidirectional, connected to the buildings microgrid and are considered in the building energy management strategy. A control system decides when and in which amount to charge or discharge the battery, meaning to buy or sell energy from/to the microgrid link towards the chargers. The goal of the charging/discharging control system on the vehicle is to minimise the charging cost under the given constraints. There are multiple constraints related to storage capacity, power ratings and microgrid link towards the chargers.

Microgrid connection capacity is put in the constraints form:

$$P_{min} T_s \leq u^F_k \leq P_{max} T_s, \tag{36}$$

where $u^F_k = \sum_{i=1}^{N} u^i_k$ is the total EV fleet consumption in time step k, N is the number of vehicles in the fleet and T_s is the sampling time period. If vehicle i is not connected to the microgrid in the moment k, then energy $u^i_k = 0$. Limits P_{max} and P_{min} are the maximum power that charging system can take from (P_{max}, positive sign) and give back to (P_{min}, negative sign) the microgrid. The system is often designed not to withstand the peak operation of all chargers at the same time. Furthermore, each charger has own individual constraints. Power ratings of individual chargers form constraints:

$$u^i_{min} \leq u^i_k \leq u^i_{max}, \tag{37}$$

where u^i_{min} and u^i_{max} are 0 if the vehicle is not connected to the charger. To avoid damage or rapid degradation of the car battery, SoC is only permitted to be inside the recommended working limits, i.e. in any time instant, the following constraint has to be satisfied:

$$x^i_{min} \leq x^i_k \leq x^i_{max}. \tag{38}$$

If the vehicle is leaving the charging station at the time instant k, then the state x_k has to be equal to x_{final}, making sure that the vehicle need is met. In a form of constraints that is:

$$x^i_k = x^i_{final}, \quad if \quad k \in z^i, \tag{39}$$

where z^i are instants at which the vehicle gets disconnected from the charger. The conditions (35), (36),(37),(38) and (39) form an overall set of constraints that should be satisfied while minimising the cost function.

A conventional centralised approach takes all the constraints within the same problem formulation and minimises the cost function. Two types of cost functions are considered here, linear and quadratic. The optimisation problem for achieving the smallest charging cost is formed as a linear program (LP):

$$J := \min_{\mathbf{u}} \mathbf{c}^\top \mathbf{u}, \quad \text{s.t.} \quad (35), (36), (37), (38), (39) \tag{40}$$

or quadratic program (QP):

$$J := \min_{\mathbf{u}} \frac{1}{2}\mathbf{u}^\top Q\mathbf{u} + \mathbf{c}^\top \mathbf{u}, \quad \text{s.t.} \quad (35), (36), (37), (38), (39) \tag{40}$$

where $c \in \mathbb{R}^N$ is a price vector containing prices for all vehicles in one interval, Q is a multiplication factor of vehicles consumption influence on the price and in this case it can be set to a constant value. In the simulation scenarios, $Q = \frac{C}{N}$ is chosen, where C is a small arbitrary constant determining the significance of the quadratic term and N is the number of vehicles. Bold notation stands for vectors stacked over the prediction horizon n.

The microgrid takes into account the grid energy price and its other subsystems when forming the price towards the chargers. The energy exchange price c^F, can be forwarded by the microgrid as a volatile market electricity price or transformed to shift the battery charging process towards the overall building cost-optimum . Volatile energy market electricity prices can be found at e.g. European Power Exchange company portal. It is assumed that grid price for energy is equal for buying and selling, which may not be the case in practice. It serves as an amortisation that compensates increased battery outwear due to a higher number of charging cycles. Consequently, the price vector is composed of two components:

$$c^\top = [c_{ch}, c_{dch}]^\top, \tag{9}$$

where $c_{ch} = c^F + c_{bat,ch}$ and $c_{dch} = c^F + c_{bat,dch}$.

From Fig. 2.4.3, which shows simulations of the total energy exchanged with the microgrid (u_k^F) for $N = 25$ vehicles, it can be seen that there is no significant difference in overall energy consumption plan between the LP and QP for a small quadratic term Q. Simulation runs for two days with a time step $T_s = 15$ min. The vehicles are selling the energy when the price is high and anticipated disconnecting time is far, while buying energy when the price is low or imposed by system constraint for fully charged battery (x_{final}^i) when disconnecting. This shows that a simpler LP performs as good as QP and therefore it is sufficient for the centralised case. In the sequel, the LP formulation is used while QP formulation is suitable for distributed problem optimal control.

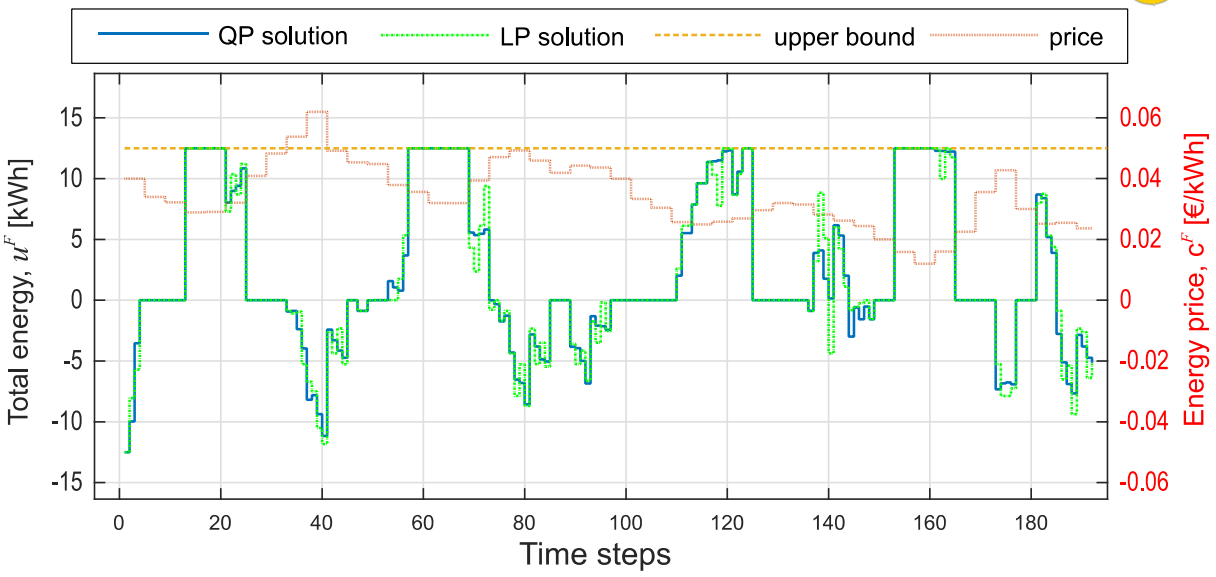

Figure 2.4.3 Result comparison of LP and QP for a fleet with 25 vehicles.

2.4.3. Results

Figures 2.4.4 and 2.4.5 illustrate the behaviour of EVs charging station for three selected EVs and total energy exchanged with the building microgrid during 5 consecutive days. Following from Fig. 2.4.4, every EV is charged to SOC = 0.9 before disconnecting from the building charger, which is illustrated as red binary signal of EV availability. The charging and discharging profile (SOC) follows the electricity price for every individual EV such that the sum of energy for all vehicles is following the optimal behaviour, which can be seen in Fig. 2.4.5 and compared with the electricity prices. The prices are in this case volatile and changing hourly, taken from EPEX portal for year 2014.

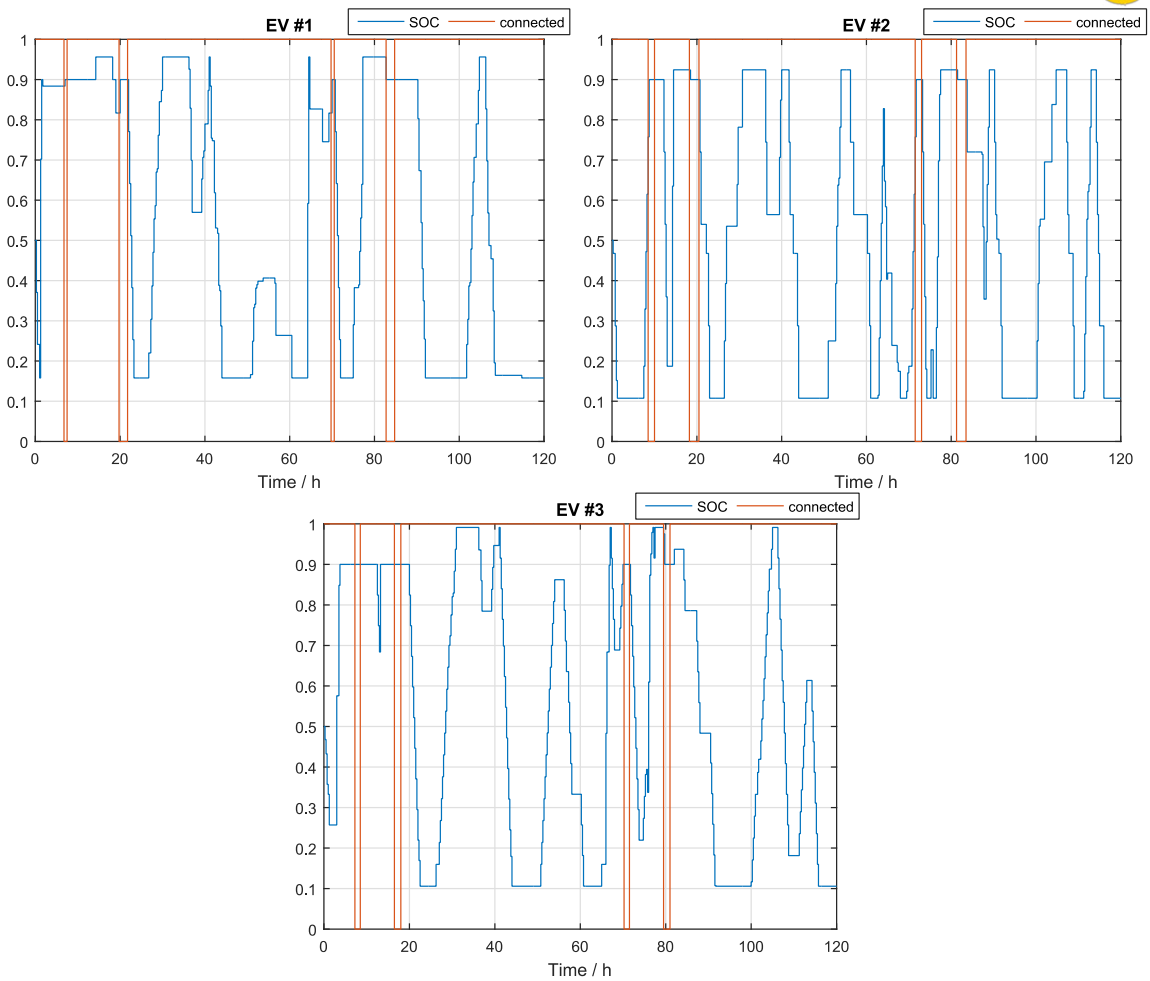

Figure 2.4.4 Illustrative case for three selected electrical vehicles.

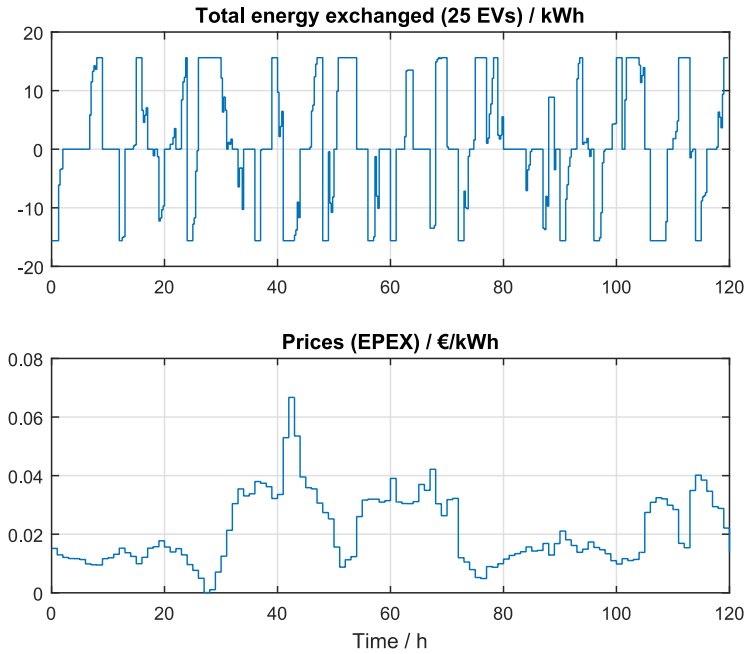

Figure 2.4.5 Total energy exchange between charging stations and building / grid compared to the volatile pricing.

2.4.4. Flexibility provision study

Possibility of flexibility provision by the electric vehicles charging system is analysed in a simplistic way for the purpose of this case study. The flexibility provision is considered for the same conditions as for the building and water distribution system, i.e. as follows.

From the grid side the following flexibility intervals are assessed:

- 11:30-11:45
- 13:00-13:30
- 14:30-15:00

The prices determined for flexibility are:

- 0.027 EUR/kW/(15 min) for flexibility reservation
- 0.109 EUR/kWh for flexibility activation
- 0.219 EUR/kWh penalty for non-delivered flexibility within the 90% threshold with respect to the activated flexibility

The day-ahead electricity price is used from EPEX portal for year 2014.

Simplified analysis is performed in a way that the optimization is performed with disregarding flexibility provision in order to compute the optimal overall cost of the electrical vehicles batteries system. Then the optimization was performed with enforced all input flows in the flexibility intervals equal to the maximum value – in this way the declared consumption profile of the EVs for the case of flexibility provision is assessed. Finally, the optimization was performed with enforced all input flows in the flexibility intervals to be minimal (i.e. attain negative, discharging values). When flexibility is activated, in the electricity cost also the cost for deviation from the declared energy consumption is accounted (deviation is priced with 20% higher prices than day-ahead prices). For this case, EVs are disconnected randomly between 6 am and 10 am, for the following 5–9 hours, and returned with randomized SOC, from 20% to 90%. The total SOC of all vehicles is set to 50% at the beginning and at end of the day.

Possible flexibilities of the considered electric vehicles charging infrastructure obtained in this way in the three grid flexibility intervals are as follows:

- for 11:30-11:45 : -29.2909 kW
- for 13:00-13:30 : -56.5226 kW
- for 14:30-15:00 : -107.2532 kW

The flexibility contribution to the results are very dependent on the time schedule of EV availability and the chosen timing of flexibility intervals. For the chosen intervals, EV schedule is more beneficial to commercial than residential buildings. The total possibility for the current case, when all 25 EVs are plugged, is -125.0 kW. The results of the three chosen optimizations are summarized in the following table.

Table 2.44.2 Economical analysis of daily operation of the considered EVs with flexibility provision. Positive sign denotes economic cost while negative sign of cost denotes economic gain in operation (earned money).

	1: Operation without flexibility provision	2: Operation with reserved flexibility, but not called	3: Operation with reserved flexibility called in the entire amount
A: Optimized electricity consumption cost (including deviation from the declared amount) [EUR]	0.663	1.246	1.2985
B: Daily cost for flexibility reservation [EUR]	-	–9.635	–9.635
C: Daily cost for flexibility activation when called in the entire amount [EUR]	-	-	–9.724
D: Overall daily electricity cost (A+B+C) [EUR]	0.663	–8.389	–18.060
Daily gain when flexibility is not called (D1-D2) [EUR]		7.726	
Daily gain when flexibility is called in full amount (D1-D3) [EUR]		17.397	

From the table it follows that it pays off to the EVs to participate in the flexibility provision scheme: if flexibility is not called per day it has an increased overall gain of operation by 9.635 EUR; if flexibility is called (activated) by the grid in full amount the EV charging system has an increase of daily operation gains by 17.397 EUR. Considering that the overall daily electricity cost is on the level 0.6 to 1.3 EUR, the increase induced by flexibility provision is very significant. Batteries are inherently suitable for providing flexibility, which is evidently reflected in the results. The results do not incorporate battery degradation, which may be easily taken into account as 1 day represents 1 cycle of the operation. Therefore, the gains are decreased by cca 1/5000 of battery value with 5000 cycles as full life span of Li-Ion batteries, which yields approximately 4 EUR for UNIZGFER pilot batteries setup. As an overall conclusion, the operation of EVs connected to the grid without utilizing flexibility option is not profitable.

The optimized daily electricity consumption profiles in the performed analysis are shown in Figure 2.4.6. The optimal operation without flexibility provision is denoted with ‘Optimal’ in the graph, the operation of the system when flexibility is not called is represented with ‘Declared’ in the graph, and the operation of the system when flexibility is called in maximum amount is represented with ‘Alternative’.

One may also see from Figure 2.4.6 that flexibility in batteries also means the storage system needs to carefully balance with the flexibility and prepare itself for the reserved interval (time span from 10:00 until 11:15), which introduces deviation costs from declared day-ahead profile. The costs are not reflected significantly to the final gain as the flexibility gains are much higher.

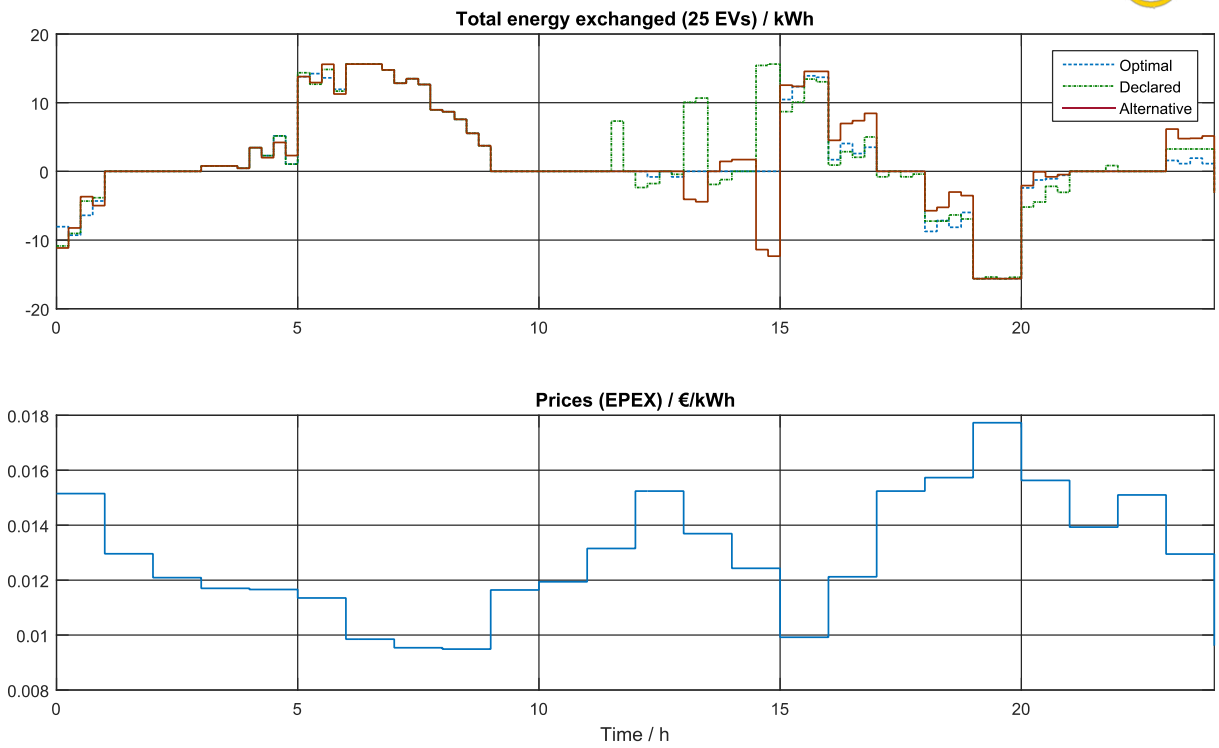

Figure 2.4.6. EV energy consumption profiles for the cases of: optimal operation without flexibility provision ('Optimal'); operation when flexibility is just reserved, but not called ('Declared'); and for the cases when flexibility is reserved and called in maximum amount ('Alternative').

2.5 Central heating distribution system

Description of the district heating systems operated by HEP in Croatia

HEP-Toplinarstvo d.o.o. (HEP District Heating) is a member of HEP Group that performs the activities of production, distribution and supply of heat energy as well as the activities of a heat energy buyer for households and industrial entities in the areas of the cities of Zagreb, Zaprešić, Samobor, Velika Gorica, Sisak and Osijek. The company consists of four (4) operative areas: Heating Networks Operations, Special Boiler Plants Operations, Osijek Operative Area and Sisak Operative Area. Heating Networks Operations, the biggest unit operating on the territory of the city of Zagreb, is supplied by heat energy from two Zagreb CHP plants (EL-TO and TE-TO) via the district heating system. The Special Boiler Plants Unit operates on the area of the cities of Zagreb, Zaprešić, Samobor and Velika Gorica. It consists of autonomous boiler rooms and a sealed heating system.

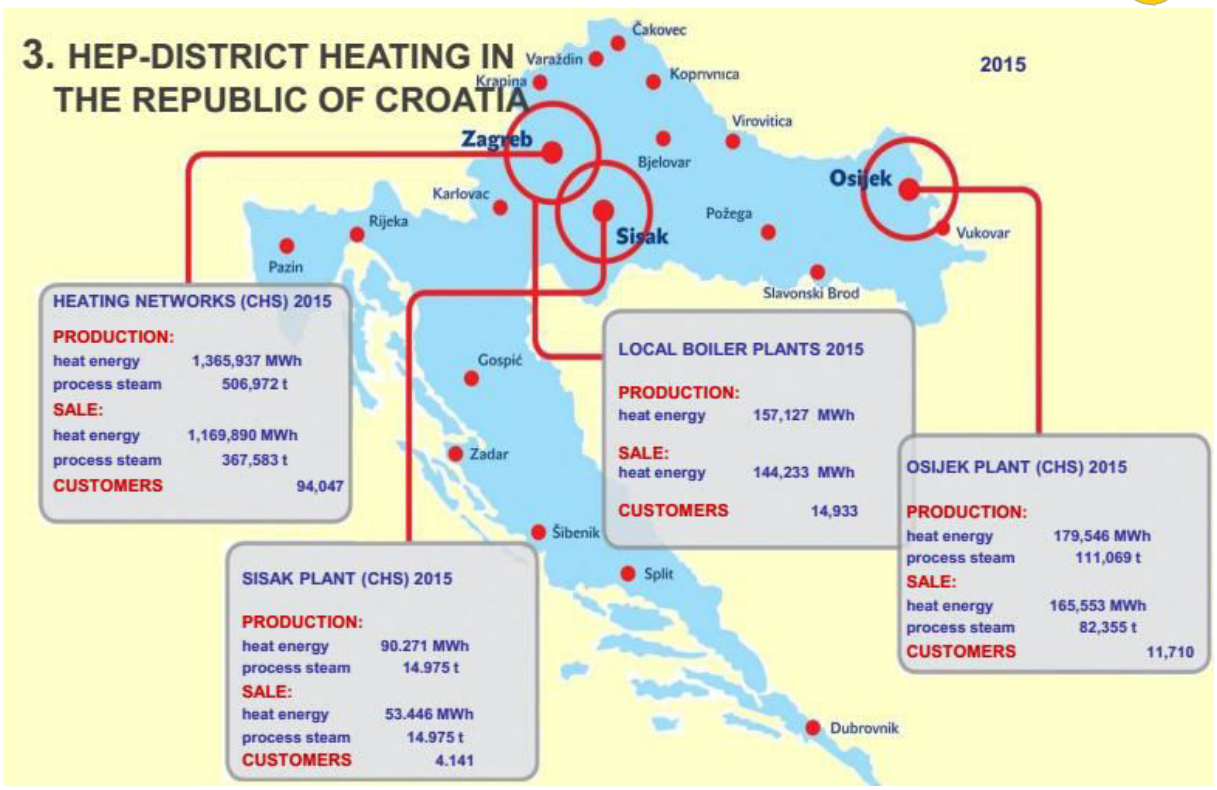

Figure 2.5.1: HEP-district heating in Croatia.

Development of heating in Zagreb

The district heating system (DHS) in the Republic of Croatia has a long tradition, especially in the city of Zagreb. The first hot water pipeline in Zagreb was constructed and put into operation in 1954 connecting EL-TO CHP and 'Rade Končar' factory. The first steam pipeline was built in 1958 running from EL-TO CHP to 'Mladost' Swimming Pools. The DHS was primarily developed in the period from 1962 until 1970, when new cogeneration units in EL-TO and TE-TO CHPs were built followed by the expansion of the hot water and steam network. The DHS major development continued until 1985 keeping up with a growing number of citizens and the industry development of the city of Zagreb. It has continued post 1985 albeit at a slower pace.

A significant growth of Zagreb's DHS heating demand first occurred in 2002 by connecting the Gajnice suburban settlement, and then in 2004 by connecting the Prečko suburban settlement to the DHS of the city of Zagreb. 3,750 meters of steam pipeline was built in 2005 connecting the DHS to the University Hospital Center Zagreb.

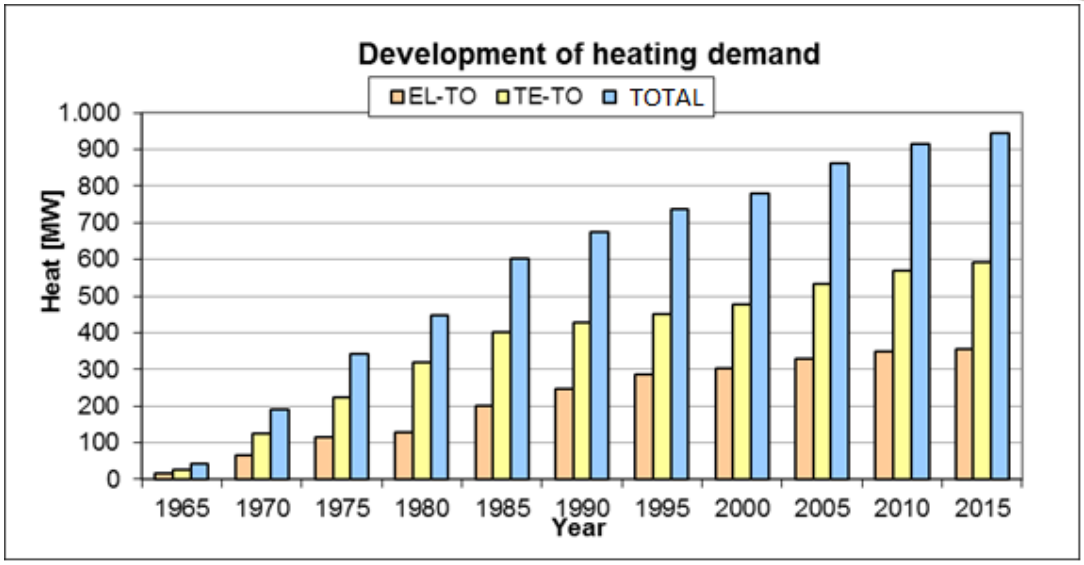

Figure 2.5.2: Development of heating demand from 1965 until 2015.

A further DHS development continued in 2011 by commencing the connection of the Dubrava suburban settlement to the DHS of the city of Zagreb, including the construction of about 16.3 km of new hot water mains and facilitating the network expansion to other settlements in the area. The Dubrava project has provided the supply of heat energy from the district heating system to the east part of the city supplied from autonomous boiler rooms. The replacement of the supply and the connection to the new DHS hot water network will result in reduced heat energy supply costs in that part of the city i.e. the supply of expensive heat energy from the unit and house boiler rooms will be replaced by cheaper heat energy from TE-TO CHP units.

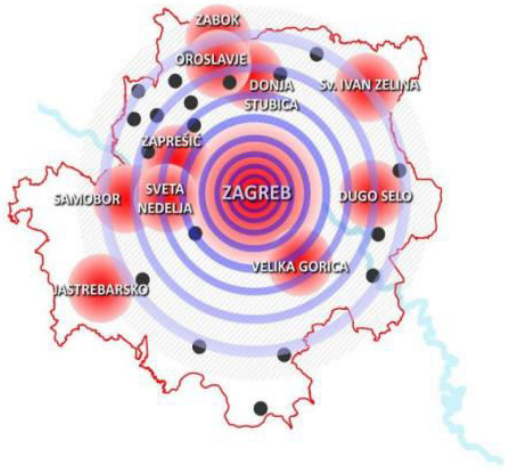

ZAGREB *Urban Agglomeration* – 11 cities: Zagreb, Donja Stubica, Dugo Selo, Jastrebarsko, Oroslavje, Samobor, Sveta Nedelja, Sveti Ivan Zelina, Velika Gorica, Zabok i Zaprešić and 19 municipalities as follows: Bistra, Brckovljani, Brdovec, Dubravica, Gornja Stubica, Jakovlje, Klinča Sela, Kravarsko, Luka, Marija Bistrica, Marija Gorica, Orle, Pisarovina, Pokupsko, Pušća, Rugvica, Stubičke Toplice, Stupnik i Veliko Trgovišće.

Figure 2.5.3: Zagreb Urban Agglomeration.

District heating system of the city of Zagreb

The district heating system of the city of Zagreb consists of the central steam and hot water system. Heat energy production capacities for hot water and steam district heating system are located on two sites: TE-TO CHP in Savica settlement and EL-TO CHP on Zagorska Street.

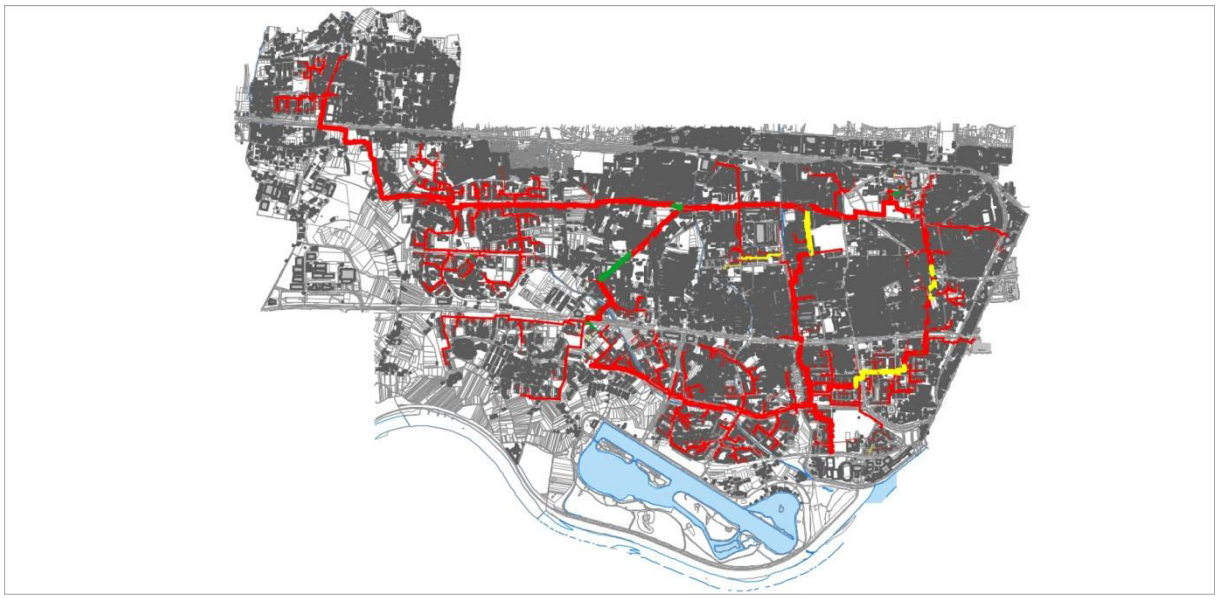

Figure 2.5.4: Hot water network West – supplied from EL-TO CHP.

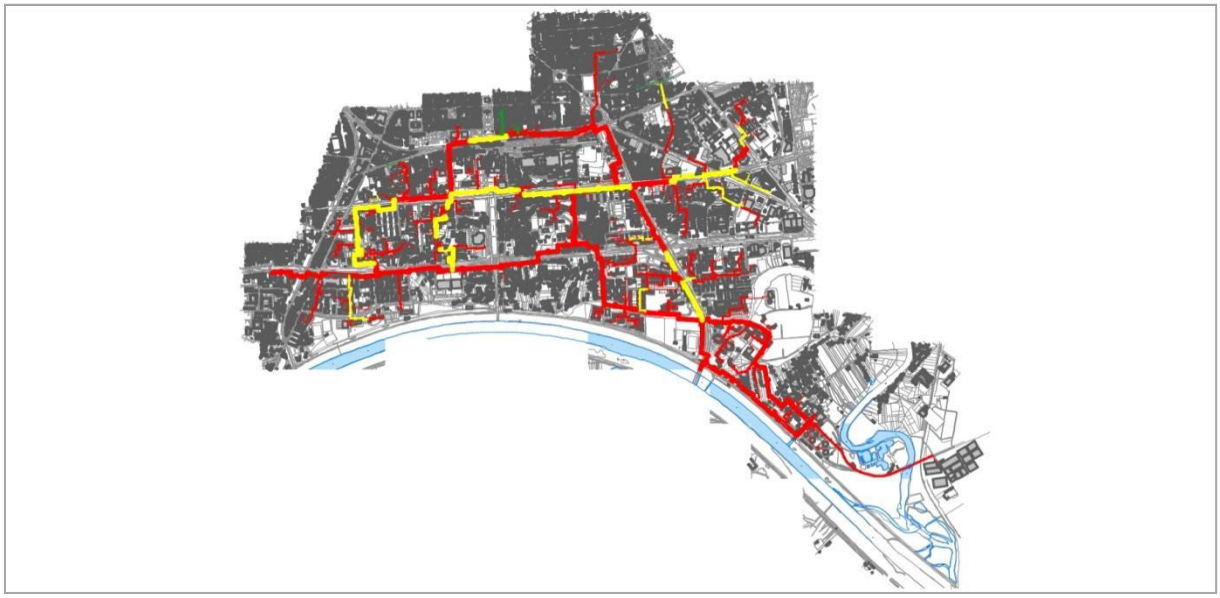

Figure 2.5.6: Hot water network South – supplied from TE-TO CHP.

Hot water distribution is conducted via a 268.6 km long hot water network (about 91 km of main lines and about 177 km of branches and connection points in settlements). The NPD structure of the hot water network mains ranges from DN200 to DN850, and of hot water branches and connection points from DN15 to DN200. While the mains account for 34% of

the overall hot water network structure, branches and hot water connection points cover the remaining 66%.

The hot water system of the city of Zagreb supplies heat energy for space heating and domestic hot water use to over 90,000 households and offices i.e. about 1/3 of the overall housing stock of the city of Zagreb. The total thermal power of the heating demand amounts to 1.120 MW. The existing hot water system is rather old, with some of its parts built more than 40 years ago. The average distribution-related energy losses of the hot water system account for 14.35 percent. Apart from those, there are also water losses incurred by the Zagreb hot water system of an average 57 m3/day. The hot water system is connected to 1,851 housing facilities with 2,199 indirect heating substations and 503 direct heating stations.

The hot water district heating system consists of a total of 268,602 km of lines (which is double the length of the feed and the return line), which differ by age and the construction method:

- About 48% of the system or 129.3 km of lines was either refurbished or initially constructed by using the ductless installation technology with pre-insulated pipes.
- About 9% of the system or 23.6 km of lines was built by using a traditional method of laying steel pipes in a concrete structure, insulated by mineral wool and a protective aluminium coat, age under 30 years.
- The remaining 43% of the system or 115.6 km of lines was built by using a traditional method of laying steel pipes in a concrete structure, insulated by a layer of mineral wool and a protective aluminium coat, more than 30 years old.

<u>Strategic determinants of further operation and development of HEP's central heating systems</u>

- <u>Production</u>
  - DIVERSIFICATION OF PRODUCTION PORTFOLIO
  - Optimization of HEP-Proizvodnja d.o.o.'s production systems - production should depend on meeting heat consumption needs
  - The analysis of the possibility for obtaining a status of an eligible electricity producer by facilities which production may be carried out as highly efficient cogeneration
  - The use of heat accumulators
  - The analysis of the possibility of electricity-generated heat, the analysis of the possibility to use alternative fuels on existing sites, production from RES, the use of heat pumps, by waste incineration.

- Distribution
  - Revitalization of the existing distribution hot water and steam network aimed at reducing distribution energy losses and refilling the system with process water; development of the condensate recovery system, where possible
  - Analysis of the possibility of introducing remote cooling (e.g. University Hospital Center Zagreb (KBC Zagreb) – steam cooling, absorption cooling system, c. 7 MWr)
  - Connecting new demand
  - Implementation of the IT monitoring and distribution network operation system
  - Implementation of the heat energy meter remote reading system and establishing the connection with the heat substation monitoring and control system
  - All the above complies with general objectives of EU's energy policy
  - The main objective is to reduce, cost effectively, the use of fossil fuels and CO2 emissions, as well as increase the security of customer supply
  - Central heating systems must be observed via a prism of integrated systems which include buildings as consumers as well as their energy characteristics, distribution network and production systems
  - Central heating systems are a natural part of urban infrastructure in the cities, they are not a novelty, however they provide a new meaning to practical solutions for reducing environmental pollution (cities account for 70% of EU's energy consumption)
  - The latest, 4th generation of central heating systems, enables city planners to increase energy efficiency while simultaneously increasing the possibility of producing heat energy from RES

Construction of a high-voltage boiler for low-pressure steam and hot water production

Due to the occasional low electricity prices (eg. weekend, holidays, vacations) on European stock exchanges, potential savings can be made using these, if the real market for this electricity could be found. EL-TO Zagreb supplies consumers with thermal energy 24 hours a day throughout the year. Therefore, it is justified to consider the possibilities of using electricity for the EES regulatory requirements, which are growing especially by increasing the share of renewable energy in electric energy production in Europe, and in cases of very low electricity prices even for CHS heating and steam production (less frequent). As the EL-TO Zagreb uses primarily gas for the supply of heat to consumers, it is also necessary to pay attention to contractual obligations with gas suppliers. The analysis carried out through the Feasibility Study of High-voltage Low-pressure Boilers concluded that the construction of electric boilers is a highly cost-effective investment. It achieves significant savings and benefits. Additional unquantifiable benefits of this kind of technical solution are:

- ''smoothening'' daily load curve; straighter curve - lower system costs and HEP's costs;

- the ability to provide EES balancing services, as well as balancing the gas system of the Republic of Croatia;
- lower emissions, the need to adopt HEP's production when it is forced to sell/export energy;
- substitution, virtual reversible power plant in RH system;
- extremely fast coverage of heat consumption in the event of failure or inability to start a production unit, so that consumers would not feel the disruption;
- the possibility of guaranteeing greater security in the heat supply;
- supply safety of heat consumers in case of gas supply interruption;
- maneuverability of electric boilers consumption;
- participation in the tertiary regulatory system:
    - Decrease, as well as increase of power;
    - Currently valid prices from HOPS-HEP Production contract;
- Payment by power and energy (engagement);
- Boilers work at full strength about 20% of the year, and are not engaged more than 50% of the year;
- Conservative estimate of possible income: approximately 250 thousand € per year

Approach for the case study regarding the district heating system in the considered city district

Heating energy supply is provided intensively between 06:00 and 22:00, and outside these hours it is also performed, but in reduced quantities. Thus every morning during the heating season a significant peak in consumption occurs at about 06:00 due to warming up of facilities by the end consumers which poses a significant pressure on the distribution system and of course causes higher losses. Technically calorimeters used for billing of thermal energy to end-customers already now record the consumption on the 15-minutes intervals and store it for approximately last 10 months such that the usage of time-shaped consumption for billing already has practical potentials without high technical barriers or needed investments.

The distribution system would especially benefit if the buildings can be coordinated on the district level such that they jointly reduce consumption in some period of the day or coordinate the instances of consumption between themselves which would enable that the temperature on the common distribution line towards the group of buildings can be reduced which then reduces losses for the distribution company.

Given next is the obtained day-ahead heat consumption under electricity flexibility provision for UNIZGFER building, for a sunny day in January.

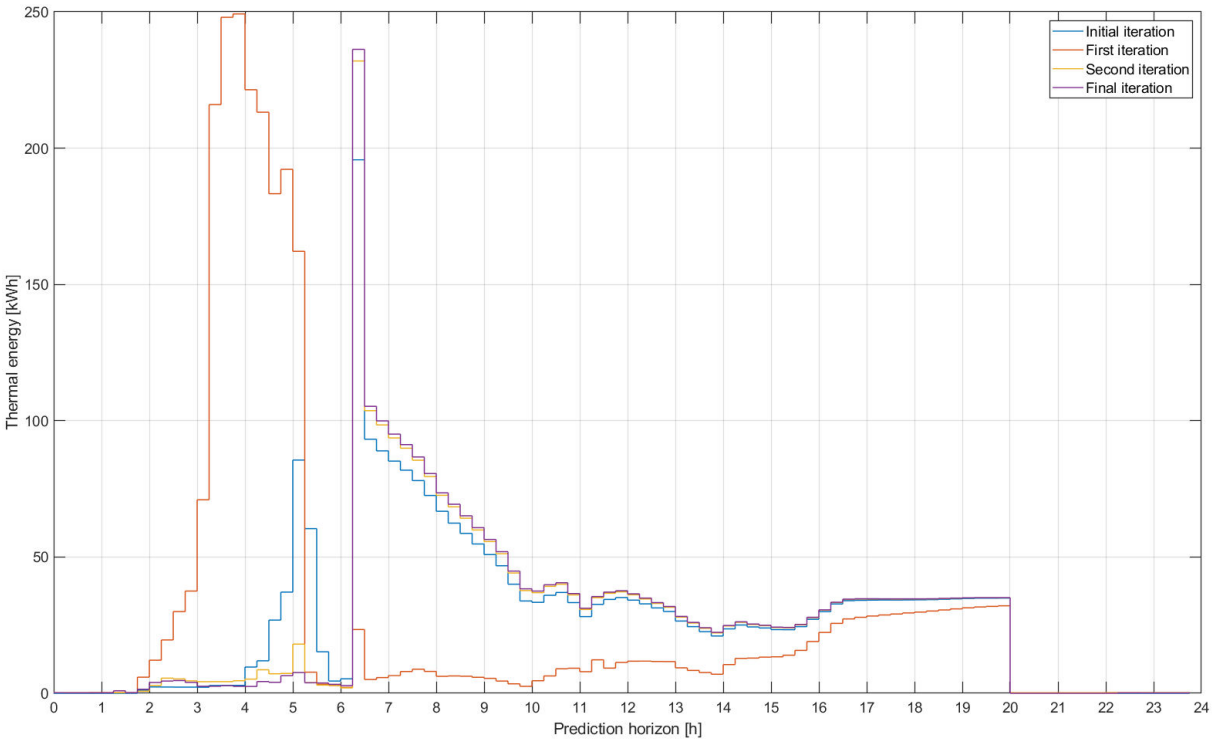

Figure 2.5.7: Heating energy demands: optimal operation (blue), declared heat consumption when electricity flexibility is not activated (violet) and the realized heat demand when flexibility is activated (red).

Figure 2.5.7 shows that the heating energy consumption can be efficiently displaced in time via pre-heating, if it pays off to the building – this would be especially so if favourable prices for night consumption would be in place.

2.6 City upscale load-flow analysis

The city upscale load-flow analysis includes:

- Voltage, current and power-losses calculations for feeder Savica for average workday in July
- Determining the optimal point of common coupling (CPP) for flexibility services providers
- New stages of the network with utilized flexibility services

Zagreb Savica is 30kV feeder with six 30kV/10kV substations with end-point customers. Input for load flow analysis are grid topology and technical specification, taken from national DSO, and load profiles based on correlated measurements from 2018. Figure 2.6.1 shows load profiles for all LV substation based on correlated measurements and voltage state of network. Basic case scenario for load flow analysis does not consider the consumption of water distribution system and EV charging station, only the UNIZGFER building consumption.

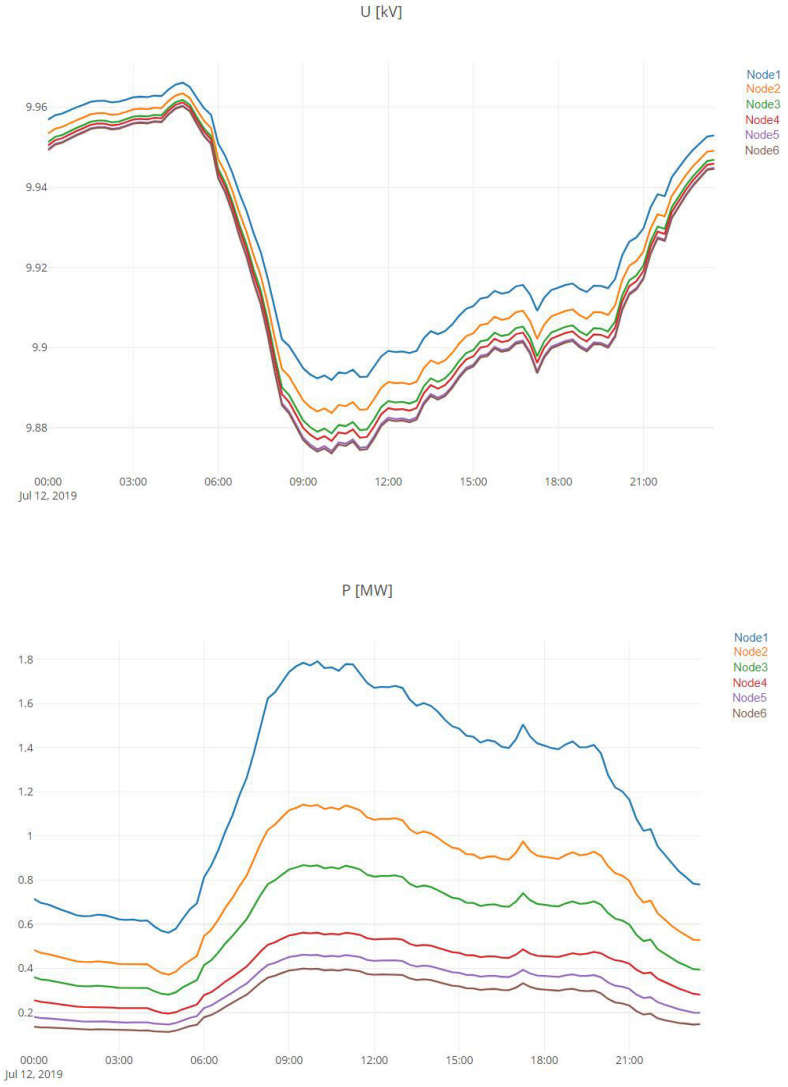

Figure 2.6.1 Voltage and active power stage of the feeder Savica

The network stages can vary for different points of connecting those customers to distribution grid. The point of common coupling (CPP) was determined for water distribution system and EV charging station based on Monte Carlo methodology. Total power losses were calculated for all possible combinations of CPP. The WDS and EV charging station electricity consumption was submitted to the different measured data of the observed node. In the case where EV charging station and water distribution system are connected at the begging of the feeder, the power losses were the least. Figure 2.6.1 shows that nodes at the begging of the feeder have the larger active power load and better voltage stage. The power losses are highest in the case where they are connected at the end of the network.

Analysis is based on AC optimal power flow calculation with the cost function to minimize power losses in the network. Optimization cost function is described in deliverable 5.2.1 "Short -term day ahead module". City upscale load flow analysis includes power loss comparison in the case of utilizing flexibility services and not utilizing flexibility services.

Four scenarios were used to compare:

- Scenario A – CPPs are at the begging of feeder (node 1) and flexibility services were not utilized
- Scenario B – CPPs are at the end of feeder (node 6) and flexibility services were not utilized
- Scenario C – CPPs are at the begging of feeder (node 1) and flexibility services were utilized
- Scenario D - CPPs are at the end of feeder (node 6) and flexibility services were utilized

In both scenario C and scenario D, AC OPF determined maximum capacity of offered flexibility services (Figure 2.6.2).

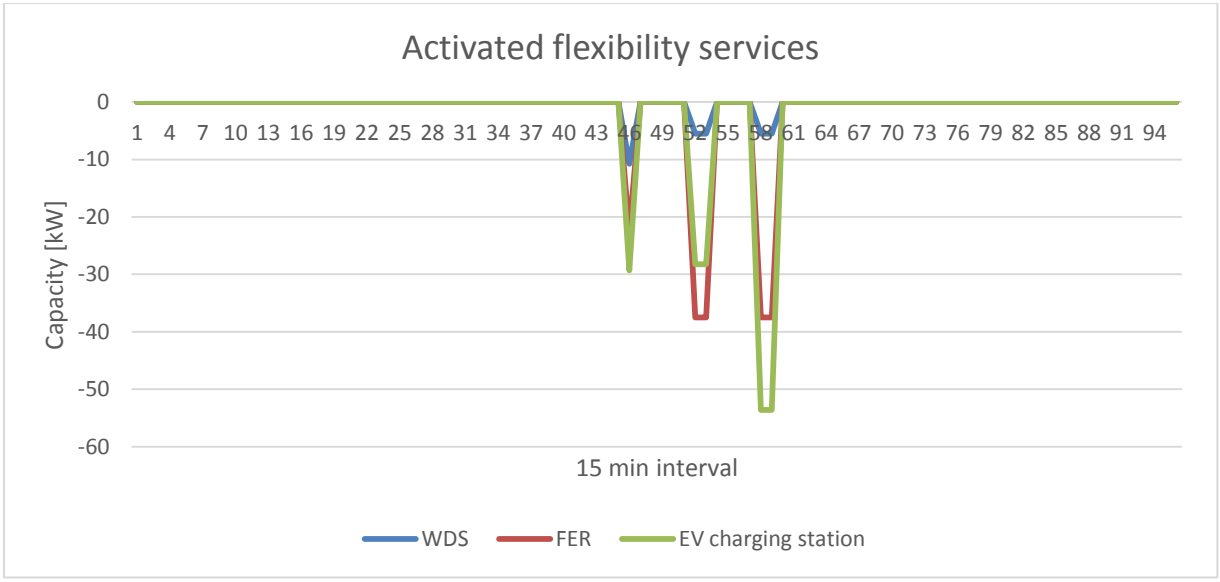

Figure 2.66.2 Utilized flexibility services

After utilizing flexibility services, the total power losses in the case where CPPs are at the begging of the feeder, drop 8.08%. In second case the total power losses drop 8.18%. Figure 2.6.3 shows how power losses changed during the day in all the scenarios. Charts for scenarios A and B, and, C and D, are slightly different due to small power loss differences.

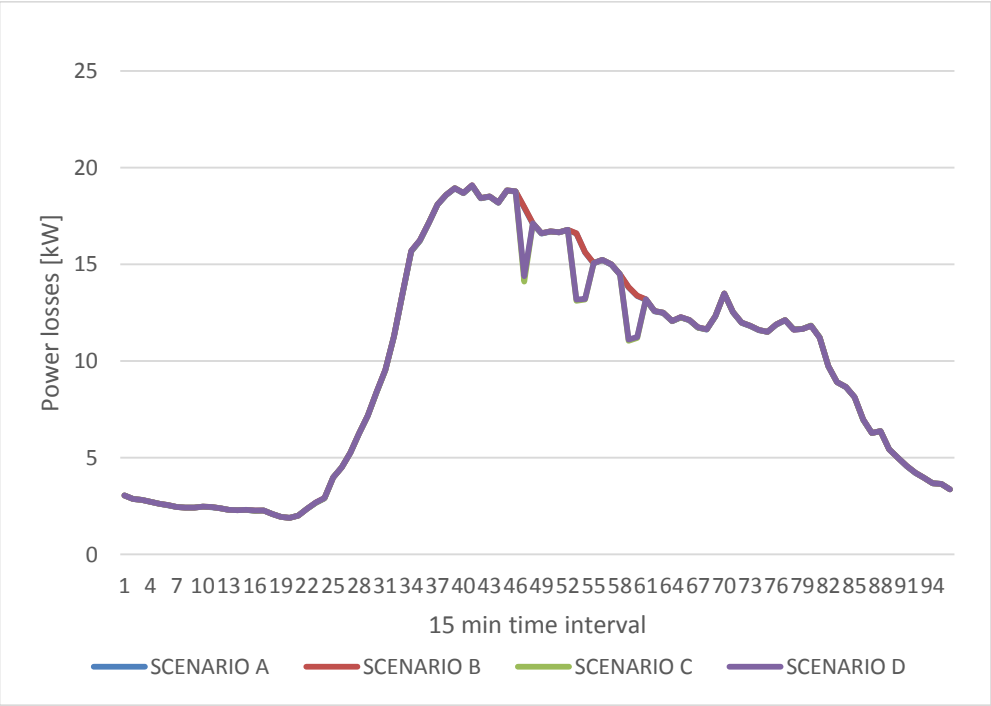

Figure 2.6.3 Distribution power losses

3 Idrija

There are two units in Idrija which are evaluated in case study for 3Smart EMS deployment:

- Mine pumping system,
- business and Households.

3.1 Infrastructure and other buildings included in technical analysis

In this section, the area under study is presented. Since there would be too much data to process and study for the whole town of Idrija, we focused on a region around the town centre, which we claim to be representative of the whole town. In the next picture, we see the main grid of transformer stations in Idrija and the highlighted circuit, which will be under study.

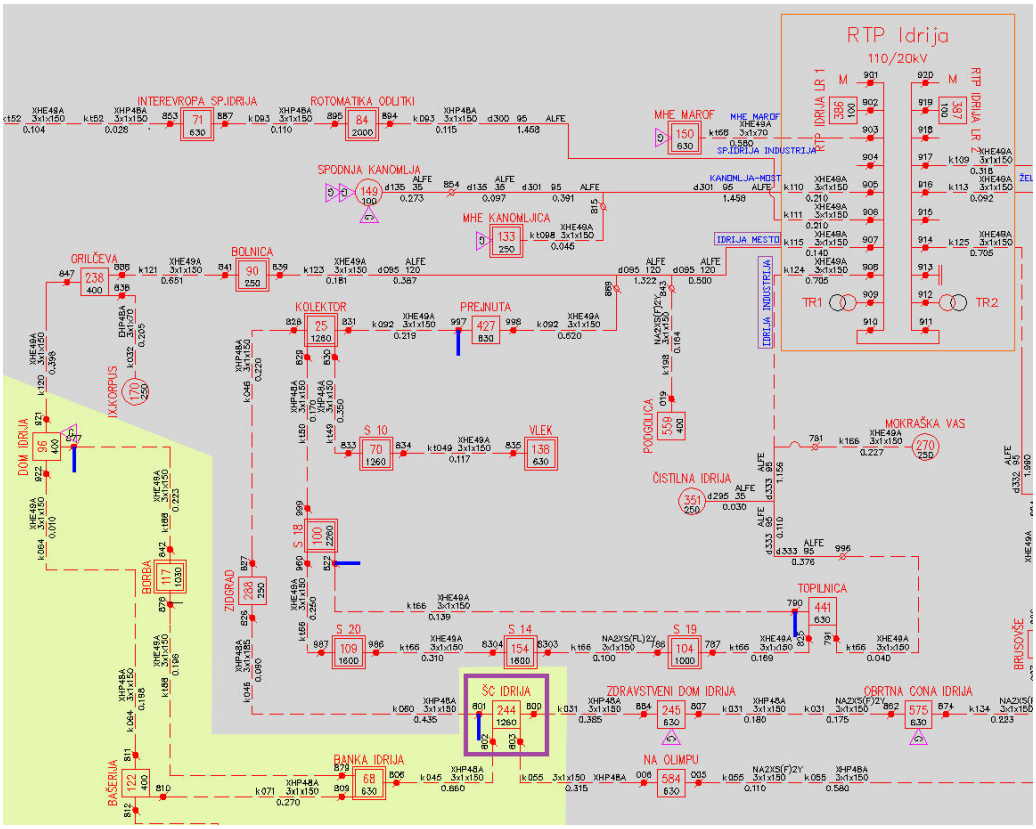

Figure 3.1.1: Electrical grid in Idrija.

We can see that we will focus on five main transformer stations (ŠC IDRIJA - 244, BANKA IDRIJA - 68, Bašerija – 122, DOM IDRIJA – 96 and BORBA – 117).

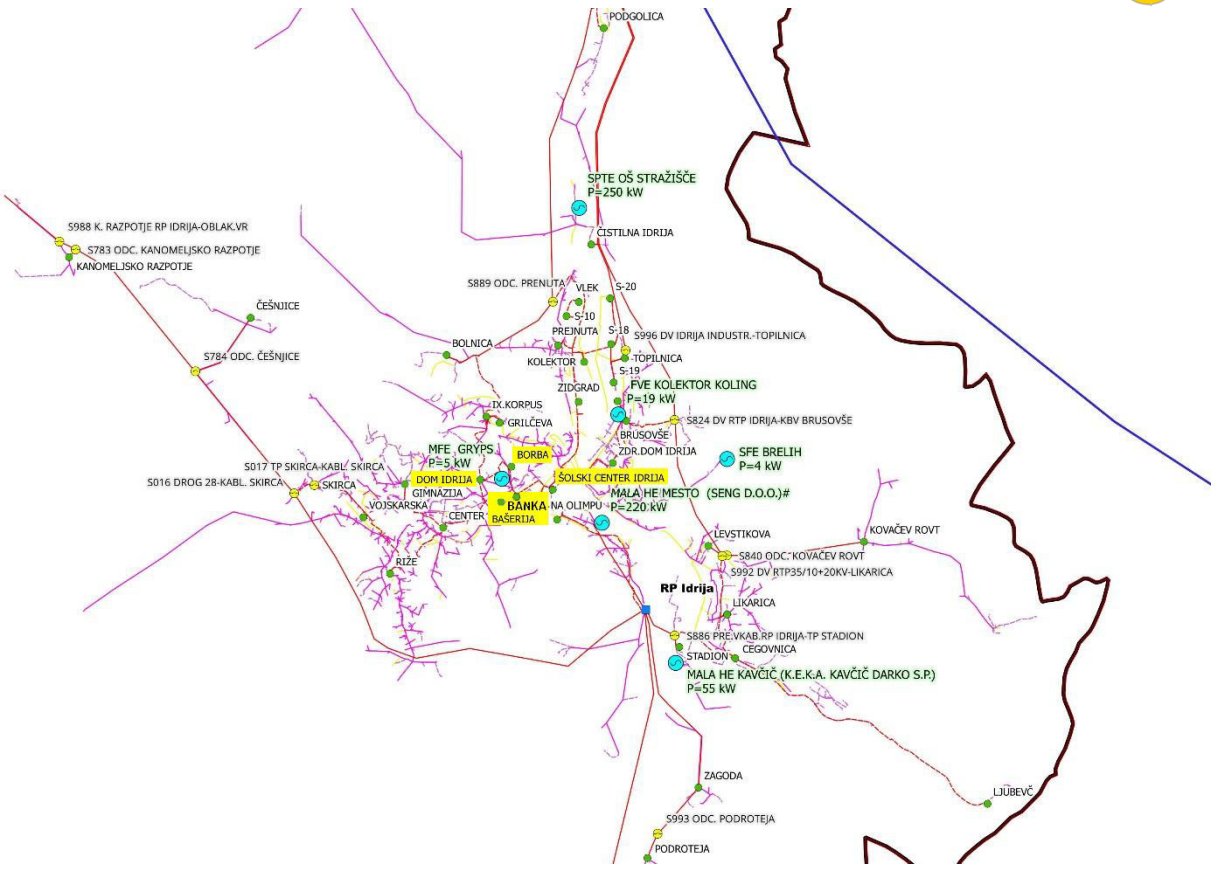

Figure 3.1.2: Schematic map of Idrija and its transformer stations with highlighted stations under study.

From the obtained data, we can extract that there is the total of 713 connection points included in this study in which there are 668 households, 41 smaller business customers, 1 bigger business customer and 3 street lightings.

3.2 Street lighting

Cost rates in Slovenia

There are three different electricity tariffs in Slovenia: Peak tariff ("Višja dnevna tarifna postavka - VT"), off-peak tariff ("Manjša dnevna tarifna postavka - MT") and flat rate tariff ("Enotna tarifna postavka - ET").

1. VT – high cost rates are charged every workday from 6:00 a.m. to 10:00 p.m. During the daylight saving time (DST) the high cost rates are also shifted for an hour, so they last between 7:00 a.m. to 11:00 p.m.
2. MT – low cost rates are charged any remaining time, at the weekends (Saturdays and Sundays) and at holidays from midnight to midnight.
3. ET – Unified cost rates apply for the customer, who uses one-rate measuring device or decides to use one-rate way of charging his consumption. This type of rate is charged equal at all times.

Data analysis

In this section, the analysis of the street lighting electrical energy consumption is made. All the analysed data is collected in intervals of 15 minutes from year 2017. The connection points included in the study are listed below.

Connection point ID number	Address	Yearly consumption [kWh]
7-1263	Lapajnetova ulica 48	29014
7-1407	Ulica IX. korpusa	7151
7-1244	Grilčeva ulica	875

Table 3.2.1: Connection points of Street lighting.

Let us now look at these street lightings locations on the Idrija's map.

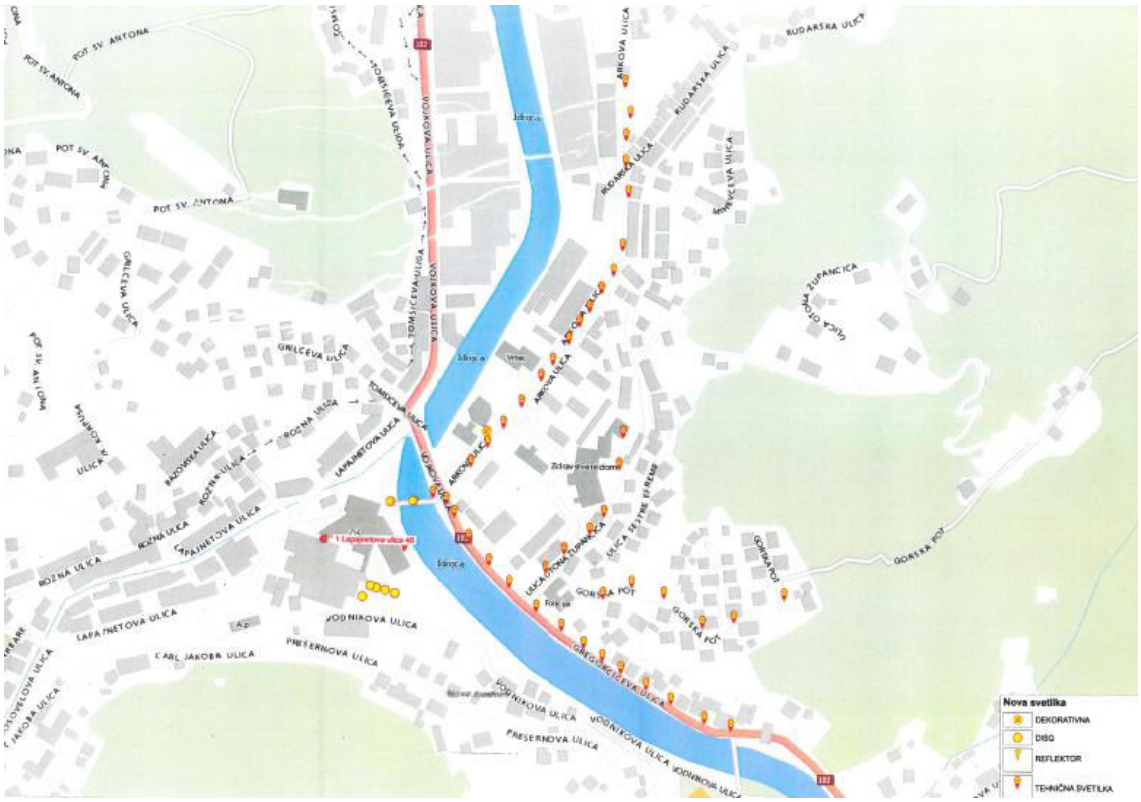

Figure 3.2.1: Street lighting 1263 on Lapajnetova ulica.

Figure 3.2.2: Street lighting 1407 on Ulica IX. Korpusa.

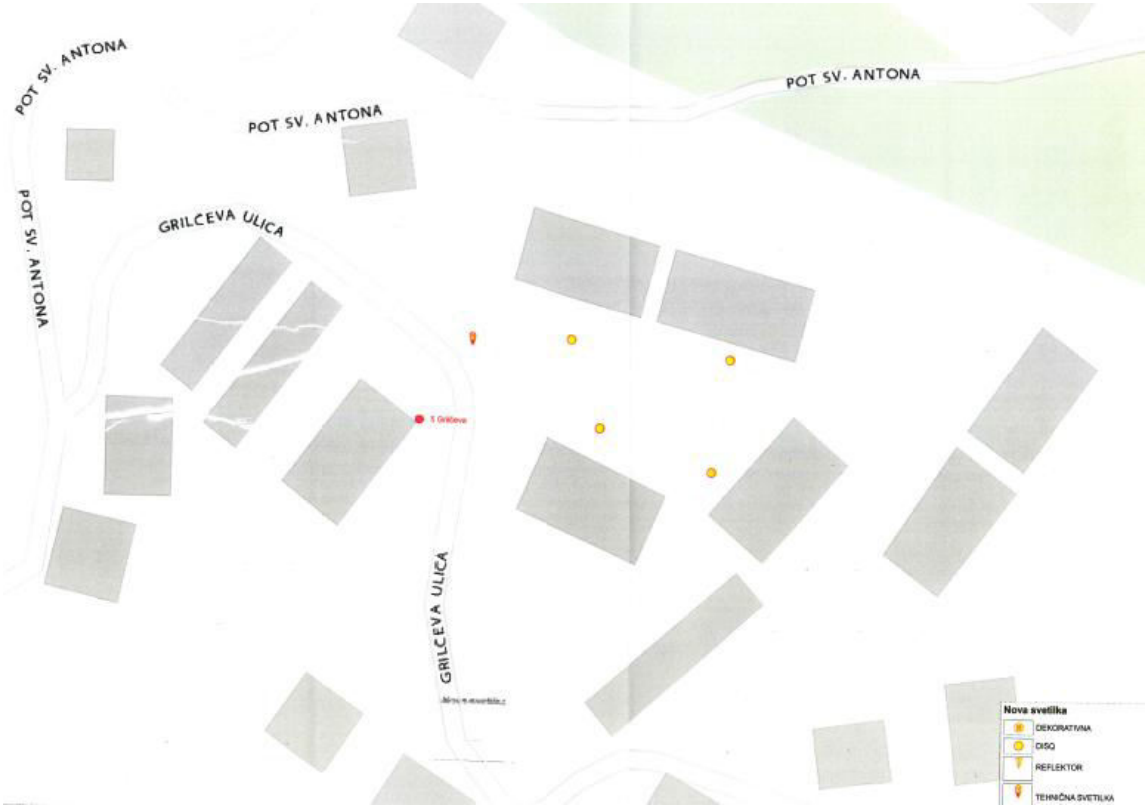

Figure 3.2.3: Street lighting 1244 on Grilčeva ulica.

To get the feeling of the energy consumption course, some daily profiles are shown below.

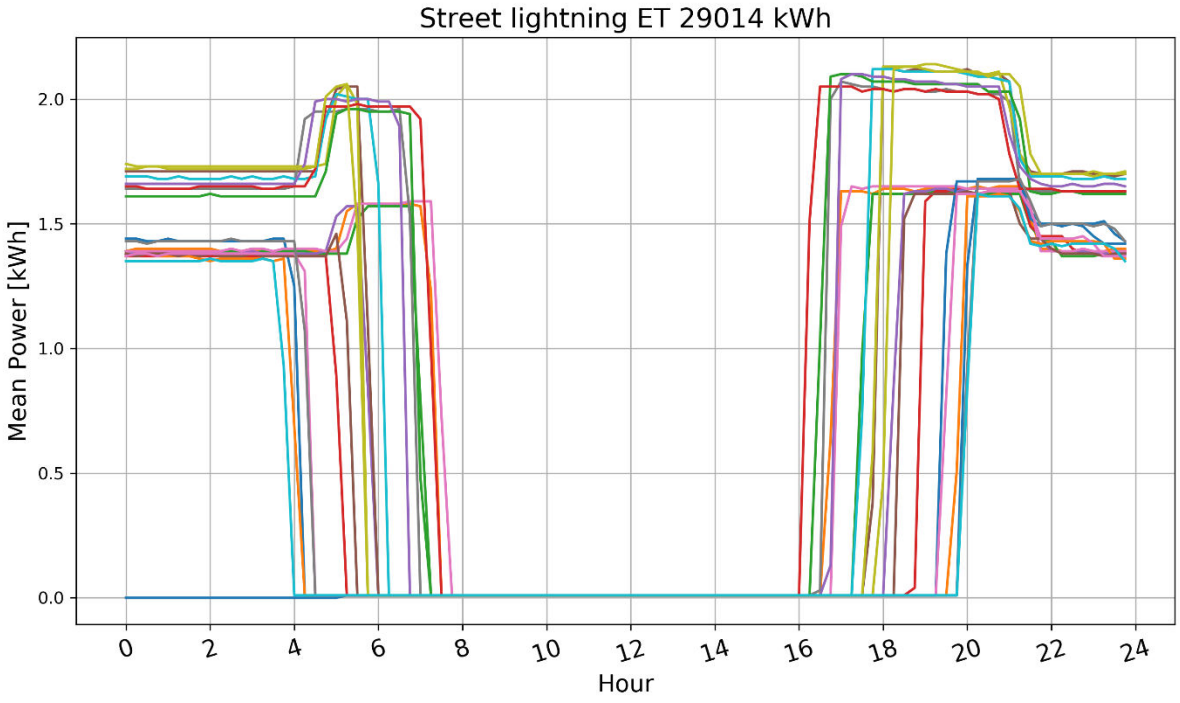

Figure 3.2.4: Twenty randomly chosen daily consumptions of the main street lighting consumer.

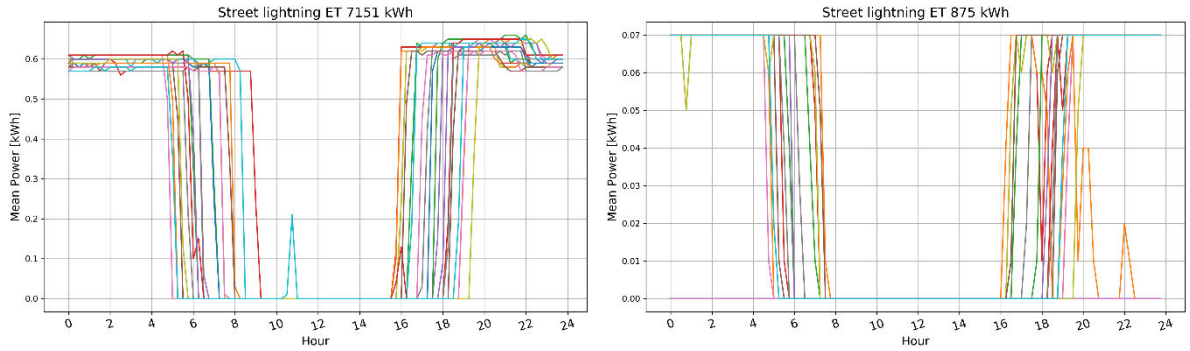

In the figures above, daily electrical energy consumption is shown, where 20 random days of the year were chosen. There is also a cumulative energy consumption listed in each figure's title, where SL means street lighting and ET means flat rate tariff. One can clearly see that the turn on/off time of the street lighting is not equal throughout the year and this is due to the daytime length, which is for the town of Idrija depicted below.

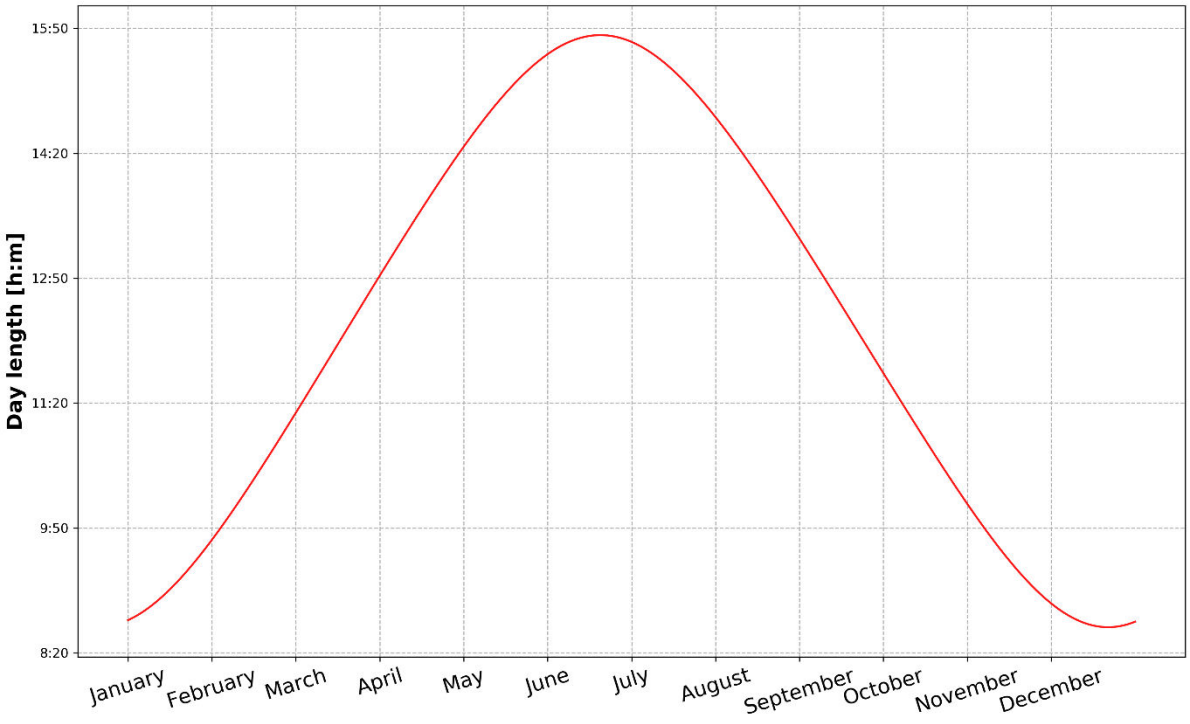

Figure 3.2.5: Day length for Idrija. Data is taken from https://www.timeanddate.com/sun/.

In order to get the estimation of the total electrical energy consumption of the given data, the sum of all the connection points throughout the whole month is taken and shown in the next figure.

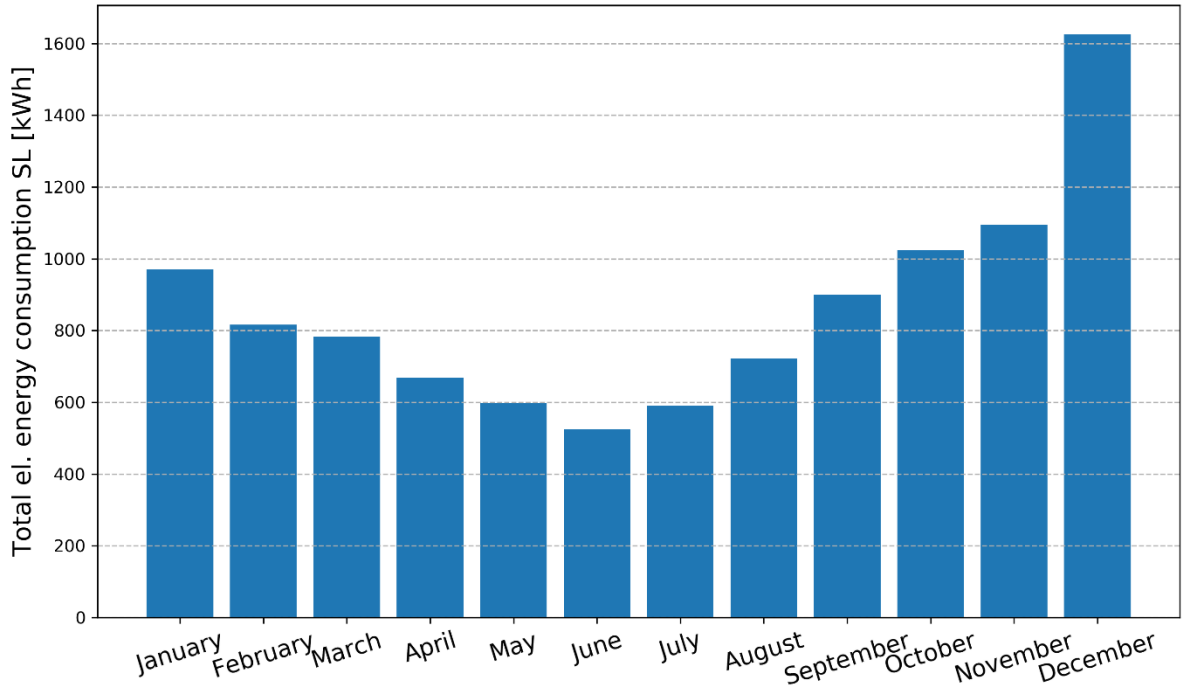

Figure 3.2.6: Total energy consumption of street lighting.

We see that quite big variations in energy consumption occur during the year. There is a factor of approximately 2.9 between June's and December's consumption. If we plot the temperature and day length course on top of this bar chart, we get the following dependencies.

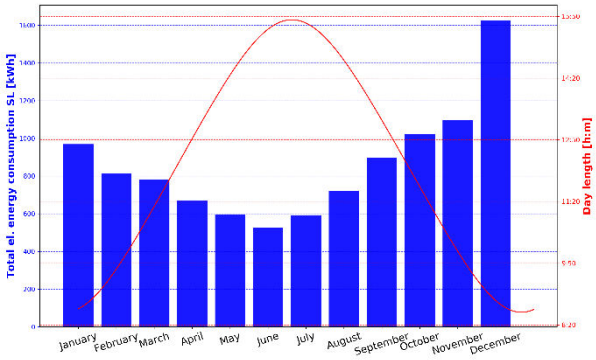

Figure 3.2.7: Day length dependence.

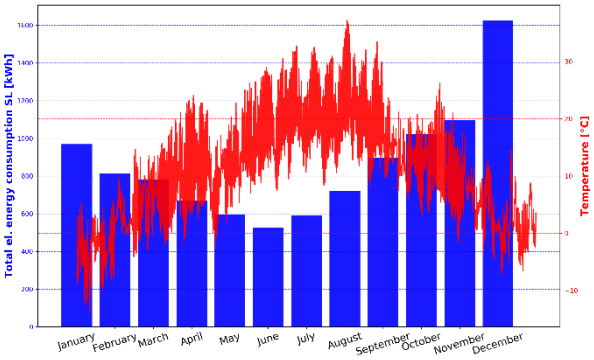

Figure 3.2.8: Temperature dependence.

The best way to visualize which connection points consume most power is to draw a pie chart, which is shown in the next figure.

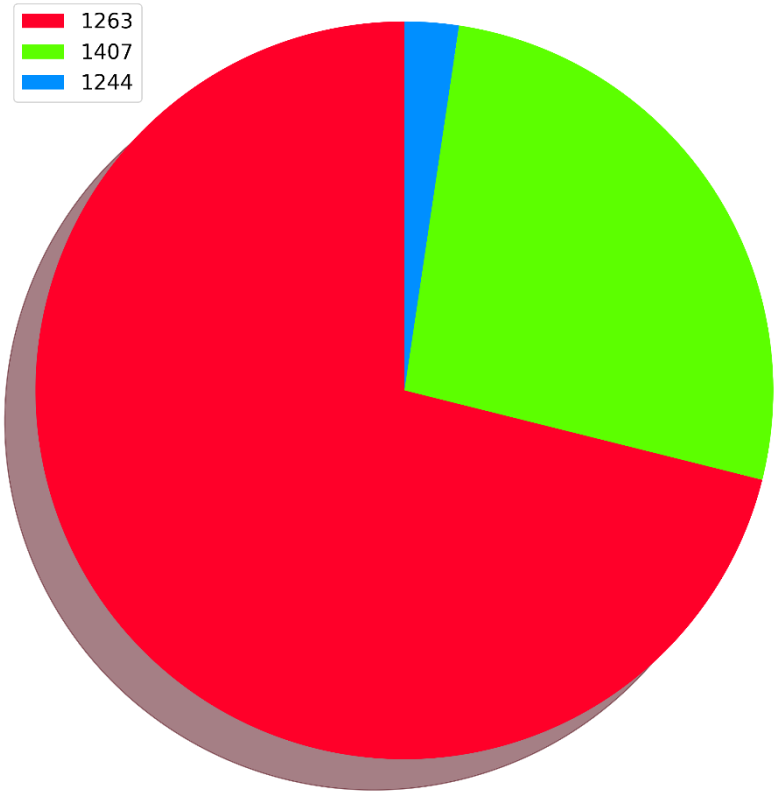

Figure 3.2.9: Pie chart of street lighting consumers in the analysed area.

Mean weekly consumption during four seasons

We can also plot street lighting consumption for an average week in individual season, which is maybe more representative.

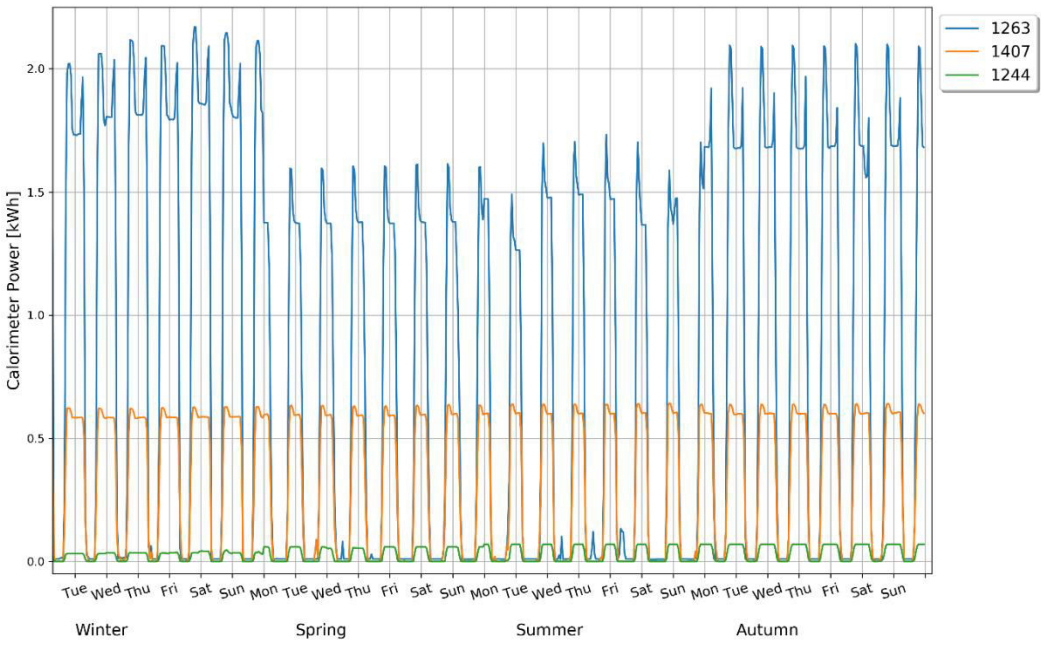

Figure 3.2.10: Average weekly consumption during seasons.

From the figure above, we see that the consumption of two street lighting stays almost the same during the whole year, while one dramatically changes due to already mentioned reasons. It is nicely seen, (especially from a blue consumption line from connection point 1263), that electrical energy consumption has two peaks per day in cold seasons (which is again probably because of a day length and daylight saving time) and no peak in the mornings in warmer seasons. For the reference, we at this point enclose other Idrija's street lighting, to show that these connection points from above are really the main consumers.

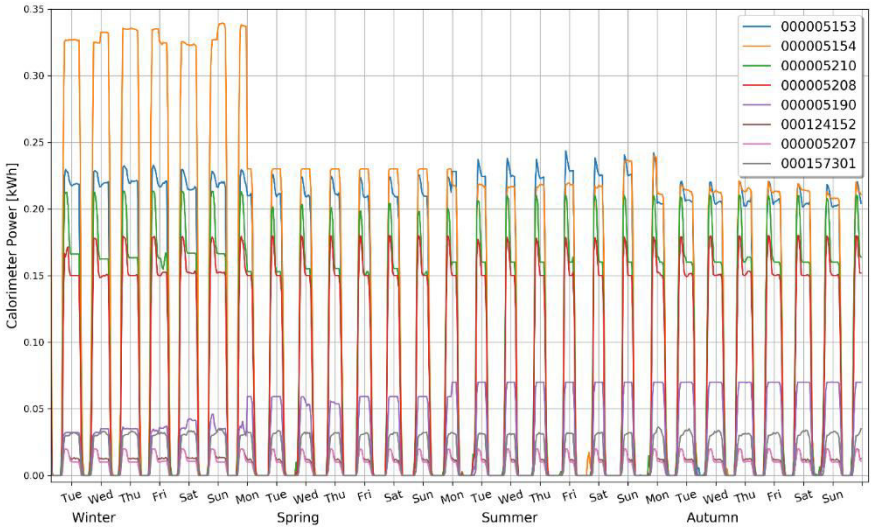

Figure 3.2.11: Street lightings that consume small amounts of energy.

3.3 Idrija Mine

Description

Idrija Mine was former mercury mine located in Idrija. It was second biggest manufacturer of this kind of ore in the world. The legend says that a simple man named Škafar found elementary mercury when he was filling his pail in Idrijca stream. The ore is said to be dug for the first time in the last decade in 15th century and was in its peak in 18th century. After the First World War, the mine went through another flowering, since the mercury prices were high, but due to the stricter environmental rules over the time, the decision in 1977 was made to gradually close the mine. In 1987 the plan how to properly close and restore the mine came out. In total, there was 12,757.731 tons of ore dug, from which they extracted 107.691 tons of commercial mercury.

There are 15 horizons in the mine, where the deepest point is 382 m below surface. This gives total elevation of -33 m. Deepest six horizons (XV. – IX.) are flooded with water (its volume is estimated on 2mio m^3), while the horizons from IX – III are filled with concrete, which is nicely depicted in figure below.

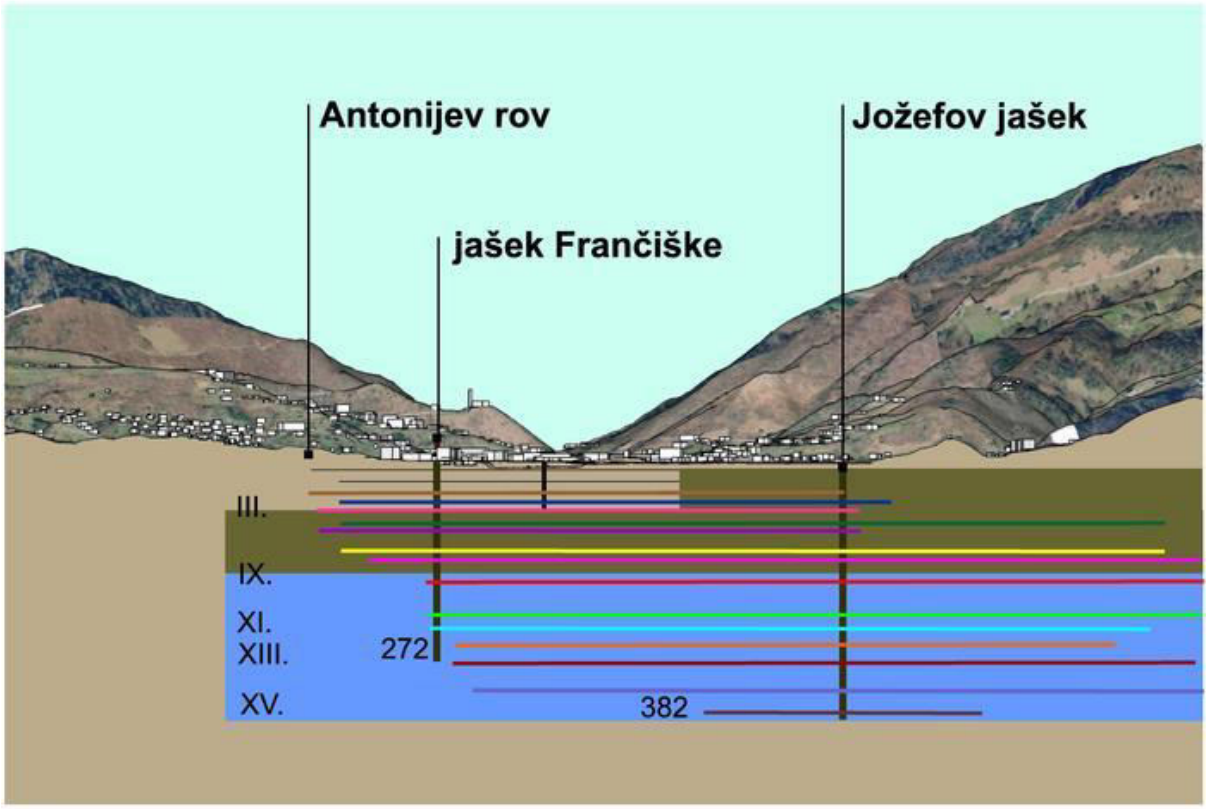

Figure 3.3.1: Idrija mine and main shafts.

By the 1987 plan, the water level should increase through time, but since people noticed some surface damage (the surface was settling constantly) the water level raising was decelerated. The water level is shown in the next table.

Year	Water level
2009	120
2014	133

Table 3.3.1: Water level through time.

There are three major shafts, which lead to the mine, the biggest and deepest of them is called Jožefs' shaft, which was built in 1768, when the mining in Idrija was at its peak.

Water pump

There is only one electrical consumption counter for the whole mine and the main consumers are the water pump and compressor.

Figure 3.3.2: Spare water pump.

Mining pump consists of wooden drive wheel, which measures 13.6 m in diameter and is therefore the biggest preserved wooden water wheel in Europe. The wheel was driven by Idrijca stream, which came to the wheel in 3.5km long water canal. The pump was pumping 300l per minute, while the wheel needed 13s per revolution.

In 1895, a new steam pump in Frančiškas' shaft took a majority of water pumping and was made by Klay in Plzen, CZ in 1893. They disassembled it in 1955 and put it on its first place as sights. It is also the biggest preserved mine machine, biggest steam machine in Slovenia and one of the biggest in Europe.

The present pump is powered by electricity and is placed in Frančiškas' shaft, too. The water is pumped from nineth horizon from the depth of 215 m below surface.

Technical specifications of the present water pump:

1. Number of pumps: 1
2. Motor 1000V, 140kW
3. Pumping height: 200m
4. Capacity: 3400 m^3/24h = 141,66 m^3/h
5. It is powered from grid of 400V,
   which is then auto transformed to 1kV.

Water inflow is 2200 m^3 per day and is weather dependant. The inflow is shifted for approximately 48h considering precipitation. At heavy rainfalls, the pump barely pumps out enough water, to maintain the

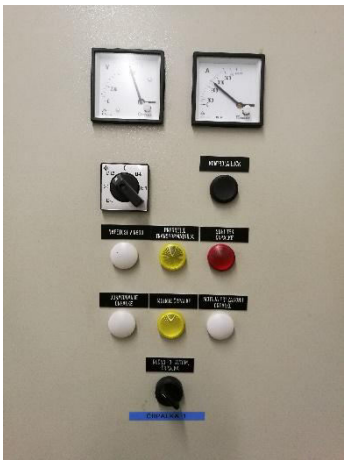

Figure 3.3.3: Control panel.

demanded water level. The pump is working constantly – on average 21 days a month and it is only stopped for refit or due to low water level in mine, because pump stopping can damage the system due to high-pressure shocks.

Water level is kept between 142 m and 145 m of elevation and is slowly raising in accordance with closing of the mine procedure. The water temperature ranges from 17°C to 18°C and some ideas of heat pump construction already arose, but dissolved substances (iron, sulphates) would be the problem this way.

Electrical energy consumption of the pump

Electrical energy consumption of the whole water pump system is listed in the next table:

Consumer	Power needed [kW]
Water pump	140
Elevators	54
Working machines in workshops	30
Indoor lighting	3
Outdoor lighting	1
Administration and offices	5
Boiler room and pumps	2
Compressor	55

Table 3.3.2: Energy consumption of water pump system.

Data of the energy consumption from the mine connection point were obtained for the period from 1.1.2015 to 30.6.2017 and is shown in the next figure. The energy consumption data was taken every 15 minutes, so there are 96 measurements per day and 35040 per year. In the figure, we see that the majority of time, the mean power average is around 140 kW, which means that the water pump is working. There are also many spikes visible in the figure, which are loaded on “boxed” water pump consumption. Since their height is approximately 50 - 60 kW, one can immediately assume that at those times, the compressor or the elevators were working.

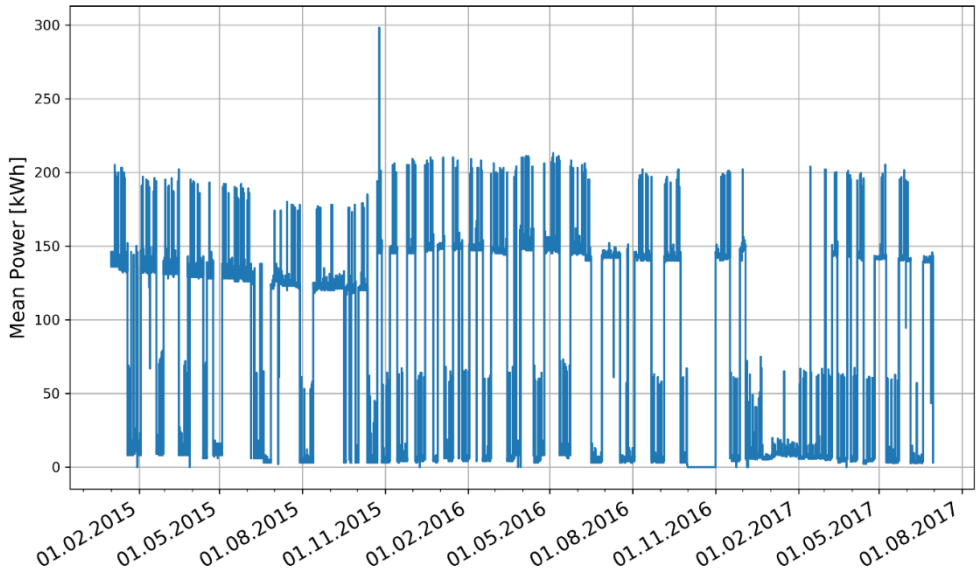

Figure 3.3.4: Energy consumption during the whole obtainable period.

For better visualization, the weekly energy consumptions for the same period are depicted in the next figure, where red background represents high cost rate, while green one represents low cost rate. This background colouring does not take into account holidays (which are charged at low cost rate) but is still enough informative, since we immediately see, that the pump mainly works at high cost rate VT.

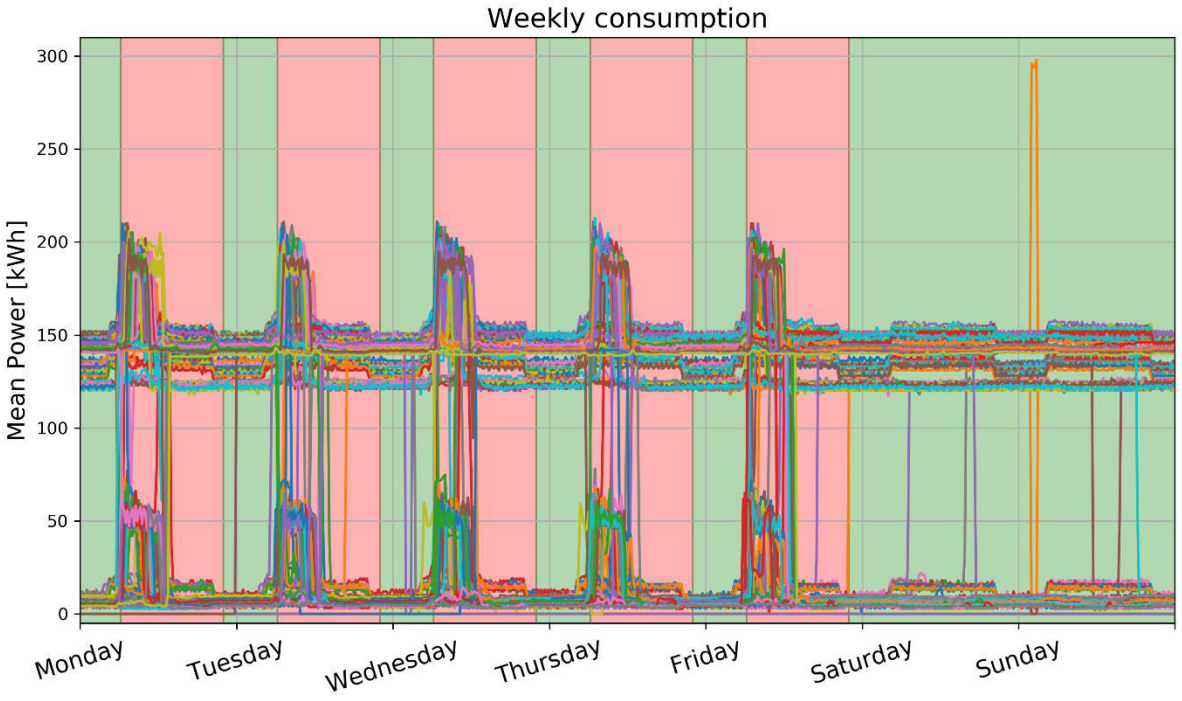

Figure 3.3.5: Weekly consumptions.

If we filter out energy spikes from compressor, we can see the actual water pump consumption and estimate approximate working time of both water pump and compressor/elevators. The filtered data for 2016 is shown in figure below.

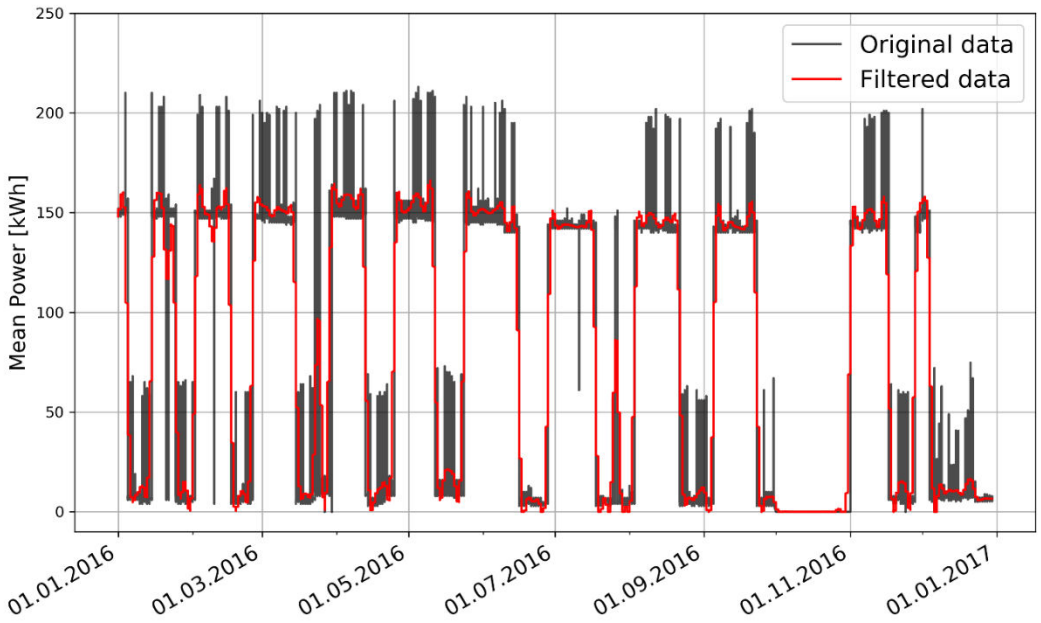

Figure 3.3.6: Filtered water pump data.

If one calculates the working times of both water pump and compressor for the 2016 year, one gets the following outcomes:

Consumer	Working time [%]
Water pump	48.3
Compressor	24.4

Table 3.3.3: Working time of the pump system.

In the figure below, an average weekly consumption is plotted for each individual season.

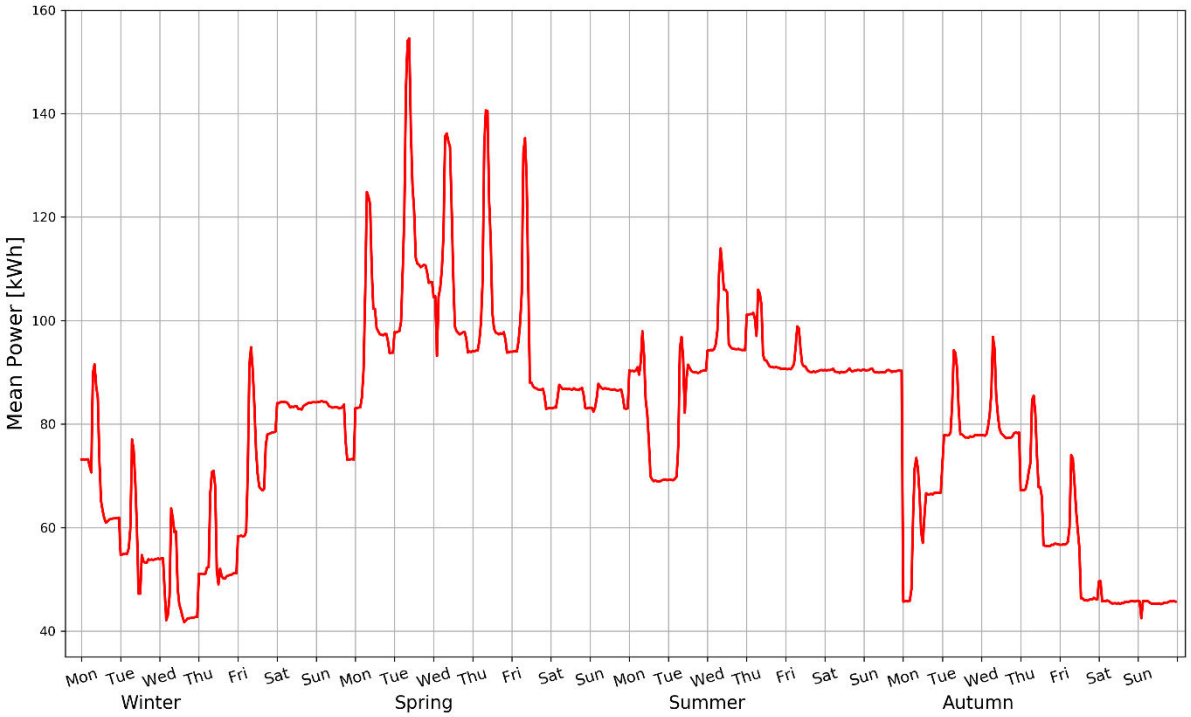

Figure 3.3.7: Average weekly consumption for individual season.

From the figure above, one can hardly extract any schedule, when the water pump is turned on. The electrical energy consumption is lower in cold seasons, while it is the greatest in Spring, when there are the most rainy days in this region.

Amount of pumped water

We are able to obtain the data of pumped water from SCADA program for approximately five and a half years since the summer of 2012. The whole plot of the pumped water during this period is shown in figure below.

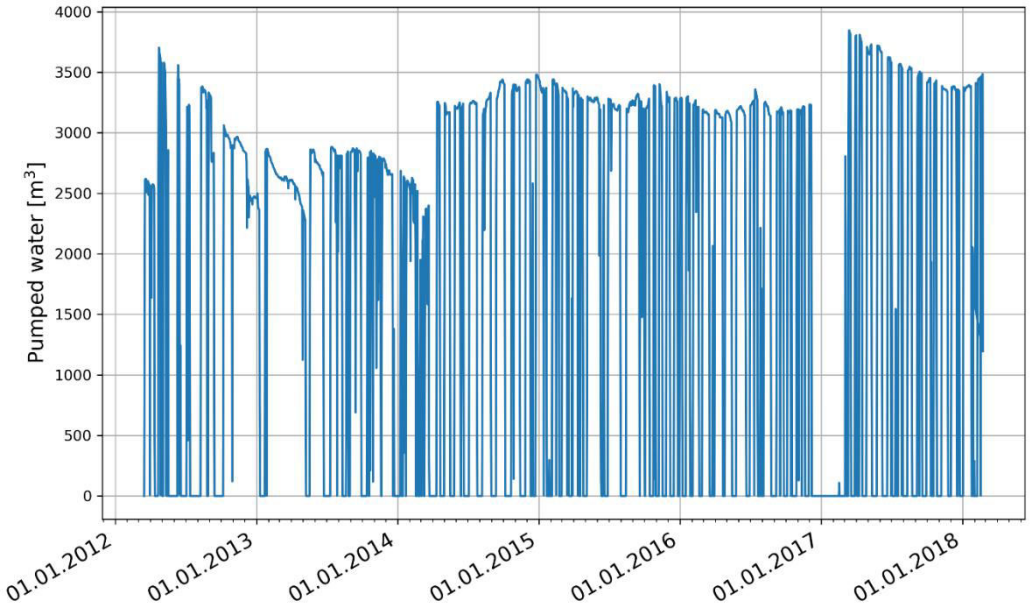

Figure 3.3.8: Pumped water during the period of five and a half years.

We see that the amount of pumped water is not changing dramatically. There are some deviations in some periods, which probably occur due to weather conditions (heavy rainfalls or droughts), where they had to regulate the amount of pumped water. What is interesting is the period around the 2017 New Year, where the pump was not working for quite a long period. There may be a drought or the pump was turned off due to maintenance.

At this point, we can compare the graphs of pumped water and the electrical energy consumption data, which we already plotted above. The period taken into account is again year 2016 and the comparison is shown in the figure below.

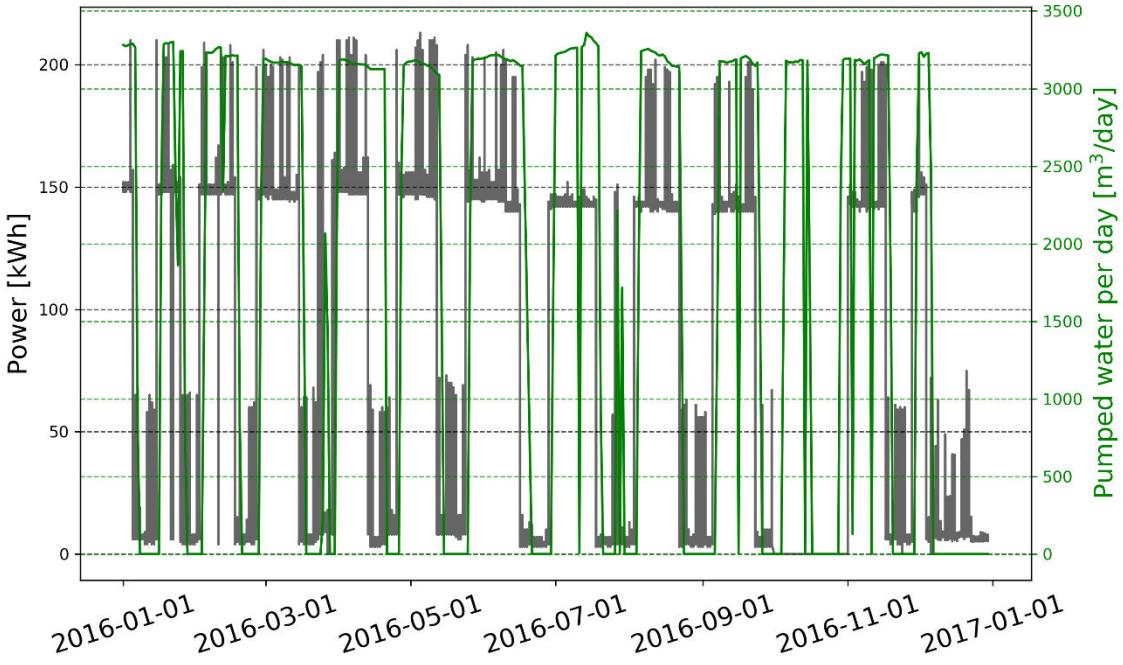

Figure 3.3.9: Comparison between the pumped water and electrical energy consumption data.

From the figure above, we can easily conclude, that the two different data is nicely getting along, so that when the pump is turned on (consuming power), the water is being pumped out of the mine.

Water level in Idrija mine

There were only a few SCADA files, from which we were able to obtain a water level during the period of six days from 25.12.2008 to 1.1.2009, and we include them into this document only to show the response of water level in mine to turning the pump on. It is shown in the figure below.

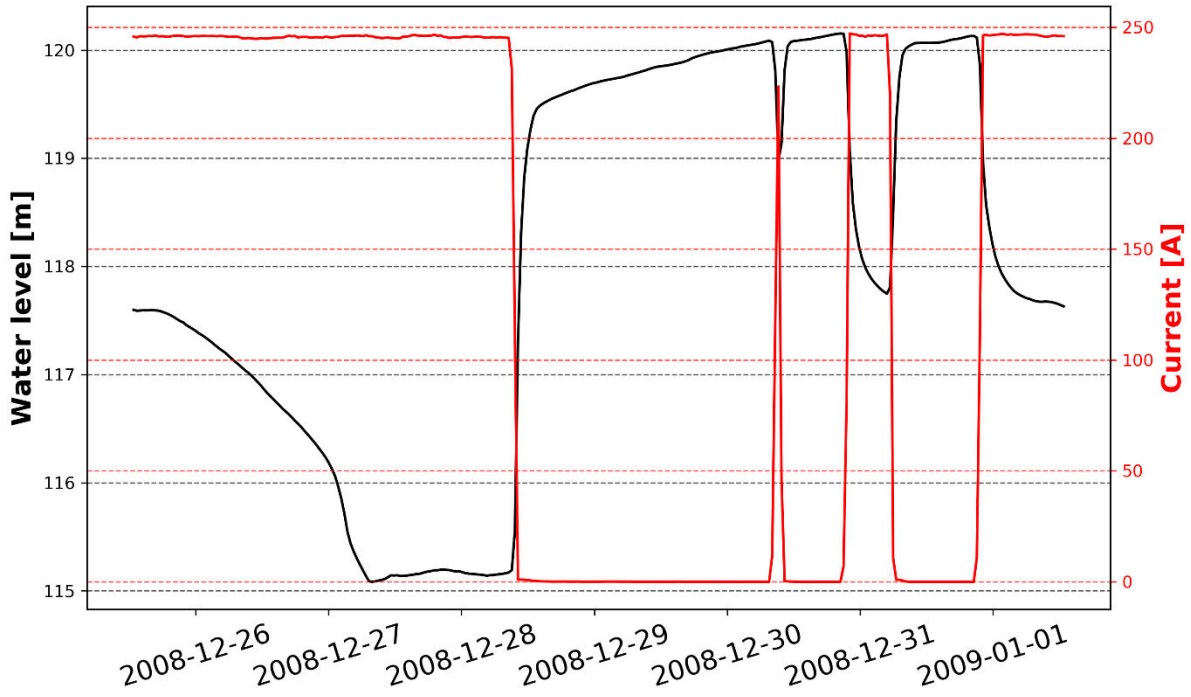

Figure 3.3.10: Water level in mine to pump consumption.

We see, that the water level has a quick response to turning the pump on or off, and that when the pump is turned on, the water level firstly exponentially falls, but then slowly approaches some value.

3.4 Primary School

History

Schooling in Idrija dates back in 1580, when first Protestant school was built with a teacher who was paid by Idrija's' miners. The school then came under catholic control up until 1778, when the main school was established. It was one of the best schools in this region with much success, but as the population in Idrija grew over time, number of school age children grew too, so the need for a bigger school occurred. It

Figure 3.4.1: Old primary school.

was in 1876 when the nicest and most fashionable elementary school in Carniola region was built and was also financed by Idrija's mine. During the First World War, Idrija came under Italian authority, so the Slovene word died out for a period of two decades. After the war, the school needed renovation, but the whole work was done only in a school year of 1959/60. In 1966, there were 1018 pupils in school, so the idea for a new, bigger school arose. It was finished in 1991 on a place called "Lenštat" next to the gym, where it stands up to the present.

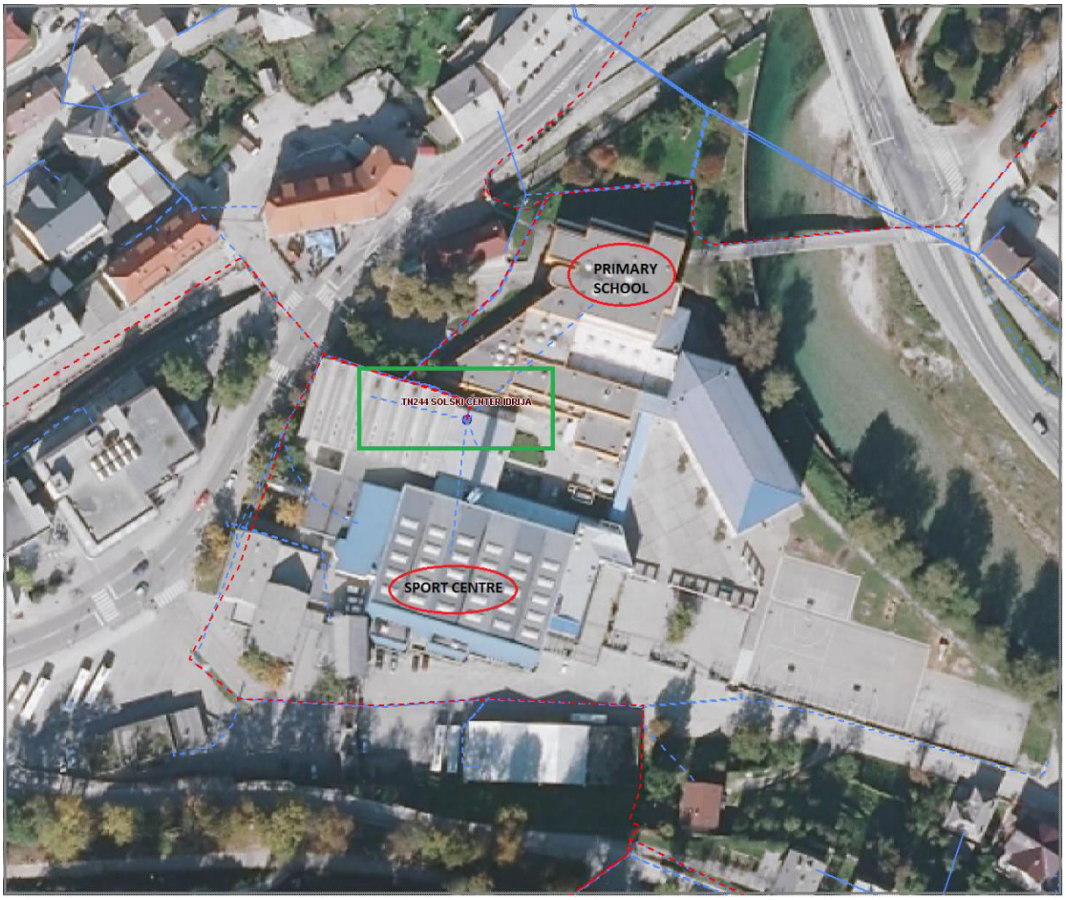

Figure 3.4.2: Pilot building location.

Since this school is one of the biggest energy consumers in our region of study, it is important to focus on the effects of 3smart on its consumption. Let us first look at its heat energy consumption data from calorimeters, for a year of 2016 taken once a day from four measuring places labelled above – School, Sports centre, Blue Hall and Boiler room.

Consumer	Connection point ID numbers	Connection power [kW]	Consumption type*
School	7-1516	148	T < 2500 h
Sports centre	7-1265	53	T < 2500 h
Blue Hall	7-1266	66	T < 2500 h
Boiler room	7-1270	66	T < 2500 h

Table 3.4.1: Consumers data (*T means yearly operating hours).

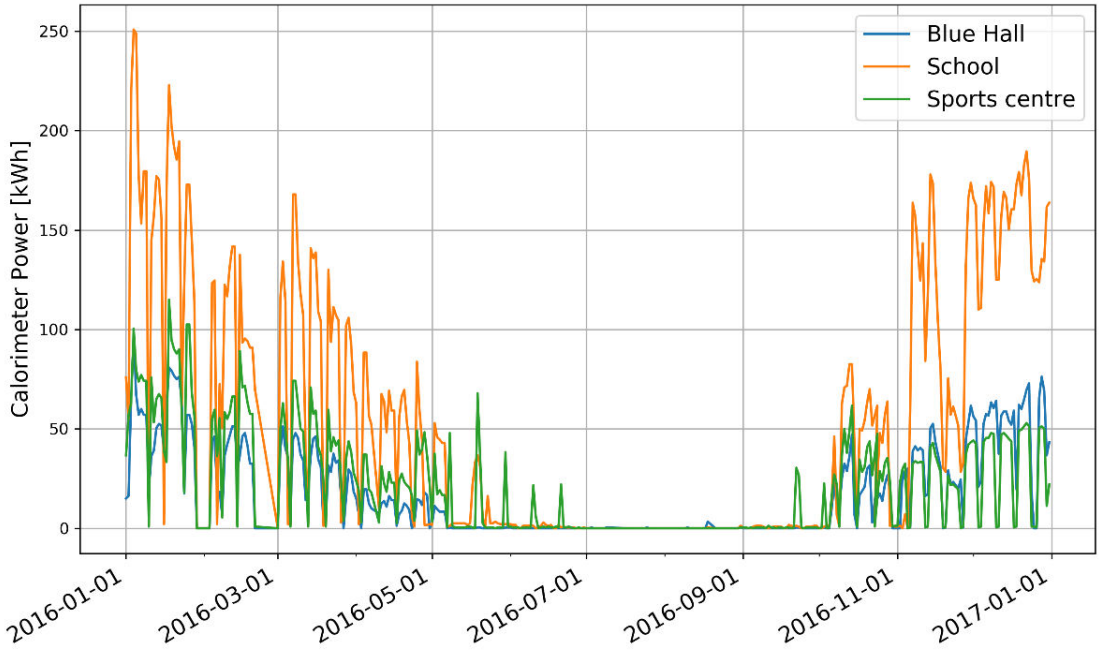

Figure 3.4.3: Heat energy consumption.

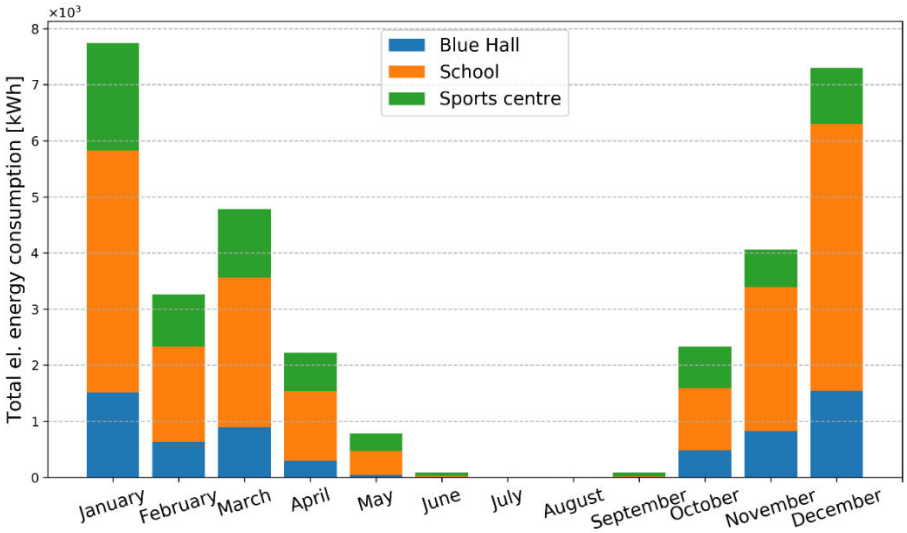

Figure 3.4.5: Monthly heat energy consumption.

From the figures above, one can clearly see, that the consumption is small during summer, when it is warm outside but another reason are also summer holidays, which take place during 24.6. – 31.8. in Slovenia, when schools are mainly closed.

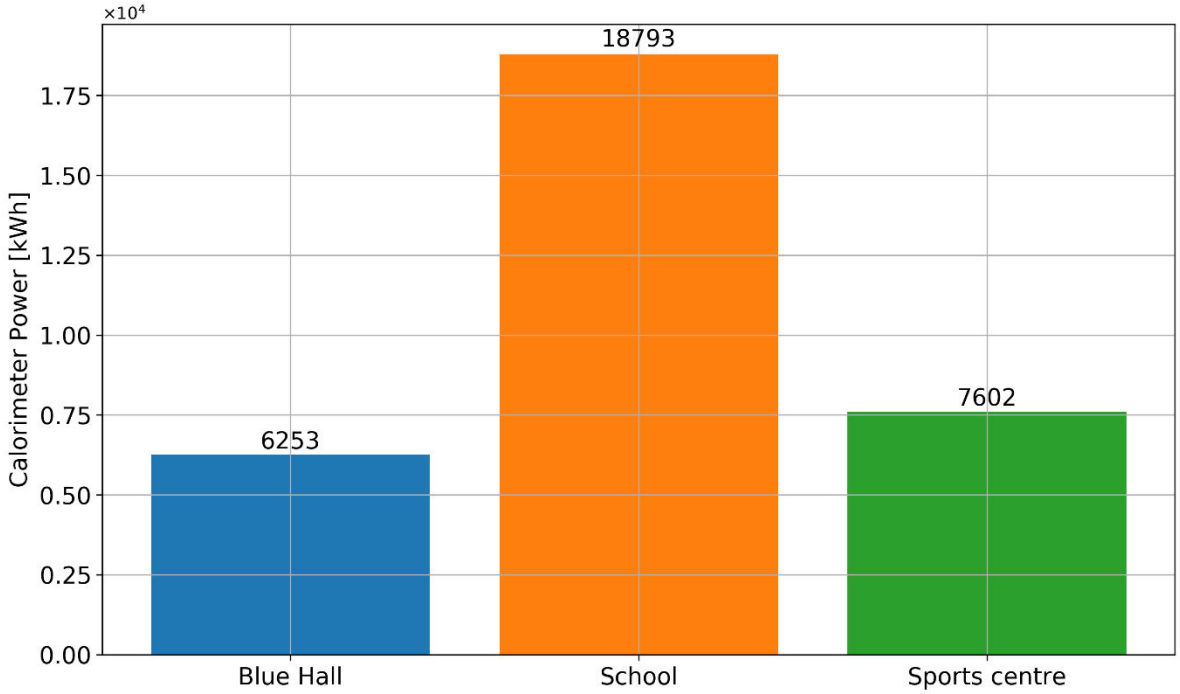

Figure 3.4.6: Total energy consumption for 2016.

The figure above shows us yearly consumption of three consumers. For example, the consumption of School nicely coincides (+3%) with the number from the electrical energy bill, which states, that the school consumed 18176 kWh. Let us now look at the average electrical energy consumption during the week for all four seasons, where the data for Boiler room are included.

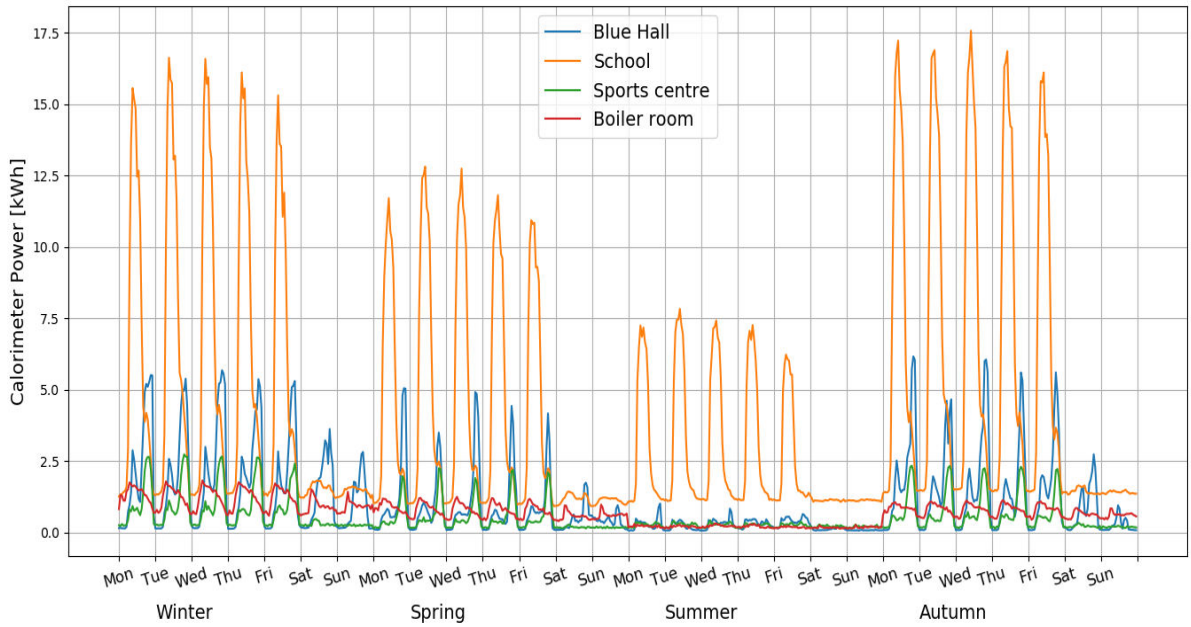

Figure 3.4.7: Average weekly consumption during a year.

We again see that consumption is larger in cold seasons, while it is the lowest in summer. It is also nicely seen, that consumption is lower during weekends, but on the other hand, we see similar patterns during working days. Again, school is the main consumer, while boiler room needs the least electrical energy.

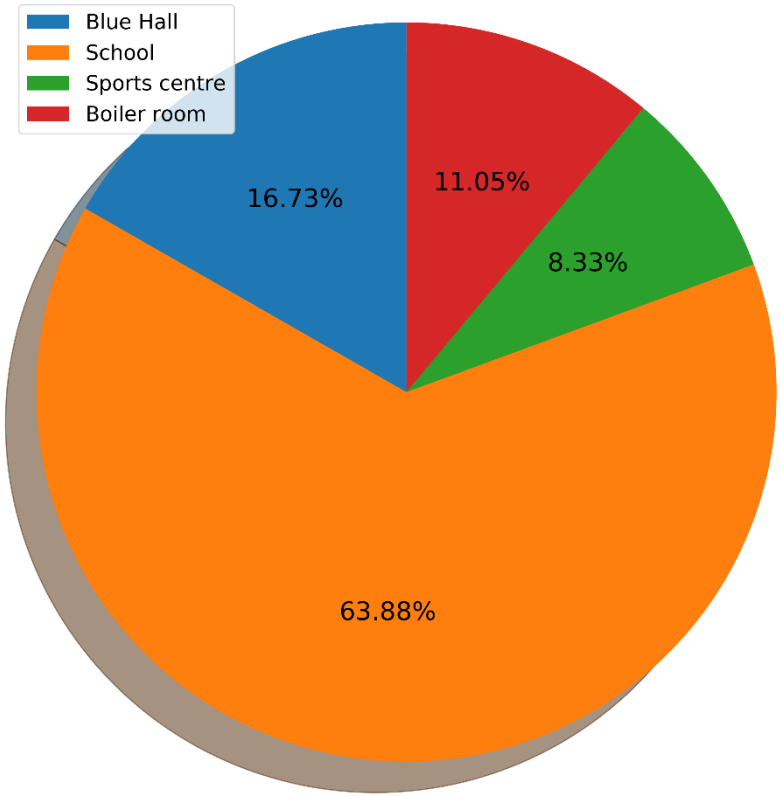

Figure 3.4.8: Consumption distribution.

3.5 Households

Description

We focused only on some connection points in Idrija, from which we obtained consumption data of households. Since Slovenian law is quite strict about obtaining electrical energy consumption data as it is considering it as personal information, there is no much information about individual consumers. This way we took into account around 670 household customers in the Idrija's centre, which are all connected to the grid shown in the previous chapter and have the connection power less than 22 kW.

Load profiles

As said before, load profiles for each household is impossible to obtain, but it was manageable to obtain the average customer's profile. The same situation is for the business customers.

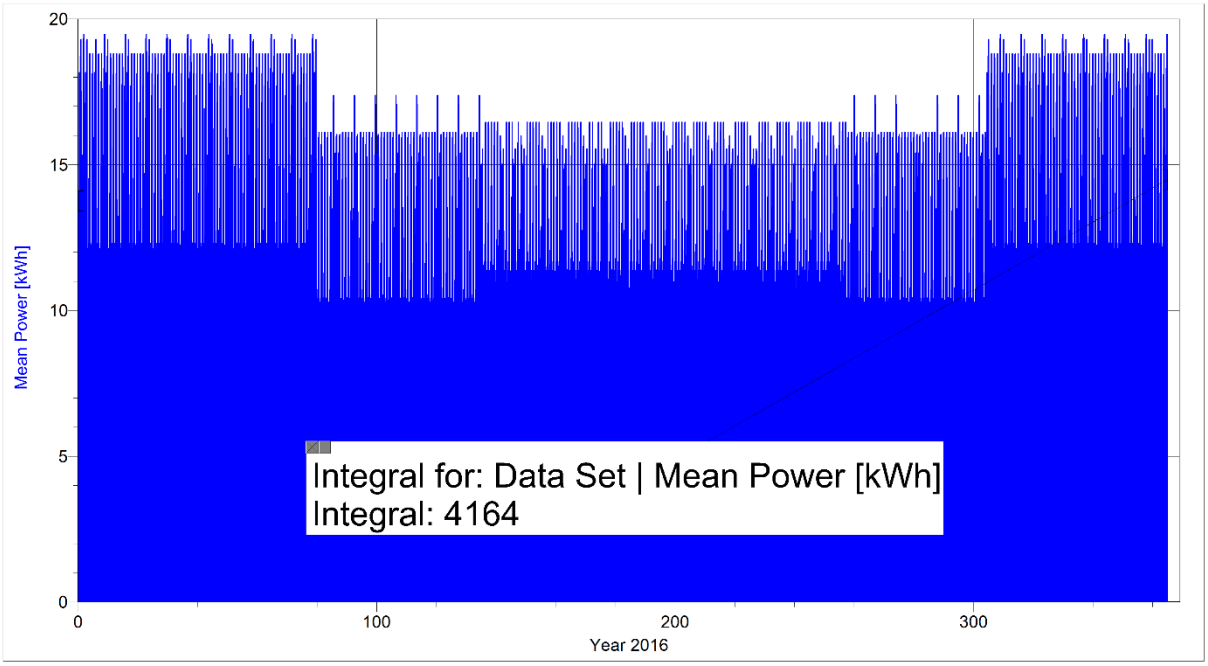

Figure 3.5.1: Average 15min household customer consumption during a year 2016.

Load profile of a household during a year changes, but not much. The results are very symmetric, which is in a way strange, but let us just trust the measurements. This figure does not say much, the only thing we can calculate from it, is load profile's integral over the whole year, which gives us a total yearly consumption of an average household, which is also denoted in a figure above and adds up to 4164 kWh/year.

The most informative graph is the one, where we present average week in an individual season as shown in figure below. If we do this, we can get the idea of a shape of a weekly and daily consumption. We see that an average household customer has two spikes in his daily load profile,

one smaller in the mornings and a greater one in the evenings and that Sundays are in this way different, which makes sense.

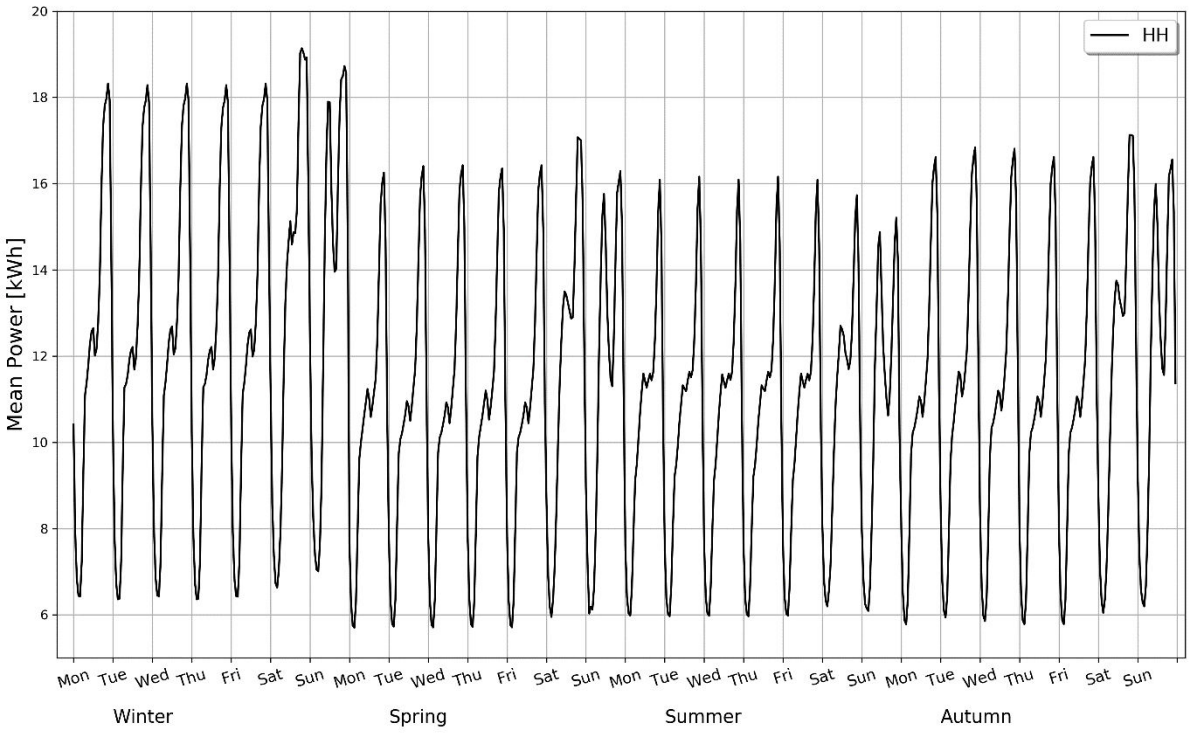

Figure 3.5.2: Average weekly household consumption during an individual season.

3.6 Business consumers

Load profiles

Let us do the same analysis for a business customer. Firstly, let us look at an average whole year load profile. We see a similar trend as in household load profile, only slightly higher values of consumption occur. The total yearly consumption in this case is 8320 kWh.

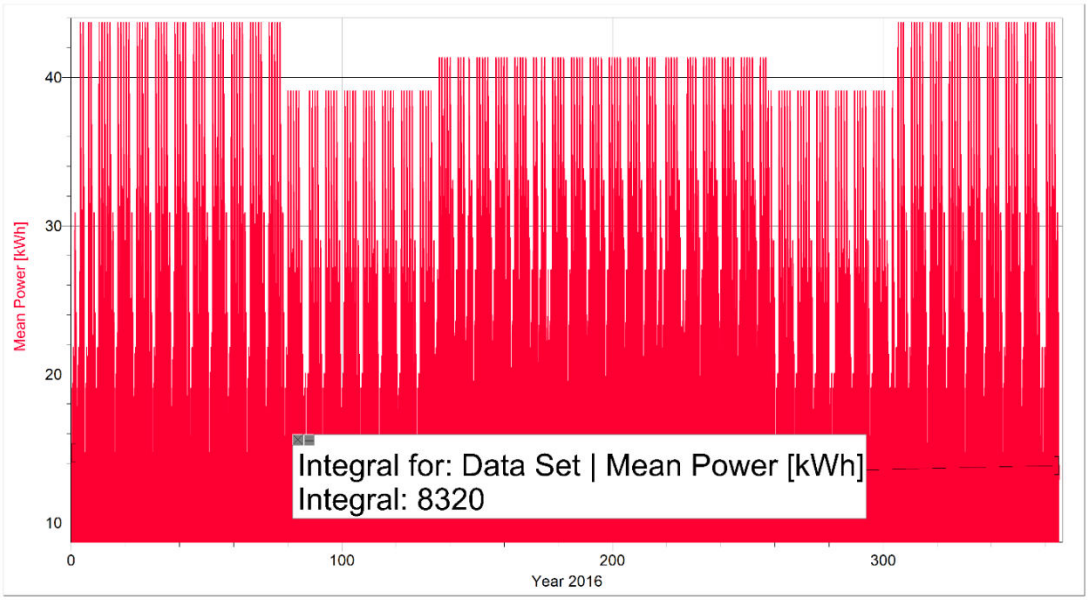

Figure 3.6.1: Average 15min business customer consumption during a year 2016.

At this point, we can sum individual days to months and see what an average monthly consumption is for a household and for a business customer.

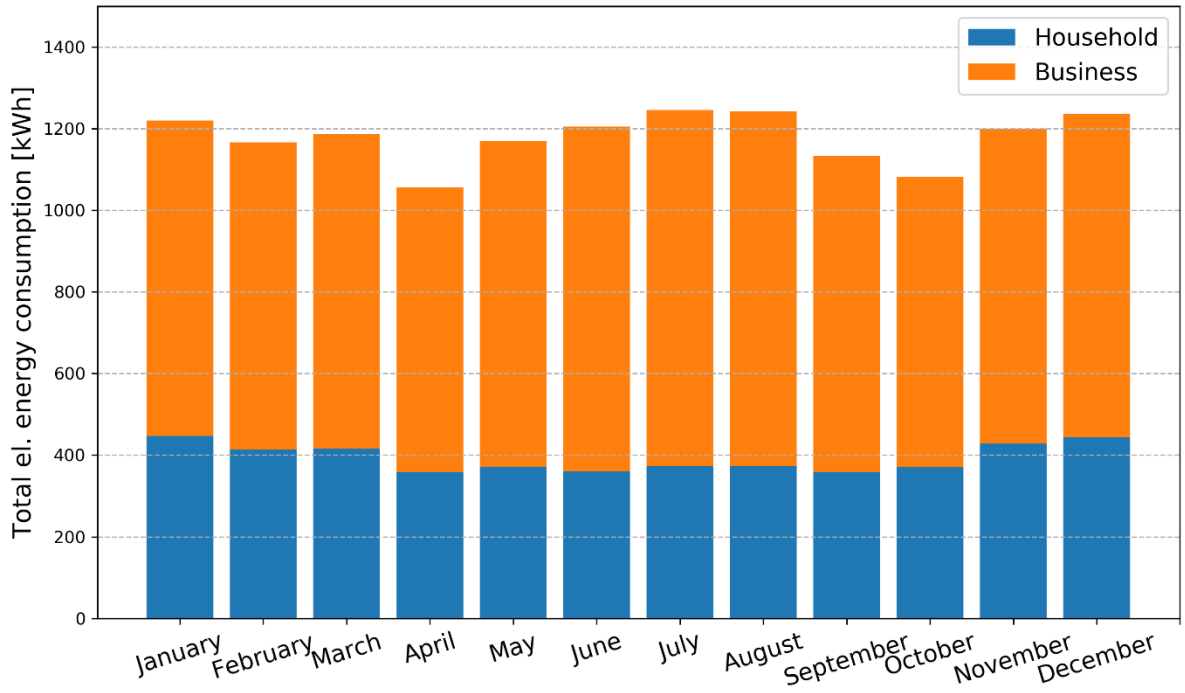

Figure 3.6.2: Stacked diagram of monthly consumption for an average household and business customer.

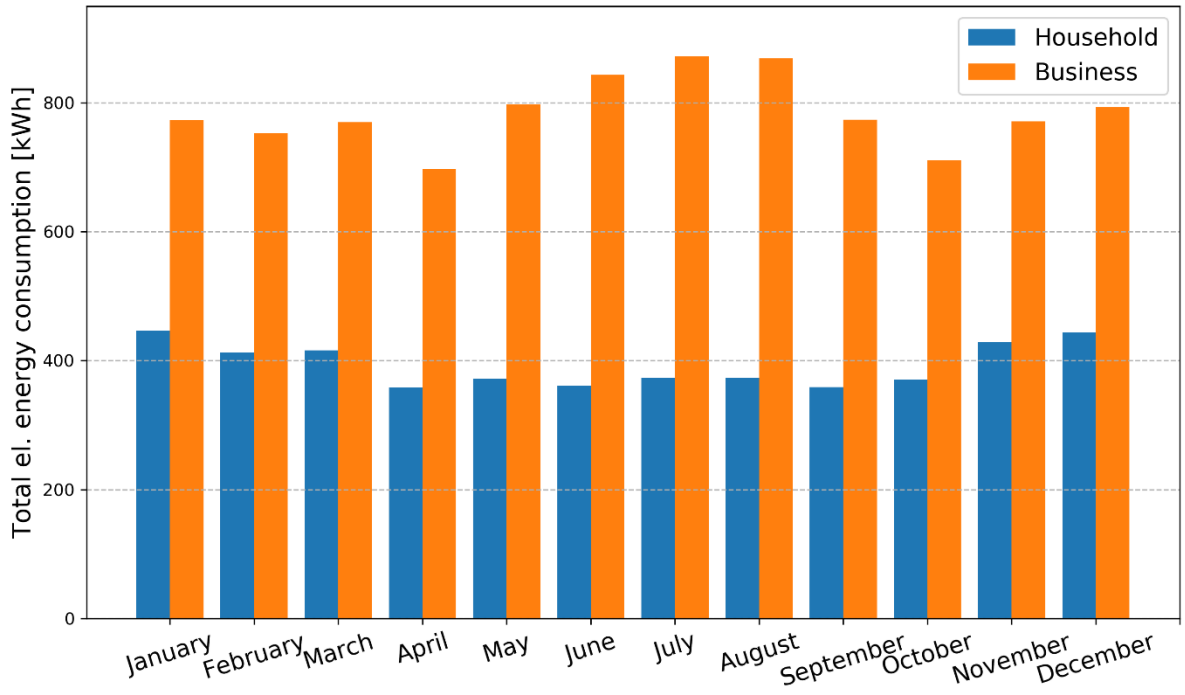

Figure 3.6.3: Bar diagram of an average monthly consumption.

From the figures above, one can extract that an average business customer consumes roughly twice as much electrical energy as a household and another thing to see is the difference during different seasons. Household consumption decreases during summer, while the business consumption is greater then. The average monthly household consumption is 390 kWh and 785 kWh for business customer, which confirms the idea, that it consumes twice as much as a household.

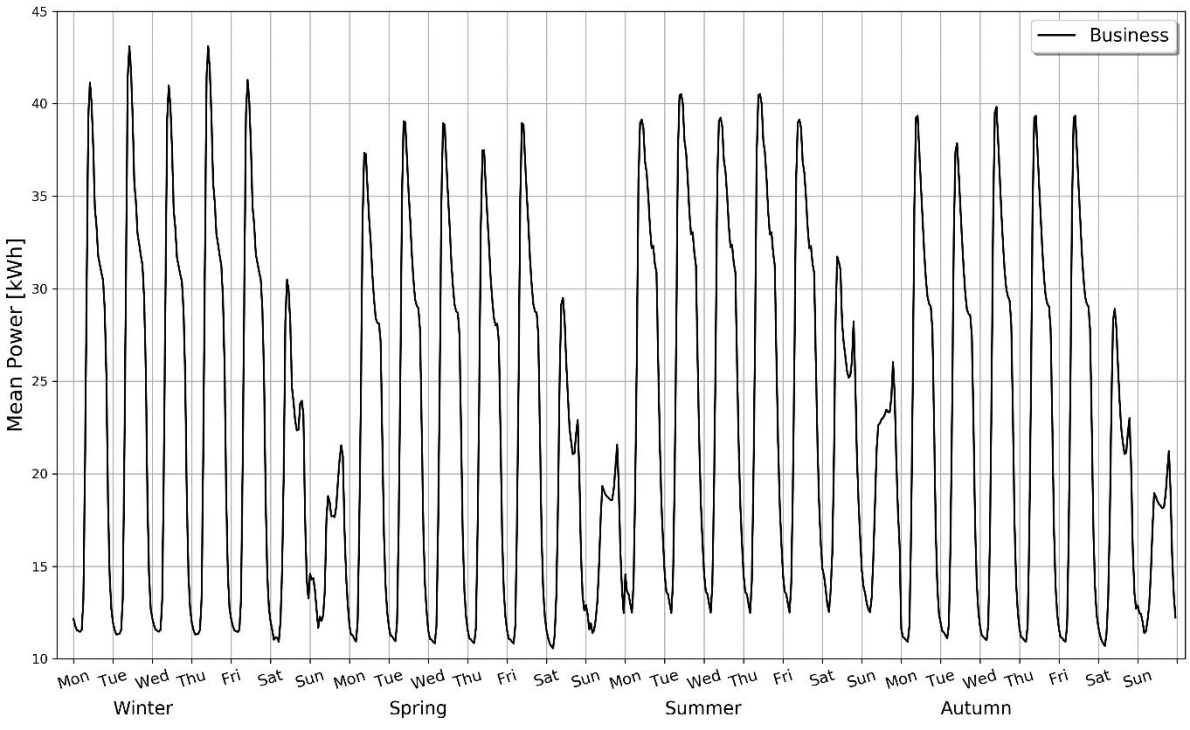

Figure 3.6.4: Average weekly business customer consumption during an individual season.

In the figure above, an average business customer's load profile is shown. It has slightly higher peaks than the household ones, and are also quite different from them. Load profile has tallest consumption peaks in the mornings, while they are shorter during the afternoons and in the evenings. Business customers have also slightly higher consumption than household customers do during the night-time, while in the weekends, the business customer's consumption significantly drops.

Peak demand

Maximum demand occurs when there is a large demand for electricity from customers simultaneously on the network - typically, these peak demand events result from customers increasing their electricity consumption due to temperature changes (cold winter evenings or hot summer afternoons).

While the overall system peak demand highlights the network wide impact of peak demand, localized electricity infrastructure such as cables, transformers or zone substations may experience localized peak demand events at different times of the day and year depending on the electricity demand from customers in that local area.

When the demand for electricity at peak times approaches the capacity of network infrastructure, the energy supplier must act to maintain reliable electricity supply to customers. Reliable electricity supply to customers can be maintained by either increasing the network capacity (supply side management) or reducing the peak electricity demand on the network (demand side management).

Demand management is an important part of efficient and sustainable network operations. It can involve either the voluntary moderation of customer electricity demand at peak times or the supply of electricity from generators or storage batteries connected at customer's premises or to the distribution network. Effective network investment considering demand management is used for both replacement of aged network assets and network expansion due to growth in demand. Demand management solutions are also referred to as non-network solutions and similarly, a demand management provider may also be referred to as a non-network provider. Effective use of demand management reduces the cost to maintain the network and helps lower electricity charges for the entire community.

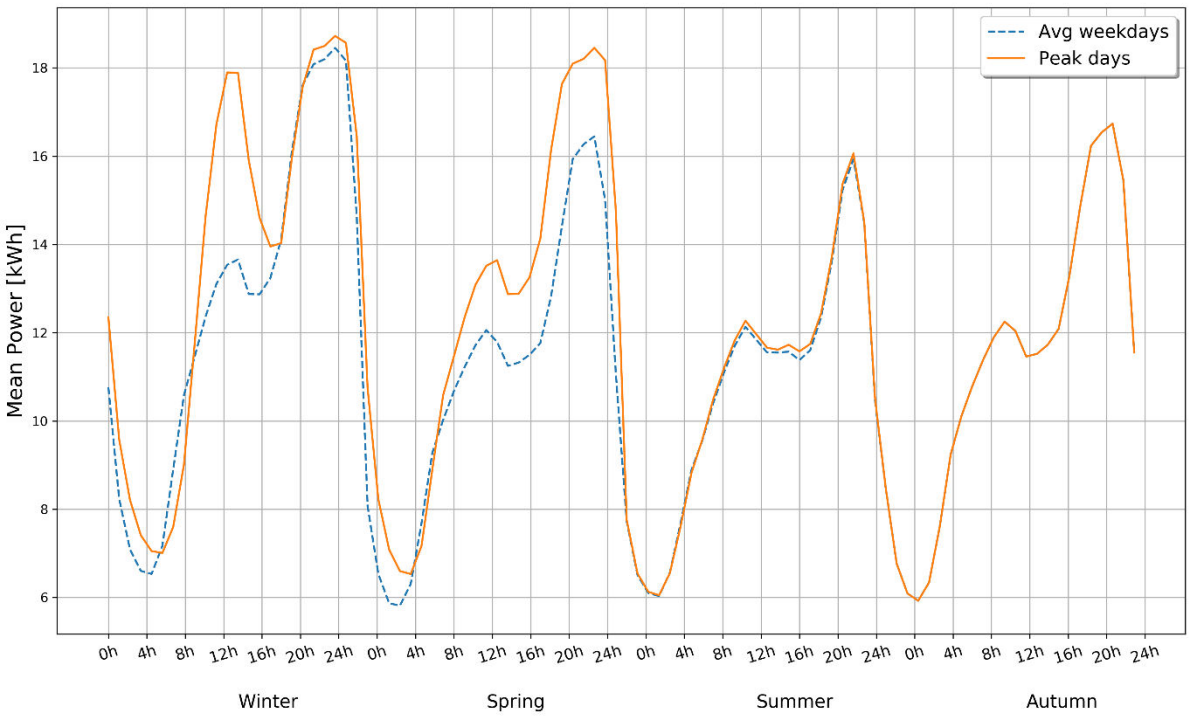

Figure 3.6.5: Average and peak daily demand profiles in Idrija's housholds.

3.7 Algorithm for management and scenarios

Idrija Mine

This system is big energy consumer and as such offers great opportunity for energy management, which is beneficial for the grid and the owner.

Pumps can be easily upgraded with variable frequency drive. About 25% of the world's electrical energy is consumed by electric motors in industrial applications, which can be more efficient when using VFDs in centrifugal load service.

Fixed-speed loads subject the motor to a high starting torque and to current surges that are up to eight times the full-load current. AC drives instead gradually ramp the motor up to operating speed to lessen mechanical and electrical stress, reducing maintenance and repair costs, and extending the life of the motor and the drive equipment. The starting method typically allows a motor to develop 150% of its rated torque while the VFD is drawing less than 50% of its rated current from the mains in the low-speed range.

Fixed-speed motor can save energy when they are operated at variable speed by means of VFD. Such energy cost savings are especially pronounced in variable-torque pump applications, where the load's torque and power vary with the square and cube, respectively, of the speed. This change gives a large power reduction compared to fixed-speed operation for a relatively small reduction in speed. For example, at 63% speed a motor load consumes only 25% of its full-speed power.

The system is allowed to be stopped for few hours at any time. Operation can be scheduled or delegated from 3Smart EMS. System as such will be very attractive for aggregating companies in the future. Equipped with 3Smart EMS it will be ready for advanced services.

A VFD allows continuous power control and this is ideal case for 3Smart EMS.

Used method is load shifting in week period. Time and energy amount is defined based on Street lighting consumption profile.

Primary School

There is a modern central control system placed in the boiler room, where two different ways of regulation are possible: boiler automatics control all the heating circuits, or the heating circuits are controlled by central control system. Boiler automatics can control up to three heating circuits, but there are nine heating circuits in the relevant area. For the needs of 3Smart, it will be necessary to adapt this system and upgrade it for the connection with EMS platform. It is reasonable to include all the data from heating measurements in 3Smart EMS.

There will be an electric power plant with different sensors built near the primary school, which will be connected to EMS. With all these upgrades, the school will be able to produce its own electrical energy. This energy, in addition to CHP produced electricity, will in some periods exceed school’s and

sports centre's electrical energy consumption. This way, the connection point should be adjusted in such a way, that it could controllably give off exceeding electrical energy.

Economic assessment

Pumping system for mine water, offers flexibility which can be used for 3Smart. Variable speed control that was discussed earlier in this document is not possible to be implemented. Pumps can operate only at fixed power, but operating time can be shifted. This means, that DSO can request switching off the pump during high power demand on distribution grid. The flexibility is three hours per day.

The owner of system that offers flexibility wants to have some revenue. The DSO must know what is the marginal price acceptable for it. The base document is long-term contract. It defines the technical and economic parameters. These parameters include frequency of activation, activation time, avoided cost, the method of deriving the flexibility price from avoided cost.

The maximum price on flexibility products for the DSOs will be set from the DSOs' alternative costs in reinforcement. This will form a sort of price-cap on flexibility products for the DSO. The final price will depend on what price the Aggregator offers its flexibility products at. If it is sufficiently low, the DSOs are likely to use the offered flexibility product.

If the DSO's only alternative to buying this flexibility product is to upgrade its grid components (cables, transformers, etc.), the price setting could be done based on the 1st year value of these upgrades.

Above mentioned approach is covered with 3Smart long-term module. The inputs are:

The owner provides these parameters:

- Asset power (nominal power of pumps): 140 kW
- Availability (flexibility duration): 3 hours every day.
- Price of system upgrade to be available for activation: 6000 EUR

The DSO provides these parameters:

- MV grid upgrade from RTP Idrija to Transformer station TP ŠC: 227.000,00 EUR
- WACC: 4,69% (This is a risk-free return of the distribution industry to the recognized capital cost in the tariff)
- Inflation: 2,50%
- Year: 2019

The long term module outputs give quite interesting results:

- Unit price of Reservation (EUR/kW) 16,959 (0,0039 EUR/kW/(15 min))
- Unit price of Activation (EUR/kWh) 0,0161

The flexibility provider – owner revenue from reservation part is 140 kW * 16,959 EUR = 2.374,26 EUR for one year contract period.

Estimation of activation ratio is 50% of. available time. This gives yield of 76.650,00 kWh/year and 1.234,065 EUR.

Total revenue: 3.608,325 EUR per year

Capital costs are 6000 EUR. Break-even point is 1,66 years. This means, that at least two year contract is reasonable to conclude.

Each year the revenue will be higher. Investment costs are 0,00 EUR but maintenance and operational cost should be taken in account.

3Smart EMS Measures

In order to get all the information needed for 3Smart system, the temperature of the rooms should be measured, the number of people in school and the number of lights, which are turned on, should be known. The electricity meters should also be installed – one for general use and one for lighting.

Households

At this point we must make an assumption how much energy we can manage or in other words, over how much energy we have control. Let us assume that 5% of all households would participate in our program and all of them have ordinary household appliances, which they use daily and are listed in the table below.

Appliance	Capacity	Length of use	Energy consumption/year [kWh]	Energy consumption/day [kWh]
Washing machine B	2500 to 3000 W	48 weeks - 2x / week	130	0,35
Water heater	4000 W	365 days - 3h / day	4300	11,78
Air conditioner	2000 W	150 days – 4h/day	2920	8
Heat pump	1500W	150 days – 4h/day	3000	8,20
Tumble dryer C	2500 to 3000 W	32 weeks - 2x /week	200	0,55
Dish washer	1200 W	48 weeks - 5x / week	288	0,79
Fridge + freezer C	200 to 350 W	365 days - continuously	500	1,39
Iron	750 to 1100 W	48 weeks - 1h / week	52	0,14
Vacuum cleaner	650 to 800 W	48 weeks - 2h / week	70	0,19
Computer	70 to 80 W	240 days – 2h /day	36	0,10
		∑	11496	31,49

Table 3.8.1: Household appliances and their energy usage.

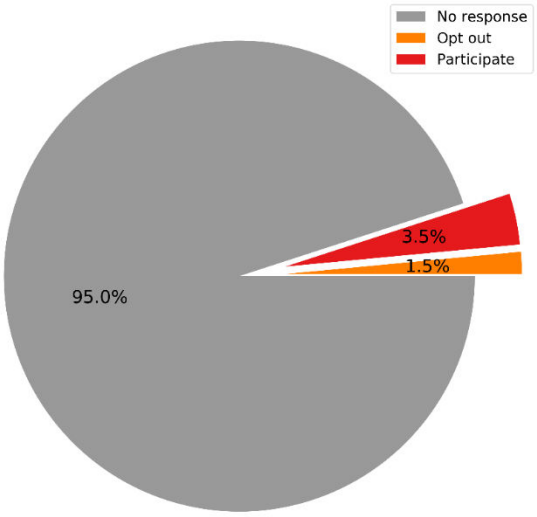

Figure 3.8.1: Households participation in 3Smart share.

Motivation

Let us first think what are the reasons to participate in 3Smart project. We assume, the most popular reason is that people would think it would help save on costs and reduce their energy bills. On the other hand, of those who will not be willing to allow remote switching, the most common reason would probably be that they would not want to lose control over the energy supply and consider it inconvenient.

Three demand management innovation projects can be developed and implemented by 3Smart with the aim of exploring innovative approaches to reducing the impact of peak demand from residential hot water systems using load control solutions. These projects can have different objectives including testing different technology and load control options, discovering customer take-up rates from various incentives and marketing approaches, customer satisfaction and response to load control solutions.

Control of small hot water systems

What we can extract from Table 3.8.1 above is that one of the main consumers are water heaters, so the first idea is to focus on investigating a demand management solution for electric hot water systems on continuous electric supply. As mentioned above, we estimate there are around 670 customers with small hot water systems with storage of less than 100 litres. If we assume 5% would participate in this project for a modest incentive of 50-100€ per year, this means that roughly 33 households would participate in 3Smart.

However, it is important to know how are the costs, associated with the supply and installation of the controlled load devices, in relation to the demand reductions, so that it would be considered a cost-effective alternative to other network and non-network solutions.

4 Strem

4.1 Introduction to the district heating system

As additional infrastructure for the case of the municipality Strem, where the pilots are located, the central district heating system is proposed.

Description of the district heating system

Based on the activities of the municipality Strem in the renewable energy sector, different plants based on renewable energy sources to produce heat and electricity were established. One of those energy projects was the implementation of a local district heating grid. The heat for this district grid is provided by two energy plants, the biomass heating plant (based on forestry biomass) and the biogas CHP plant (based on agricultural biomass). The district heating grid is owned by the municipality.

Main data of the grid:

Start of operation: October 2003

Number of consumers: approx. 150

- 85 private households
- 55 flats (generation village, apartment building block Kapellenstraße, apartment building block Hauptstraße)
- municipal buildings (Pflegekompetenzzentrum Strem, primary school, kindergarden, fire department, doctor, municipal office)
- different companies

Investment: EUR 2.000.000 ,-

Biomass boiler capacity: 1.000 kW

Biogas CHP capacity: 500 kW

Grid length: 5.500 m

The scheme of the local district heating grid is shown in the following figure.

Figure 4.1.1. Overview of the local district heating grid in Strem

4.2 Smart interaction of grid and building – aspects of heat supply

Regarding the structure of the district heating system in Strem, three possible smart interactions of heat grid and buildings can be seen.

- Heat sources: Biogas CHP process 500kW; Biomass furnace 1000 kW

Figure 4.2.1. Overview of the location of the plants, supplying heat to the district heating grid

- Distribution: central heat buffer (50m³ = ~ 1.000 - 3.000 kWh), pipe grid
- Heat sinks: mainly households and smaller loads
    - Biggest load is the pilot building 2 – retirement and care centre (5-7% of the overall consumption)

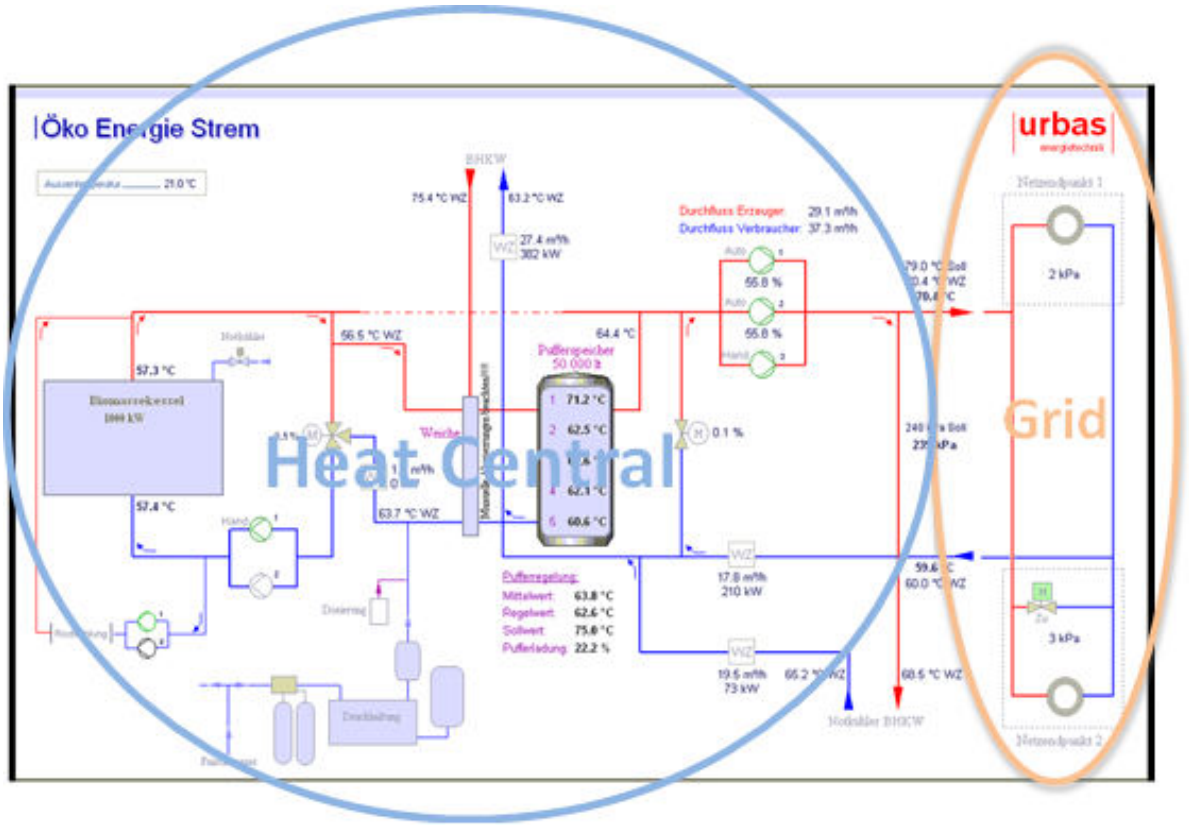

Figure 4.2.2 Scheme of the district heating grid

The normal operation conditions within the distribution grid are 80-85° supply medium temperature and 55-60° return medium temperature (in summer 75° supply medium temperature is standard), so the inclination is 30 degrees. The volume of the heating medium (water) in the grid is 20m³. The reaction time, from starting the heating boiler until the heat is arrived at the last consumer, is 1,0 to 1,5 hours. The heat is mainly provided by the biogas CHP plant, as it produces constantly electricity during the year and the off-heat of the gas engine provides constantly heat for the heating grid and this amount is enough to cover the domestic hot water demand. The heating furnace of the district heating plant only operates in the period between November and April. The heating furnace is operated during this season at basic load (minimal load).

At grid side, normally 2 or 3 grid pumps are active and can be controlled by the grid controlling system.

Flexibilities:

From the district heating grid, the main flexibility is seen on the one hand in the central heat buffer with a volume of 50.000 liters as well as on the consumers' side at the domestic hot water generation. In this part, the district heating operator has influence in the controllability of hot water preparation by the bus-system. A lot of households connected to the grid have own boilers for hot water preparations in a size of 150 – 300 liters.

In addition, buildings with a control system that is now developed within the 3Smart project can in future represent additional flexibilities. Very important is a flexibility like the pilot building 2 of the 3Smart project – the retirement and care building – which is the largest heat consumer in the grid.

Furthermore, considered from the viewpoint of the grid-operator – the grid itself could also provide some buffering capacities. The volume of the district heating network can to a certain extent itself be used as storage. Increasing the supply temperature before peak loads causes a "charging" effect in the grid, regarding thermal energy storage. By lowering the flow temperature before or during the peak, the capacity at the boilers can be reduced. An essential advantage of this strategy is that the necessary investment costs for the increased regulatory effort compared to the installation of central storages are low.

Monitoring and control:

For monitoring and control, the district heating system uses a bus-system. Following parts can be controlled:

1. boiler loading times

2. temperatures
3. control valve settings
4. pump settings

Figure 4.2.3 shows two screenshots of the monitoring system and the different parameters that can be monitored.

The consumers are controlled whether with outdoor- or indoor temperature sensors. The controller can additionally set parameters for a night setback.

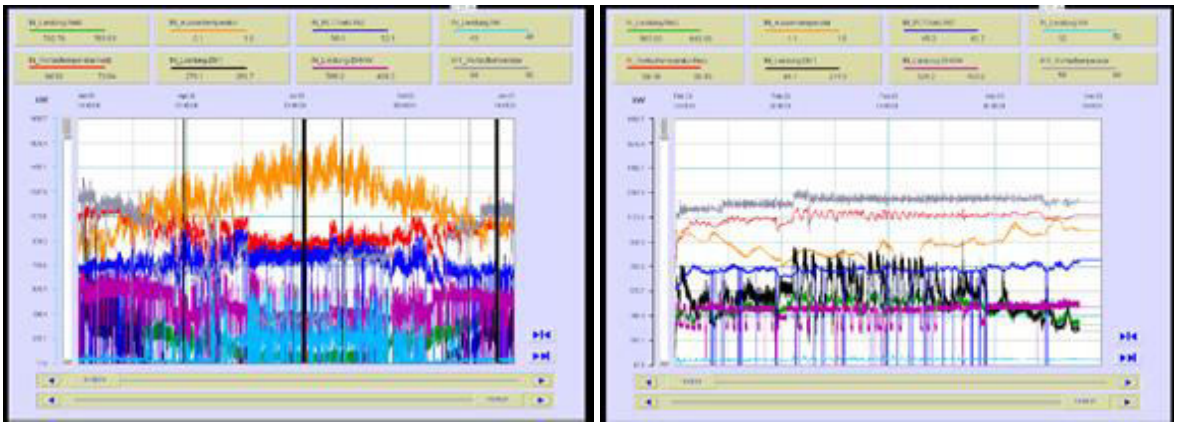

Figure 4.2.3. Screenshot of the monitoring system of the district heating grid parameters

Within the considerations of the 3Smart project for the analysis of the district heating grid within A3.3, the grid will be divided into two parts:

1. controllable part of the grid → 3Smart pilot buildings
2. non-controllable part → rest of the grid with exception of those buildings

4.3 Implementing flexibility in the district heating grid – case study approach

The following cases shall in general be considered for the analysis of the whole district heating system:

Case A:

Case A comprises a constant supply in the heat grid, as it is also now. The supply temperature is sustained by the central buffer.

On the load side, the hot water storage is directly connected to the heat switch (district heating transfer station), temperature regulation is done by thermostat – thus no change in future. The building heat side has an interface between heat switch

(and optionally, but not necessarily a heat buffer), which can be operated remotely in order to vary the temperature in the building and thus, the forward temperature level of the heating system. In case of a number of participants this is replacing the through simultaneity factor estimated load by a precise load distribution management.

The case A-scheme is illustrated in Fig. 4.3.1:

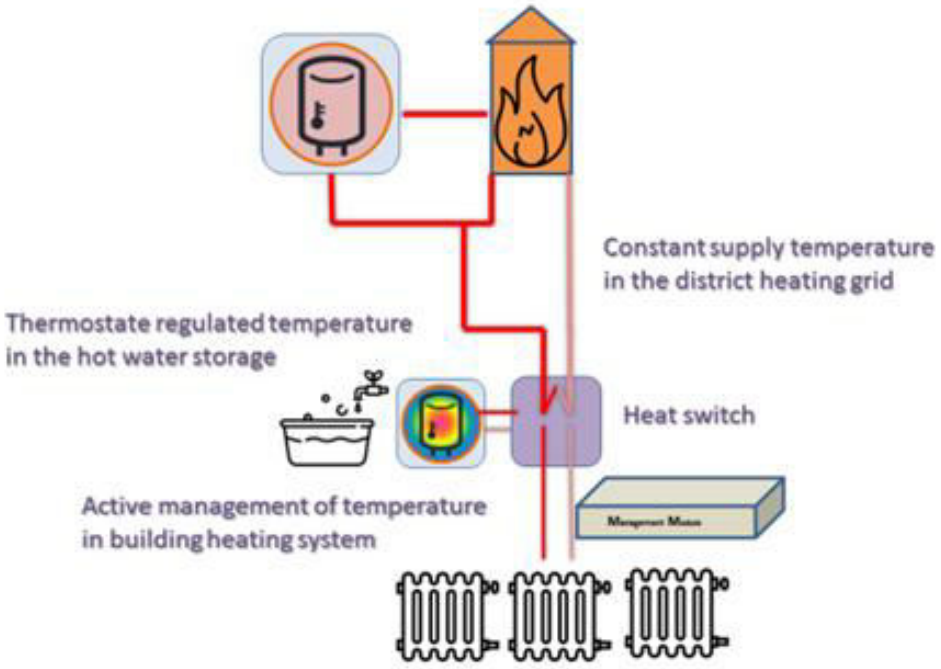

Figure 4.3.1: Case A-scheme

Case B:

Case B comprises a variable temperature throughout the grid by involving also the thermal central storage with higher priority in the distribution process. The thermal level of the storage is actively managed by an interface between the furnace and the buffer. In this case the forward temperature in the grid can be adapted to the expected heat demand defined by weather forecast. In order to guarantee drinking water hygienics as minimum temperature level, the building side hot water storage temperature can optionally be regulated by a simple heating rod.

The case B- scheme is illustrated in Fig. 4.3.2:

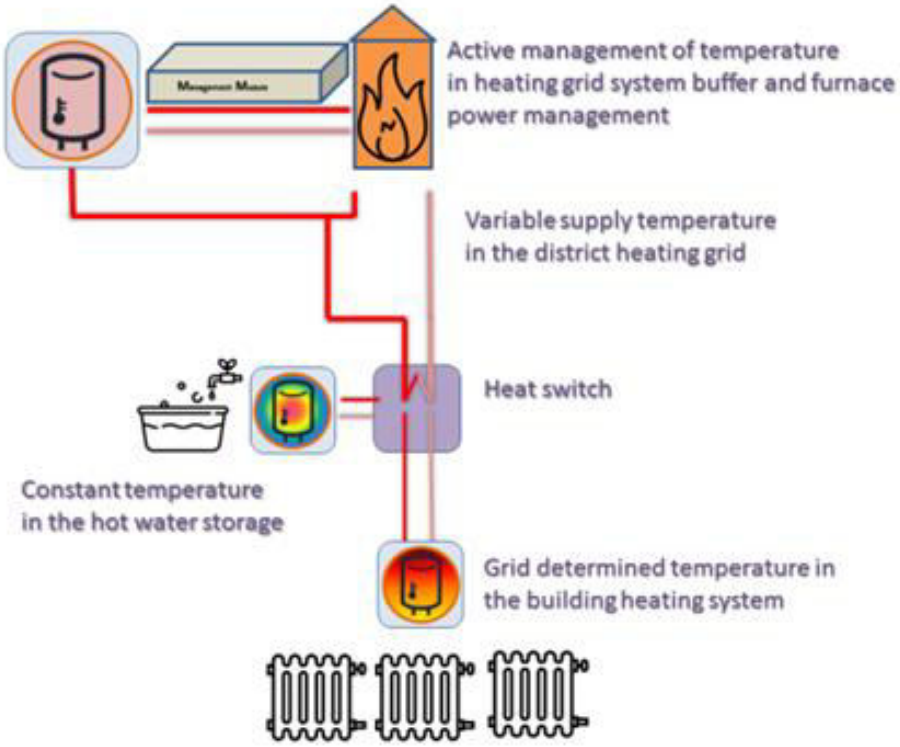

Figure 4.3.2: Case B-scheme

Case C:

Case C comprises a forward temperature level management in the heat grid, as well as a decentralised remote load management on the building side. This gives the possibility of an effective supply, as well as load management. The grid side management is located at the interface between furnace and central heat storage and allows variable forward temperature levels without lessening the furnace´s efficiency. The load side management is located behind the interface between grid and building and allows, by means of a heat pump (in the optimum case supplied by a PV facility with electric storage battery), a stable supply of the building (preferably also containing a decentral heat buffer). In this way a very effective grid and load operation can be realized.

The case C-scheme is illustrated in Fig. 4.3.3:

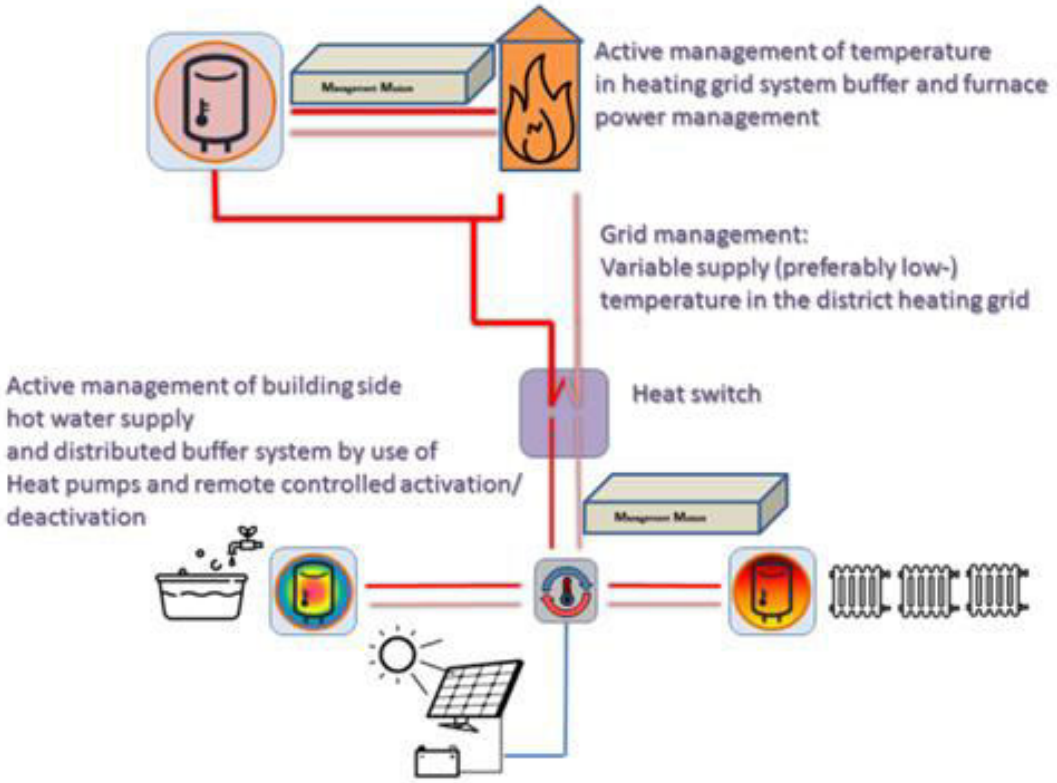

Figure 4.3.3: Case C-scheme

4.4 Potentials and consequences of large-scale EMS application in the district heating grid in Strem

For the grid analysis, it is planned to conduct "point in time" analysis. This means that "critical days" or "critical periods" in the operation of the district heating grid shall be extracted and analysed in detail. The analysis shall demonstrate how buildings that are controlled with a 3Smart EMS system can positively influence the grid performance. After the analysis on how buildings that behave according to the 3Smart EMS system is done, an analysis of the "upscaling effect" shall be conducted, that shall reveal on how numerous of 3Smart buildings would positively influence the grid operation.

Peak load reduction

Conventional control concepts for heating systems in buildings in the district heating grid in Strem are based on the definition of room temperature setpoints, usually taking into account a night setback. The night setback is in principle an efficient way of reducing the energy demand in buildings, with no major differences between light and heavy buildings. The changeover from the night to the target day value takes place at a large number of controllers at a certain time. This is often set to 6 a.m. or earlier as a predefined setting. Since this standard setting is usually not changed by the customers, this leads to a

simultaneous heat output requirement in a large number of customer installations. This collective leap of the setpoint temperatures to the daily value at the same time with a majority of the customers causes a strongly pronounced morning peak in the load course of the district heating supply. Depending on the building type and depending on their thermal storage capacity and the properties (heat inertia) of the respective heating systems (underfloor heating, thermal activation of building units, air heating by fan coil, radiator), the heating time may vary in which the room temperature reaches the setpoint. For very slow systems, therefore, the default setpoint change at e.g. 6 a.m. may not be enough to meet the customer's request (a specific room temperature at a particular time), whereas in a rather responsive system, a setpoint change may not be sufficient until shortly before the specific customer request.

In adjusting the time of the setpoint changeover from the night setback to the day-setpoint to the real time required, there is a potential on the customer side for peak load reduction on the district heating side, which could be realized by EMS systems.

If this optimization task is implemented by a large number of customers, the district heating network can certainly be expected to reduce the peak loads.

This principle is also shown in Figure 4.4.1.

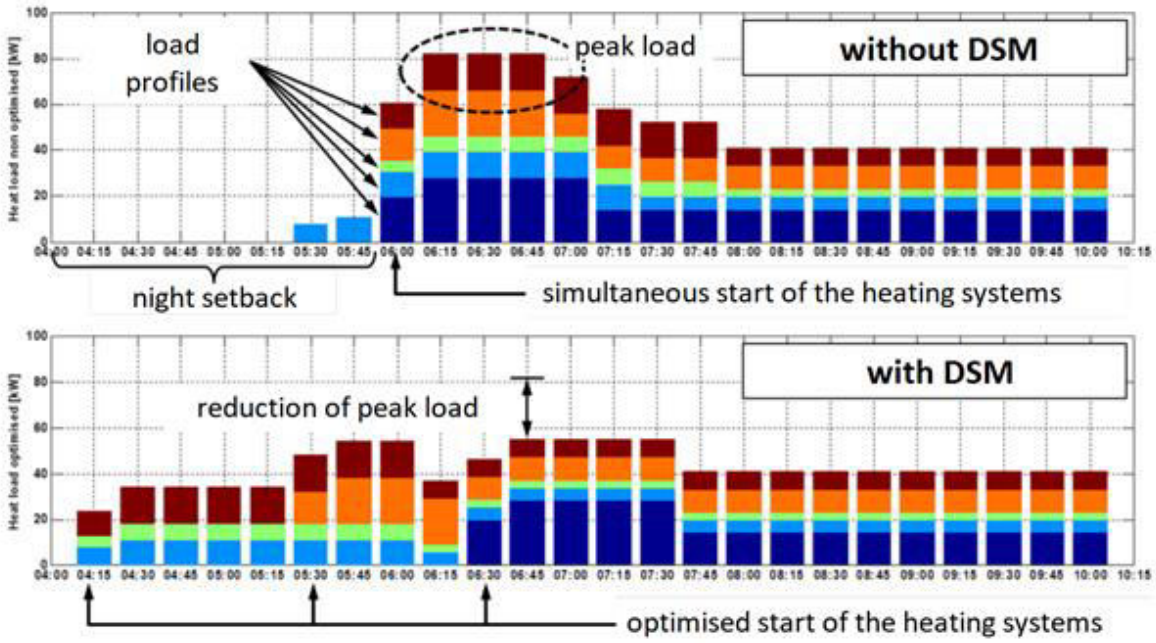

Figure 4.4.1: main principle and potential of DSM in district heating systems (Modified after Schmidt, R.; Basciotti, D.; Judex, F.; Pol, O.; Siegel, G.; Brandhuber, T.; Dorfinger, N. & Reiter, D. 2013. SGMS – SmartHeatNet. Vienna: Klima- und Energiefonds.)

The peak loads exemplarily shown in the figure above can also be found at many customers in Strem, most importantly also at the biggest customer, namely the retirement and care centre.

Potentials of peak load reduction at the retirement and care centre

Being by far the biggest consumer in the grid, the load profile of the retirement and care centre in Strem has a significant influence on the performance of the whole grid. In this context it is quite interesting, that the typical load course of the building is characterised by significant peak loads in the morning and (in the main heating period) in the afternoon. The course of the thermal loads is exemplarily shown in the following figures for this building.

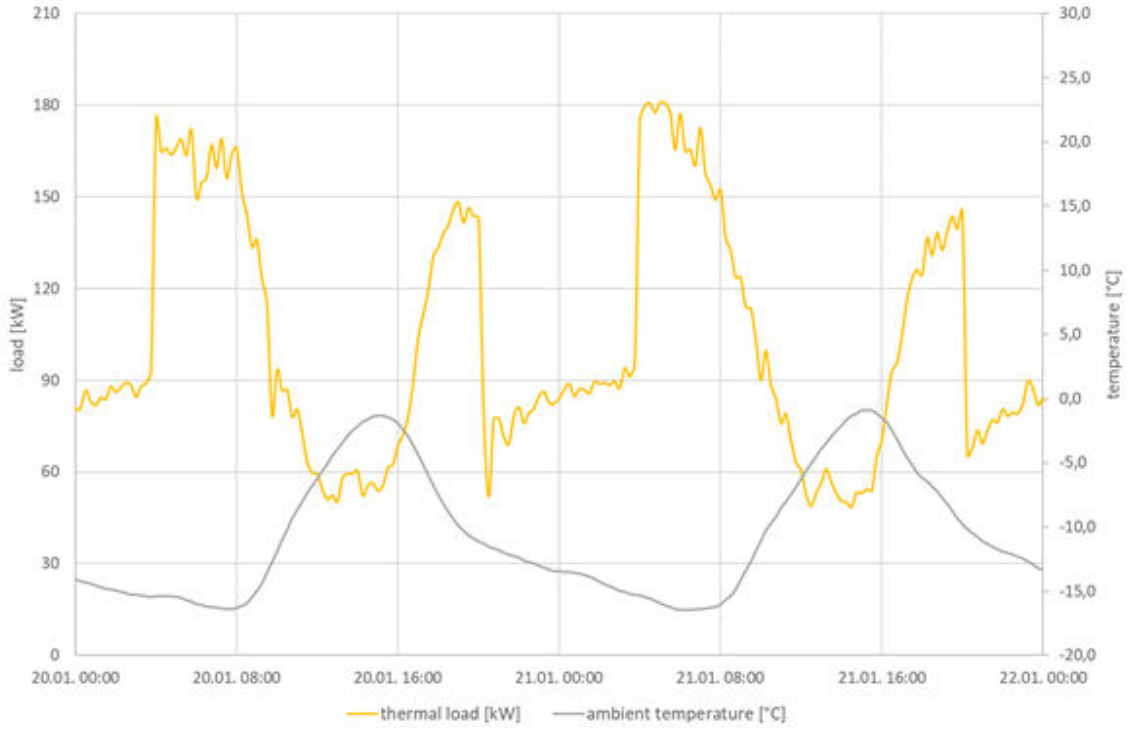

Figure 4.4.3: thermal load of the retirement and care centre in Strem from 20.01.17 to 22.01.17

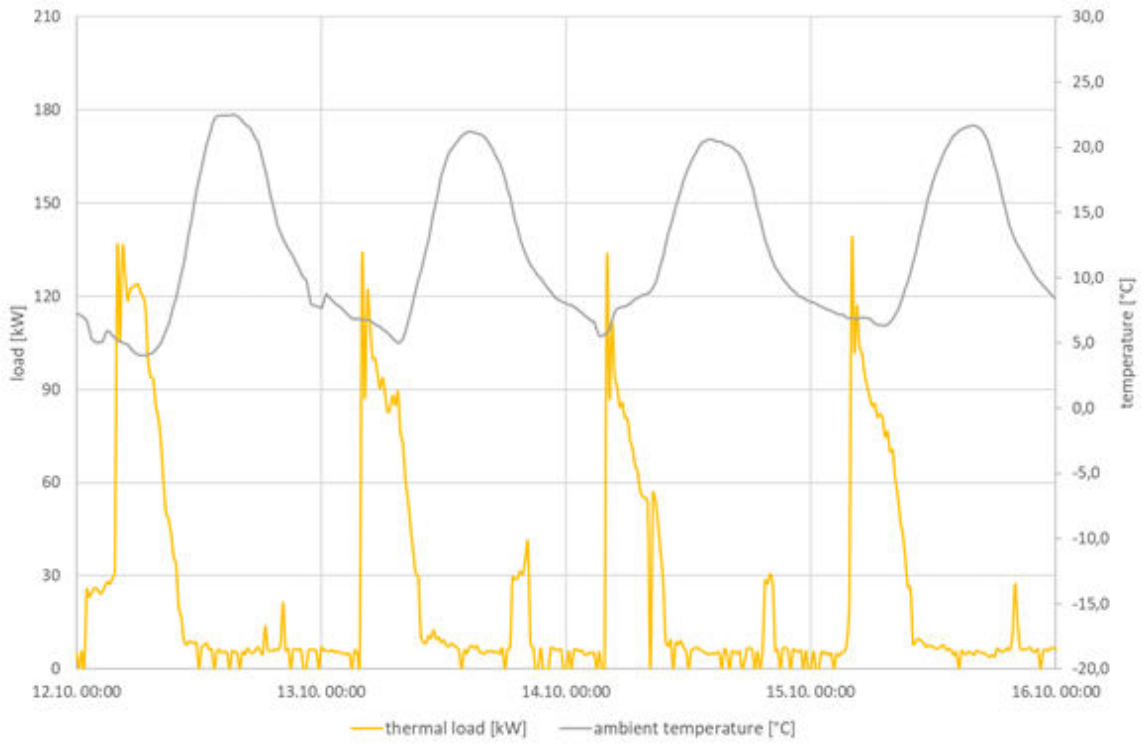

Figure 4.4.4: thermal load of the retirement and care centre in Strem from 12.10.17 to 16.10.17

Figure 4.4.3 shows the thermal load during two days in January 2017, with ambient temperatures between 0°C and -16°C. The erratic increase of the load in the early morning hours shows that the increased thermal energy demand can be led back to a setpoint-switch. The steady increase in the afternoon (beginning from 4 p.m.) may indicate just a "regular" response to an increased heat demand. What's more, the rapid decline of the heat load at 8 p.m. shows also the setpoint-switch to the night setback.

Figure 4.4.4 shows the thermal load of the retirement and care centre during four days in October 2017, with ambient temperatures between +5°C and +23°C. One can see very clearly the peak loads in the morning hours, when the setpoint switches between night setback and day set temperature. Additionally, this figure shows that peak loads come not only along with higher thermal loads, but also in periods with generally lower heat demand.

In fact, these periods are for district heating systems even more critical. In Figure 4.4.3 one can see that the thermal load in the night is roughly 50% of the peak load (90 kW to 180 kW). In Figure 4.4.4 it can be seen that the base load is only roughly 7% of the peak load, which means in relation a much higher demand.

Peak loads in the heat distribution may have a negative impact on the technical and economical performance of the district heating system, to which extent depends on frequency and the magnitude of the peaks. EMS-systems, forecasting (heat demand,

weather, etc.) and other DSM-measures can help reduce these peaks in the thermal load course of a consumer, which is exemplarily shown in the following figure.

Figure 4.4.5: possible consequences and potentials of DSM-measures at the retirement and care centre in Strem for a typical load profile in the heating period

Naturally, the concrete configuration of these measures and the settings of the control system can be implemented highly individually, in this sense the load course in Figure 4.4.5 has to be seen as one of many possibilities. The yellow load course represents the actual thermal load from 11.12. to 18.12.2017, clearly visible are the night setback and the distinct peak loads in the morning hours of each day. The orange load course illustrates how a compromise of the control strategy (taken both night setback and DSM into account) may look like. The night setback (which has advantages in the economic grid performance) is kept to a certain extent, although it is altered to shift the thermal peak loads. The overall thermal energy usage is the same in both cases. Through this (rather minor) alteration, the peaks can be reduced significantly, which not only brings beneficial effects for the building itself but also for the performance of the whole grid, as shown in the following section.

Potentials of peak load reduction in the whole grid

These characteristics of the load course of an individual customer are also reflected in the overall thermal load course of the district heating grid, shown in Figure 4.4.6 as an example for the same time period as the data from Figure 4.4.3 (20.01. – 22.01.17).

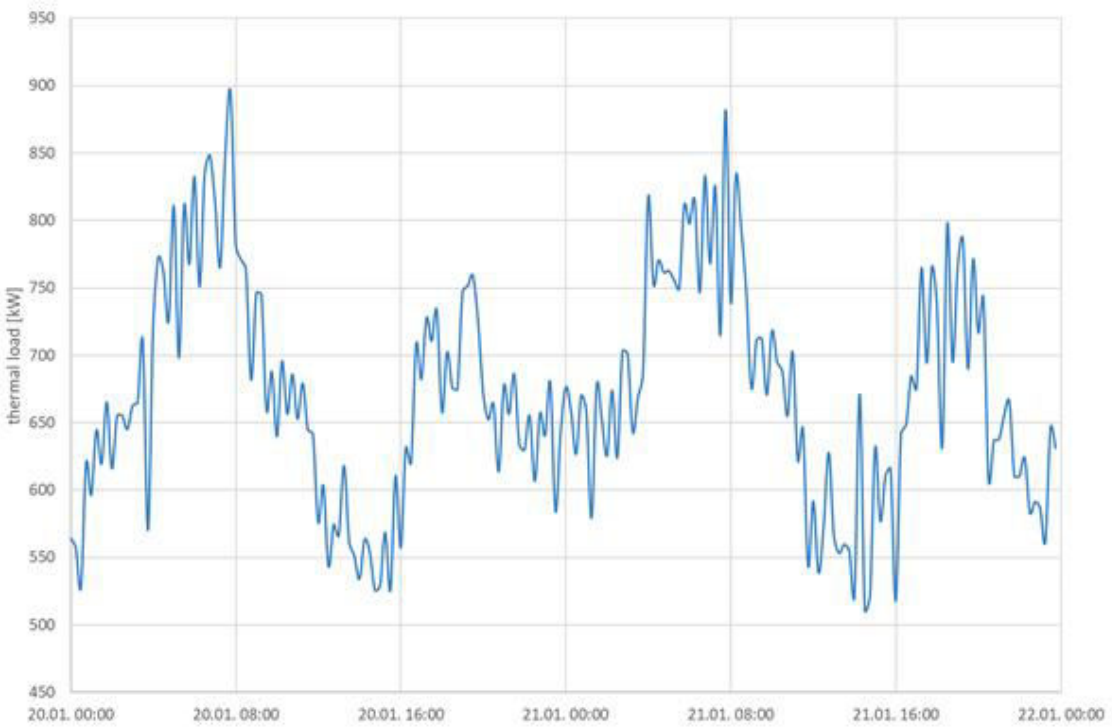

Figure 4.4.6: thermal load course of the district heating grid in Strem from 20.01.17 to 22.01.17

The peak loads, which occur very significantly at the biggest consumer (see Figure 4.4.3) can also be seen in the thermal load of the whole heating grid, illustrated in Figure 4.4.6.

These peak loads could be reduced with a large-scale implementation of EMS systems. To conclude which customers would primarily be interesting for DSM-measures, meaning which customers are the primary cause for the peak loads, it is necessary to cluster the different consumer groups, regarding their typical load profile and their heat requirement.

For this reason, the customers in the district heating grid Strem have been clustered in 6 groups regarding heat requirement in the respective period (20.01. – 22.01.17), labelled from A to F, starting with the smallest consumers (A) to the biggest consumers (F). The following figure gives an overview of the clusters and gives a first impression of the grid structure – containing mainly smaller consumers, large consumers being the minority.

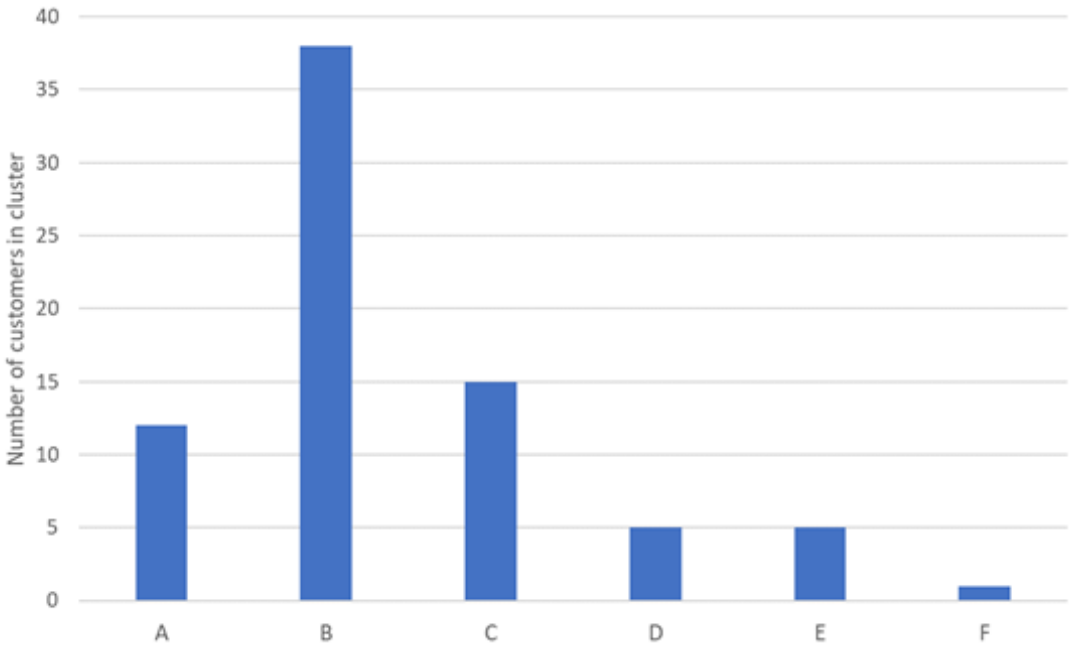

Figure 4.4.7: cluster groups of the consumers in the district heating grid in Strem regarding heat requirement in the period 20.01.17-22.01.17

Looking at the different user groups in detail, it can be seen that regarding peak loads mainly the customers in the clusters A, B and partly also C (in comparison the “smaller” consumers) contribute to the peak loads. The load profiles of these consumer groups are shown in the following figure.

Figure 4.4.8: load profiles of cluster groups A, B and C for the period 20.01. to 22.01.17

In Figure 4.4.8 the periods with peak loads are highlighted. The peak loads in the morning hours occur at all three cluster groups (most distinct in groups A and B, not so much in group C), the peak loads in the evening occur mainly at the consumers in the group B.

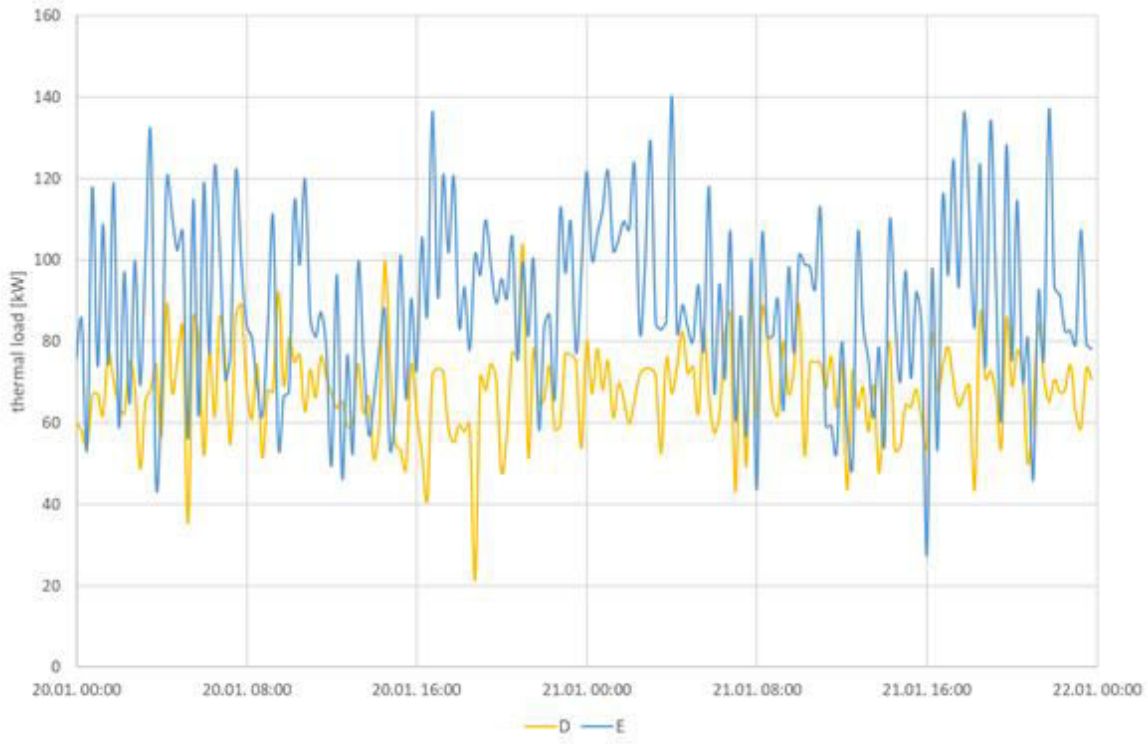

Figure 4.4.9: load profiles of cluster groups D and E for the period 20.01. to 22.01.17

Figure 4.4.9 shows the load profiles of the consumer groups D and E. The bigger consumers apparently have a steadier load profile and peak loads are not so distinct, compared to the other consumer groups. In this sense, peak load reduction via demand side management with EMS-systems seems to have a big potential with the numerous “smaller” consumers of the grid – of course alongside with some larger consumers like the retirement and care centre (as can be seen in Figure 4.4.3 and Figure 4.4.4).

Following this conclusion, it is interesting to look at the basic distribution of the customers in the district heating grid. The following figure gives an overview of the connected loads of the consumers in the district heating grid Strem, which shows a typical rural distribution structure: many consumers/households with low heating loads (single-family homes and flats), few large consumers and some consumers with intermediate heating loads.

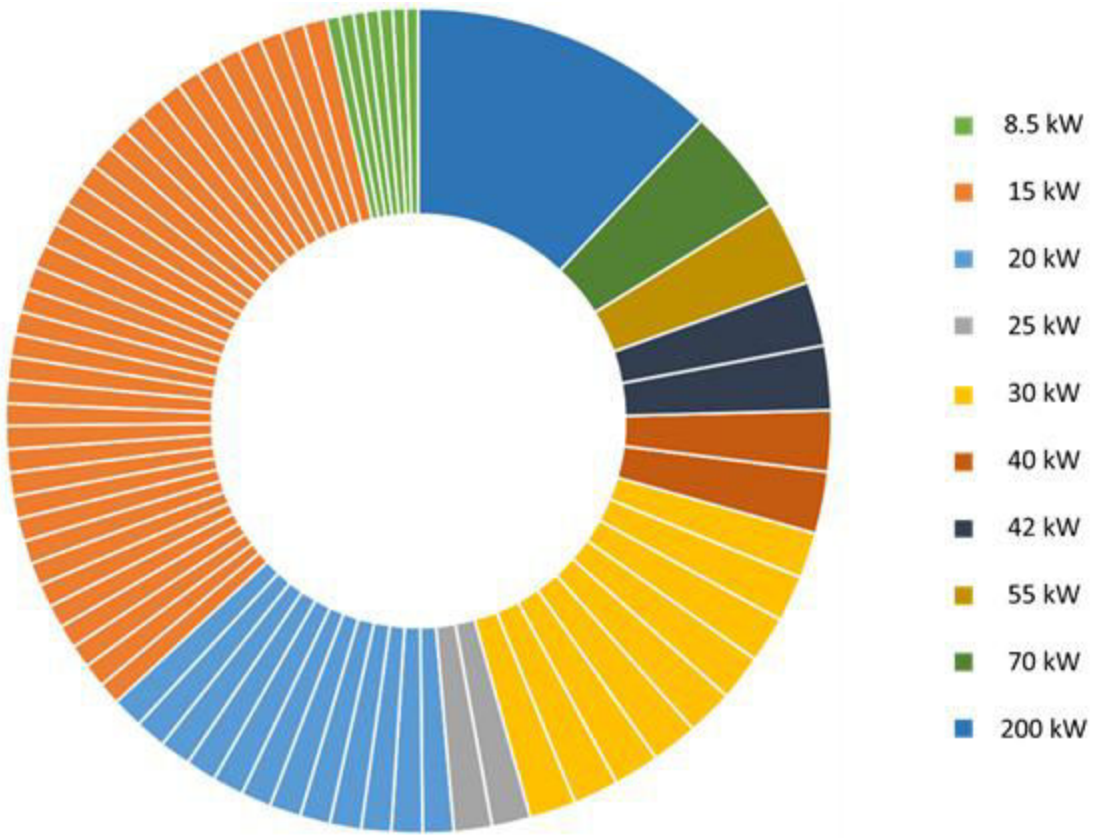

Figure 4.4.10: distribution of the consumers in the district heating grid sorted by connected loads

In this context it can be estimated that about 81% of the consumers in the grid are likely to be suitable for demand side management with EMS-systems, for the purpose of peak load reduction.

In the research project “SmartHeatNet” the potentials of demand side management have been analysed (measurements and simulations) for a heating grid in another region in Austria. Based on the results from the analysis, the authors have also developed a guideline to estimate the potentials of peak load reduction with DSM for other heating grids, provided that certain knowledge of the consumers in the grid is available.

Following this guideline with the grid-data assembled above, the potential for peak load reduction with large-scale demand side management-measures can be estimated to be about 32%, meaning that the peak loads in the grid can be reduced by a third, exemplarily shown also in the following figure.

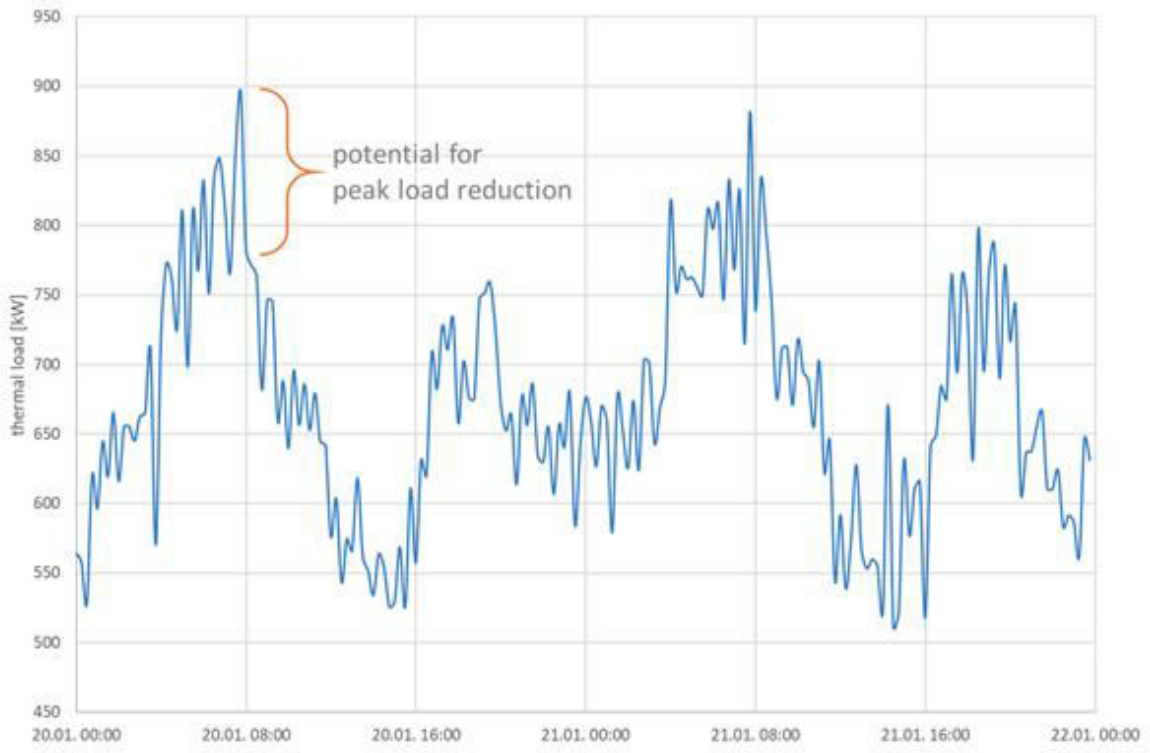

Figure 4.4.11: Thermal load course of the district heating grid in Strem from 20.01.17 to 22.01.17 including the potential for peak load reduction following DSM-measures

Economic assessment

Demand side management measures in district heating grids generally pay off quickly, when fossil fuels are used in the peak load boilers. As this is not the case in Strem (peak loads are covered by the biomass boiler), these measures become especially interesting regarding firstly the technical performance and optimisation of the grid and secondly with reinvestments in the boiler. In particular, if higher loads are to be expected due to grid extensions, the DSM measures described can be used to avoid investing in a larger biomass boiler.

The benefits for the technical performance of the grid would be a load relief, energy savings for pumping and reduction of leakage in outdated piping caused by pressure fluctuations.

As costs in this case, the control devices should be listed on the house connection heat exchangers, as well as a transmitting and receiving unit in the control center in the district heating center. Other further costs can also arise at the transfer station or at the consumer. However, without support from the suppliers, no customer will voluntarily make investments.

If these investments, especially the retrofitting of the transfer stations, have to be covered by the district heating grid operator, the economic outcome will be quite bad. Assuming that

30% of the grid participants are included in DSM measures, investment costs of approximately € 90.000 would arise, facing energy savings of annually about € 500. Thus, the amortisation period would be in the range of some dozen years, which is obviously not attractive or reasonable for the grid operator.

As a consequence it can be concluded that DSM measures are, in terms of the economic performance, mainly interesting if fossil fuels are used for the covering of the peak loads. Obviously the technical performance of the grid will be optimised by DSM measures in any case, however, investments will have to be assessed regarding their technical and economic performance and not only in the context of technical aspects.

5 Technical prerequisites and benefits for infrastructure energy management

Prerequisites

Infrastructure systems are today usually equipped with SCADA systems that allow operators to monitor their operation and to perform some supervisory control actions in them, like e.g. changing operation setpoints for different subsystems of the infrastructure.

The prospective 3Smart EMS in charge for the infrastructure management would act as a tedious operator – it needs to receive data from various sensors in the system and process them via prediction and estimation techniques to yield the information necessary for predictive control and optimization. The point of data interchange between the 3Smart modules and the physical world again would be a properly structured 3Smart database, most likely connected to the database of the SCADA system to decrease costs.

The result of predictive control and estimation modules operation are commands or setpoints that would be issued towards the infrastructure system. The logic is similar as applied in central HVAC level of buildings – no local control loops should be infringed, but rather setpoints provided for these loops, in the same way as infrastructure operators would be acting.

In the beginning most likely the 3Smart tool up-scaled on the level of the infrastructure would operate as a decision support tool and would require the operator to perform a check of the computed commands based on his/her operational experience. In this phase verifications of correct operation need to be performed, both in the outputs monitored by the operator and in the inner variables dynamics verified by a 3Smart tool expert, e.g. verification of correctness of the model used for the infrastructure, verification of reliability of the applied prediction and estimation techniques, verification of reliability of the mathematical programming software used. As confidence in system operation would be gained through time finally a supervised autonomous operation would take place where the

commands are directly sent to the system from the up-scaled 3Smart tool and the operator would intervene if deemed necessary.

The case studies performed show a considerable amount of analogy between energy management with included demand response functionality in buildings and likewise energy management with demand response in infrastructure systems. For example, analysis of operation of buildings and water distribution systems is given next.

The building:

- heating, ventilation and air conditioning (HVAC) systems represent a significant portion of the overall building energy consumption;
- HVAC and other controllable energy-relevant subsystems in a building (energy storages, controllable energy production units like combined heat and power units, etc.) induce energy exchange profiles with distribution grids for gas/heat/electricity where concern is taken related to reduction of the overall consumption, reduction of the peak consumption, reduction of the CO2 content of consumed energy, reduction of degradation of different components etc (examples of possible goals for the 3Smart tool);
- the occupants in the building should be enjoying a comfort indoor environment expressed via inequality relations on temperature and other comfort variables for individual building spaces (e.g. temperature higher than 21°C) or different units should be kept within their power limits (examples of constraints for the 3Smart tool)[1];
- the owner-centric EMSs are usually focussed on the ultimate goal – the overall cost where all goals mentioned above are combined in a single overall building costing function, but
- actually different entities from the grids side (distributors, suppliers, aggregators, etc.) and regulators shape the energy costing terms to exhibit the grids- and socially-welcome energy usage from the building, like minimized peak consumption (through peak cost terms), maximized usage of locally generated energy (through higher pricing for energy consumed than for energy exported), low CO2 content of consumed energy (lower prices for energy with smaller CO2 equivalent), demand response used for improvement of grid conditions or for energy system balancing, etc.

Water distribution system

- acceptable pressure levels in water distribution systems in the environment of fluctuating water demand are usually maintained by water storages where the

[1] The comfort of occupants can be also numerically evaluated according to different standards and that numerical evaluation used further in assessment of the occupants productivity. In that way the productivity and comfort can also be considered as operation goals.

pressure on different supply points in the water distribution network is a function of water height in the upstream storage and flow through the piping from the storage up to these points;

- for water distribution systems that exploit groundwater, pumps are used to inject the water in the storage which is then the major energy consumer in the water distribution system;
- the amount of freshwater leakage through different leaking points in the water distribution networks should be as low as possible, and they are proportional to the pressure in the pipe at the leak point in the network;
- the up-scaled 3Smart tool applied to the water distribution system should tend to reduce the consumption of electricity used for pumping and to reduce the leaked water (examples of goals of the up-scaled 3Smart tool for the water distribution system);
- the pressures in all supply points and end-points in the water distribution network should be kept above some minimum prescribed values for the sake of quality water supply and due to fire protection technical norms, which is expressed via inequality terms on pressures, e.g. pressure in the pipe higher than 2 bar, further the water level in the storage tank cannot be higher than the tank height (examples of constraints of the up-scaled 3Smart tool for the water distribution system);
- operator-centric up-scaled 3Smart tool again uses the common denominator for all the goals of the water distribution system operation by expressing them in terms of costs for the operator, one part is for electricity cost which can be priced in a similar way as for buildings (elaborated above), and the other is for leaked, non-revenue water;
- the costs determination for the leak part can be the consequence of costs related to the water delivery to the pump and its conditioning, but also can be regulated by the water authority who may put a price on water taken from the ground source.

Re-usability of the building microgrid-level modules in infrastructure

Within the 3Smart tool microgrid-level energy management is selected as the top level which interacts with the electricity distribution grid and ensures also the demand response functionality. It has been shown on different pilot sites that the microgrid-level may include specific systems for shaping energy exchange with distribution grid (like storage on UNIZGFER, HEP, EPHZHB or Strem retirement and care centre building, or production and consumption on EON or IDRIJA building), but may also exist even without any physical system for which it is directly in charge, e.g. on Strem school the microgrid-level just integrates the controllable and non-controllable consumption and governs the shaping of controllable consumption via price-based coordination/interaction with central HVAC and zone levels, as developed within 3Smart.

Microgrid-level modules developed for buildings can be used for bidding flexibility and for governing energy exchange of the infrastructure system with electricity distribution grids in the same way as done for the buildings. In a particular application the level of optimization of the overall infrastructure system behaviour needs to be interconnected via prediction and pricing signals with the microgrid level modules, as explained in D4.1.1 and D4.5.3. E.g., for the case of water distribution system, the infrastructure-specific level is in charge for computing and commanding optimal input flow into the storage tank, for the case of electrified city rail that level concerned with optimization of the train traction forces of individual trains. For the case of electric vehicles charging, it computes the commands for charging intensity towards different vehicles.

It is also important that flexible infrastructure increases significantly the potential for demand response services which makes it then a viable option for distribution system operators to exploit, instead of applying grid reinforcement measures. This then opens space for additional small flexibility providers which would not be able to provide enough flexibility to the distribution system operator on their own. One may say thus that the application on the level of infrastructure opens the local market for small flexibility providers like individual buildings.

For a considerable number of players who provide flexibility, autonomous trading can be established to further increase chances of economic gains and reduce the risk of paying high penalty according to the flexibility provision contract when the flexibility cannot be exhibited by flexibility providers due to some temporary error in them. E.g., the UNIZGFER building has during piloting in summer 2019 exhibited a temporary fault of one of the two compressors in its chiller – during the fault presence the building was not in a position to provide flexibility as calculated. Autonomous trading between flexibility providers can be then used to procure the flexibility from another flexibility provider at much lower cost than the cost of penalty.

The computed possibility for flexibility provision of the mine pumping system in Idrija has also provided a good example how the infrastructure system can increase its own economical performance and at the same way open possibility for further flexibility providers to join in flexibility service provision towards the distribution grid.

The analysis in Strem, focussed on the central heating plant and its related heat distribution grid, has shown that there is a potential in using demand response for evading existing network reinforcement for further extensions of the heat distribution grid – the existing consumers get a chance to lower their energy bills via participation in demand response while the heating operator is in position to provide heat to more users with lower infrastructure costs.

6 Conclusion

The performed case studies for application of 3Smart tools in different infrastructures of settlements of various size is performed here: Zagreb case study as a representative case study for cities, Idrija case study for towns and Strem case study for villages. They have shown a significant potential and readiness of 3Smart tools for application in infrastructure management from one side and from the other the significance of demand response potential lying in the infrastructure systems in settlements. Additionally the Strem case study has shown the gains achievable from demand flexibility provision to central heating systems.

The document further outlines the strategy how the 3Smart tools can be extended to the level of infrastructures – necessary steps are listed. High potential/readiness of already existing 3Smart tools on the building microgrid level is shown with respect to usage for the same purpose also on the side of the infrastructure – information connection with the electricity grid and shaping the lower-level infrastructure-specific optimizations towards economical optimum for the infrastructure considering energy/power pricing and flexibility provision.

Output Quality Report

Output title: Strategy of EMS take-up on city scale	
Type of output:	☐ Documented learning interaction ☑ Strategy/ Action Plan ☐ Tool ☐ Pilot action
Contribution to PO indicator:	**P23 No of strategies to improve energy security and energy efficiency developed and/or implemented**

Summary of the output (max. 1500 characters)
Please describe the output in terms of content, objective, scope and main characteristics. The potential for the application of 3Smart tool on the level of infrastructure in cities, towns and villages is analyzed. Especially emphasised is the usage of similar mathematical, optimization based, methodologies for diverse infrastructure, thus making these (potential) infrastructure-level energy management modules compatible for interaction with the modules in the 3Smart tool. To encompass settlements of different sizes, the analysis investigates three case studies in the Danube region: city of Zagreb, town of Idrija, and village of Strem. In Zagreb case study (city size), the interaction of electricity grid with buildings and with the following 3Smart-like-managed infrastructure systems is analyzed: water distribution, electric vehicles charging and electrified city rail. Also, the effects of 3Smart-managed buildings on the load in heat distribution grid are assessed. In Idrija case study (town size), the mine water pumping system is analyzed for maintaining the water level in the town mines, in interaction with electricity grid. In Strem case study (village size), the central biogas and wood pellets combined heating/electricity plant and heat distribution grid operation under demand management is analyzed. Based on the performed analyses, a strategy for up-scaling the use of building-side EMS tool is assessed. It elaborates how the modules of energy management on the side of infrastructure should look like, the envisioned IT environment, and commissioning.
Added value (max. 1500 characters)

For strategies and tools:

Please provide a comprehensive explanation regarding the added value of the output as compared to already existing strategies/ tools of similar type.

The developed strategy stems from the three case studies, which have shown: a significant potential and readiness of the 3Smart tool for application in infrastructure management, as well as the significance of a demand response potential existing in the infrastructure systems in settlements. The Strem case study has shown the gains achievable from the demand flexibility provision to central heating systems.

The document further outlines the strategy how the 3Smart tools can be extended to the level of infrastructure – necessary steps are listed. High potential/readiness of already existing 3Smart tools on the building microgrid level is shown with respect to the usage for the same purpose also on the infrastructure side – information connection with the electricity grid and shaping the lower-level infrastructure-specific optimizations towards economical optimum for the infrastructure considering energy/power pricing and flexibility provision.

The developed strategy considers the application of the modular tool for integrated energy management in buildings, city infrastructure and distribution grids, including demand response. It considers the developed elements of the tool, what IT environment is needed and what would be the steps in putting the infrastructure management into operation. To the best of our knowledge, this is the first strategy of such kind, which makes it important and relevant for the energy system transition in the Danube region.

Applicability and replicability (max. 1500 characters)

Please provide a concrete description of how the project output is to be applied in real life and could be replicated in other geographical and sectorial areas or different environments.

As the output has considered infrastructure management in settlements of different sizes and also different infrastructure types, its conclusions are directly applicable to a great variety of settlements. E.g., performed analysis of optimal operation of water distribution system with pumped storages is directly applicable in all settlements with pumped storages implemented in the water distribution system and these are practically all settlements with groundwater usage which is characteristic for the entire Danube river basin.

Further in the future is the application to the electrified rail management, and somewhat nearer, and more straightforward, the application to electric vehicles charging. The variety of infrastructure systems investigated in the case studies shows that the principles of the usage of up-scaled 3Smart tool remain the same across different sectors in city infrastructure. Thus, there is a significant replication potential. Also, the demand response potential of different infrastructure can be significant (e.g. the potential of water pumping from mines in Idrija).

Considering the large demand response potential of different infrastructure systems, in the conclusion of the strategy it is also stressed how important is the up-scale of the 3Smart tool to the infrastructure level. This can provide enough flexibility thus helping to open the flexibility market on a certain geographical location and enabling other consumers/buildings to join.

Suggestions for improvement, if applicable (max. 1500 characters)

Please provide information on possible improvements that could be brought to the current output considering the general context in which it is delivered.

Possible improvements: - Perform a deeper economical assessment that is specific to the considered infrastructure; - As a further extension, carry out the cost-benefit analyses for specific infrastructure cases. The authors should try to balance out the level of details for different infrastructure/case studies. In the Zagreb study case one gets a detailed system model and an in-depth economic analysis of the considered scenarios (in particular in sections 2.2, 2.3 and 2.4, not so much so in sections 2.1 and 2.5), while in the Strem study case there is no detailed mathematical model, and in the Idrija study case there is neither mathematical model nor similar economic analysis of the considered scenarios.	
Output Quality Level	☐ Low ☐ Average ☑ Good ☐ Excellent

Name of the Quality Manager

Prof. Mato Baotić

Signature of the Quality Manager